2013

Deep Brain Stimulation to Increase Generalized Arousal in Intact Mice and a Mouse Model of Traumatic Brain Injury

Amy Wells Quinkert

DEEP BRAIN STIMULATION TO INCREASE GENERALIZED AROUSAL IN INTACT MICE AND A MOUSE MODEL OF TRAUMATIC BRAIN INJURY

A Thesis Presented to the Faculty of

The Rockefeller University

in Partial Fulfillment of the Requirements for

the degree of Doctor of Philosophy

by

Amy Wells Quinkert

June 2013

Deep Brain Stimulation to Increase Generalized Arousal in Intact Mice and a Mouse Model of Traumatic Brain Injury

Amy Wells Quinkert, Ph.D.

The Rockefeller University 2013

Deep Brain Stimulation (DBS) is a promising neurosurgical technique that may be useful in promoting emergence to consciousness in minimally conscious state (MCS) patients. In this context, DBS of the central thalamus (CT/DBS) is intended to act as a surrogate input from the ascending arousal systems to support cortical recruitment for cognitive tasks. To test the effectiveness of CT/DBS, intact mice and a mouse model of traumatic brain injury (TBI) have been stimulated under the hypothesis that CT/DBS increases generalized arousal. Two of the three dimensions of the operational definition of generalized arousal are presented here: motor activity and sensory (specifically olfactory) responsiveness. In addition to the question of the effectiveness of CT/DBS to increase generalized arousal, this thesis explores the efficiency of a small set of parameters of stimulation. The data presented in this thesis show that 1) CT/DBS can increase generalized arousal as measured by motor activity in intact mice; 2) that a previously unexplored parameter of DBS, temporal pattern, can modulate its effectiveness;

3) a novel mouse model of TBI, multiple TBI, can produce motor activity and neurological deficits that last 10-14 days; 4) CT/DBS can increase generalized arousal as measured by motor activity in this mouse model of traumatic brain injury; and finally, 5) there is no evidence that DBS can potentiate an olfactory response in intact mice or in a mouse model of traumatic brain injury. To summarize, these data show that CT/DBS can increase generalized arousal as measured by motor activity in intact and brain injured mice and add further experimental evidence from the laboratory to support the idea that CT/DBS can be therapeutic for MCS patients. The data presented here also show that temporal pattern is important in one context of DBS, but it would not be surprising if temporal pattern turns out to be important in many other contexts of DBS. The brain does not usually work in monotonic pulses. Why should neuromodulation in the service of CNS arousal be any different? Exploring the effects of temporal patterns in DBS is certainly a promising new field of research and could ultimately benefit patients by fine-tuning the exact amount of electricity necessary to produce clinical results and thereby optimizing efficacy and reducing side effects of DBS.

To my husband, who has shared this journey with me from the beginning.

Acknowledgments

First and foremost, I would like to acknowledge my advisor, Don Pfaff. He is an excellent mentor who prodded me when I needed prodding, gave insightful and concise advise, introduced me to interesting people, and modeled how to be an effective leader, manager, and scientist. I also acknowledge the rest of my faculty committee: Bruce McEwen and George Reeke, who gave intellectual support and guidance through my years at Rockefeller, and Gary Aston-Jones, who traveled from South Carolina to hear me defend my thesis. My thesis work also greatly benefited from the support, both financial and intellectual, of Niko Schiff. It is his work with minimally conscious patients that inspired my thesis and his theories and advice which guided its trajectory. I also wish to thank Tina Schober for always being a kind ear and having apt career advice.

To those many people whose time in Don's lab overlapped with mine, thanks for the advice, training, support, and fun. Specifically I'd like to acknowledge Tom Maloney, Adesh Bajnath, and Alyssa Goodman for personally helping me manage the details of running experiments. Special thanks also go to Paola Calderon and Rebecca Leshan who helped me whip this dissertation into shape. To all the others: Cami, Khatuna, Sara, Larissa, Alex, Yoav, Eugene, Gen, Lee, Zach, Maggie, Kiri, Isabel, Ana, and Susan, thanks. To Bob Cuevas and the rest of the support staff at the CBC, thanks for your tireless efforts in managing our

mouse facilities and the Pfaff rooms especially. To the library staff, I appreciate all of those pdfs of articles you found for me through interlibrary loan.

To all my friends and family, thank you for your emotional support through all the times I was neck deep in mice, brain tissue, and numbers. And finally, to my husband: thanks for keeping me sane, making me eat, and knowing me better than I know myself. This experience would have been a much more lonely and difficult one without you there.

Table of Contents

List of Figures

List of Tables

List of Abbreviations

BL	baseline
CL	central lateral nucleus of the thalamus
CM	central medial nucleus of the thalamus
CNS	central nervous system
Counts	activity counts
CT	central thalamus
CT/DBS	central thalamic deep brain stimulation
DBS	deep brain stimulation
DOC	disorders of consciousness
EEG	electroencephalogram
Hactv	horizontal activity
IMD	intermediodorsal nucleus of the thalamus
LIS	locked-in state
MCS	minimally conscious state
MD	mediodorsal nucleus of the thalamus
PC	paracentral nucleus of the thalamus
PD	Parkinson's disease
PF	parafasicular nucleus of the thalamus
PostSx	post-surgery

PostTBI	post-injury
PV	paraventricular nucleus of the thalamus
PVS	persistent vegetative state
Re	reuniens nucleus of the thalamus
Rh	rhomboid nucleus of the thalamus
TBI	traumatic brain injury
Totdist	total distance
VS	vegetative state

Chapter 1: Introduction

Deep Brain Stimulation

Deep brain stimulation (DBS) is a popular neurosurgical technique that involves implantation of a pacemaker that produces electrical current connected to stimulating electrodes placed in specific brain targets; DBS shows promise in the treatment of many neurological and psychiatric diseases and disorders, and its use continues to expand because it is widely applicable, highly adjustable, and reversible. Since there are numerous diseases and disorders that are fundamentally neurological, there are as many potential applications of DBS as the neuroscience and neurological communities can discover appropriate brain region targets for diseases and disorders of interest. In addition to this target brain region flexibility, the stimulation itself is highly flexible. There are a plethora of parameters to optimize when using DBS, *e.g.*, frequency, amplitude, pulse width, pulse shape, and field geometry. Unlike other neurosurgical techniques such as ablation, DBS can be stopped permanently (in the case of negative outcomes) or temporarily (for optimal performance).

The Food and Drug Administration has recognized the usefulness of DBS and has approved its use in the treatment of movement disorders such as Parkinson's disease (PD), essential tremor, and dystonia, and in the treatment of psychiatric disorders such as treatment-resistant depression and treatment-resistant

obsessive compulsive disorder. DBS of the subthalamic nucleus or the internal globus pallidus are both efficacious and clinically useful in the treatment of motor symptoms and motor complications in movement disorders and are viable options for patients who do not respond well to pharmacological treatments (Fox *et* al., 2011). Treatment-resistant depression and treatment-resistant obsessive compulsive disorder patients, by definition, do not respond to any currently available pharmacological or psychological treatment options; 50% of these patients who opt for DBS respond positively to this treatment with rare serious adverse events (Goodman & Alterman, 2012). In short, DBS can and has been approved by the FDA as a safe and effective treatment option for a number of disorders and has the potential to help a host of patients control the symptoms of their disease.

Ongoing clinical trials and preclinical research into the effectiveness of DBS in several neurological diseases and psychiatric disorders are being performed in many hospitals and laboratories around the world. **Table 1.1** lists DBS trials archived at clinicaltrials.gov. These clinical trials expand on those diseases and disorders already approved by the FDA and include Tourette syndrome, Huntington's disease, multiple sclerosis, dementia, epilepsy, Alzheimer's, bipolar disorder, addiction, anorexia nervosa, anxiety, obesity, chronic pain, cluster headache and traumatic brain injury (TBI). As most of these clinical trials are ongoing,

Table 1.1 Clinical Trials of Deep Brain Stimulation.

Disease/Disorder	Brain Target (# trials)
Parkinson's Disease	Subthalamic nucleus (38) Globus Pallidus interna (8) Ventrointermedius nucleus of the Thalamus (3) Pedunculopontine nucleus (2) Caudal Zona Incerta (1) Unspecified (10)
Dystonia	Globus Pallidus interna (14) Subthalamic nucleus (4) Ventrointermedius nucleus of the Thalamus (3) Unspecified (2)
Depression	Subgenual cingulate (5) Ventral Striatum (3) Subthalamic nucleus (2) Nucleus Accumbens (2) Internal Capsule (2) Anterior Capsule (1) Medial Forebrain Bundle (1) Unspecified (2)
Obsessive Compulsive Disorder	Ventral Striatum (4) Subthalamic nucleus (3) Nucleus Accumbens (2) Internal Capsule (1) Ventral Caudate (1) Ventrointermedius nucleus of the Thalamus (1) Globus Pallidus interna (1) Unspecified (3)
Epilepsy	Thalamus (4) Subthalamic nucleus (1) Ventrointermedius nucleus of the Thalamus (1) Hippocampus (1) Unspecified (2)

Disease/Disorder	Brain Target (# trials)
Essential Tremor	Ventrointermedius nucleus of the Thalamus (4) Subthalamic nucleus (2) Globus Pallidus interna (2) Thalamus (1)
Alzheimer's	Fornix (4) Nucleus Basalis Meynert (1) Unspecified (1)
Tourette syndrome	Thalamus (1) Globus Pallidus interna (1) Unspecified (1)
Bipolar Disorder	Nucleus accumbens (1) Unspecified (1)
Addiction	Nucleus accumbens (2)
Anorexia Nervosa	Unspecified (1)
Anxiety	Subthalamic nucleus (1)
Chronic Pain	Ventral Capsule (1) Ventral Striatum (1)
Cluster Headache	Postero-inferior Hypothalamus (1)
Dementia	Nucleus Accumbens (1)
Multiple Sclerosis	Ventrointermedius nucleus of the Thalamus (1)
Obesity	Unspecified (1)
Traumatic Brain Injury	Unspecified (1)
Huntington's Disease	Globus Pallidus interna (1)

Data for this table compiled from www.clinicaltrials.gov.

publications documenting results and effectiveness are scarce. Importantly, these trials show a willingness of the clinical community to explore more applications for DBS.

Though progress continues, success of DBS in the clinic is not universal. Debate continues on its efficacy in the treatment of chronic pain syndromes, and the FDA has yet to approve any such stimulation paradigm due to the lack of controlled clinical trials proving effectiveness. Uncontrolled open-label studies suggest DBS of various regions might ameliorate chronic pain in some patients, but these results have not been replicated in randomized double-blinded controlled studies (Coffey, 2001; Rasche, Rinaldi, Young, & Tronner, 2006; Levy, Deer, & Henderson, 2010).

While the use of DBS in the clinic has been increasingly common for the last 30 years, debate persists as to the clinical mechanism(s) of action. Originally thought to be an alternative to ablation and therefore strictly inhibitory of the target, the mechanism of action of DBS has been studied by many groups, and these studies suggest local inhibition, local excitation, modulation of local firing pattern, neurogenesis, and other effects (Liu, Postupnua, Falkenberg, & Anderson, 2008; Montgomery & Gale, 2008; Bourne, Eckhardt, Sheth, & Eskandar, 2012). As these studies occur in various contexts, it is not surprising to find mutually exclusive mechanisms in this list; still, contradictory results are reported in

the literature even in studies using the same model. This contradiction may indicate that DBS has multiple effects, and the current understanding is that the clinical mechanisms of action of DBS are much more nuanced than simple ablation. Further debate surrounds the critical cell structures and types: some studies emphasize the action in local axons, others the action at the soma; there are even suggestions that the response of astrocytes to DBS is of utmost importance (Vedam-Mai *et al.*, 2012). The details of what happens at the electrical/ neurotransmitter level, cellular level, and circuit level remain unclear. Most of these studies occur in patients with PD, animal models of PD, or computational models of neuronal function, and it is important to make sure the lessons learned from these studies are generally applicable to DBS in other contexts.

MINIMALLY CONSCIOUS STATE

Disorders of consciousness (DOC) refer to a broad range of devastating states with major deficits to both cognitive and motor function (Giacino *et al.*, 2002) affecting an estimated 700,000 people in the US with only ~40% of that number ultimately regaining consciousness (Hirschberg & Giacino, 2011). **Figure 1.1** (adapted from Schiff, 2010) diagrams the spectrum of these disorders. The scales converge on coma, with cognitive function increasing along the horizontal axis and motor function along the vertical axis. The line between Minimally Conscious State (MCS) and Severe Cognitive Disability marks the boundary of

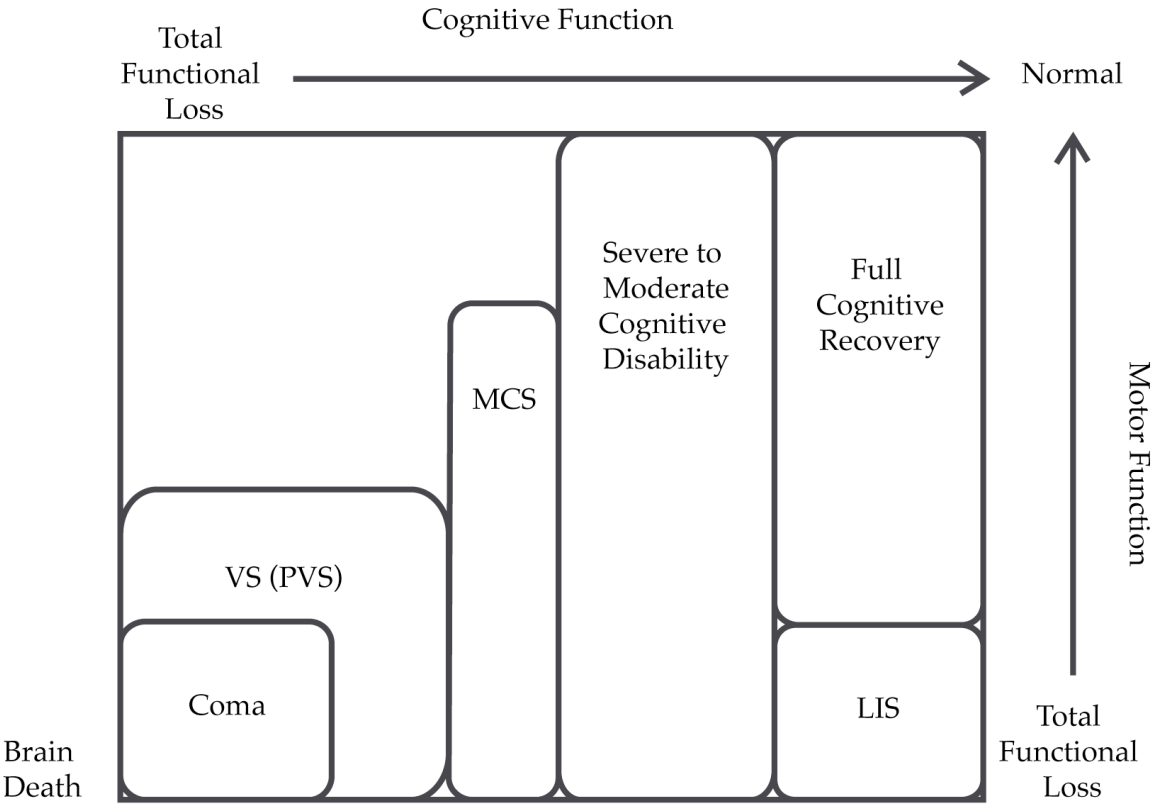

Figure 1.1 Spectrum of Disorders of Consciousness. Various diagnoses of disorders of consciousness (DOC) placed on a scale of increasing cognitive function on the x axis and increasing motor function on the y axis. With slightly more cognitive and motor functionality than coma is the Vegetative State (VS) or Persistent Vegetative State (PVS). Toward the middle of the scale of cognitive function is the diagnosis of Minimally Conscious State (MCS). VS — vegetative state, PVS — persistent vegetative state, MCS — minimally conscious state, LIS — locked-in state. Figure adapted from Schiff (2010).

consciousness. DOC are not to be confused with Locked-in State (LIS) seen in the bottom right corner of the graph. LIS can present like DOC, but is in actuality a disorder of motor neuron function with no deficits in consciousness or cognitive ability.

Unlike coma or VS patients, MCS patients show intermittent, but recurring, behavioral signs of awareness in response to external stimuli (Giacino *et al.*, 2002). In addition to this behavioral difference, neuronal differences distinguish MCS from VS patients structurally: brains of MCS patients show smaller and fewer lesions in the arousal circuitry, lesser axonal injury and thalamic cell loss, and greater cortical connectivity (Hirschberg & Giacino, 2011). While our understanding of what differentiates MCS patients from other DOC patients continues to evolve, this group comprises the most likely candidates to respond to intervention and to eventually emerge to consciousness.

Despite the fact that little is known about what sets MCS patients apart from others with DOC, theories exist. Dr. Nicholas Schiff (2008), Weill Cornell Medical College professor and neurologist, theorizes that while most DOC patients lose connectivity throughout the brain, MCS patients largely retain thalamo-cortical networks and lack only the arousing input to these circuits from the brainstem and midbrain. He proposes that MCS patients show occasional awareness when their ascending arousal systems manage to innervate the

thalamo-cortical networks that support cognition, but as this connection is weak, consciousness cannot be maintained for any length of time. Schiff further theorizes that if a surrogate arousing input to the thalamus can be artificially maintained, the thalamo-cortical circuits may have enough innervation to support emergence to consciousness: that surrogate could be DBS.

DBS in Minimally Conscious State Patients

In a double-blinded single subject cross-over study, Schiff and colleagues (2007) implanted stimulating electrodes into the central thalamus of one patient 6 years after initial injury and 4 years after termination of initial rehabilitation therapy. After implantation surgery, a titration period allowed optimization of stimulation parameters; the patient was then observed for a total of six months while monthly alternating the stimulation on or off. Throughout the study, the patient's progress was tracked using a standard test for functionality in coma patients, the JFK Coma Recovery Scale — Revised, which measures functionality in 6 modalities (auditory, visual, motor, oromotor/verbal, communication and arousal). Some of these metrics showed significant increases during stimulation on versus stimulation off. By the end of the study, the patient was capable of feeding himself and communicating with simple words and gestures. While this success in a MCS patient has not been replicated in another controlled study, it is a heartening result for those who provide care to such patients.

In addition to this single controlled study, several preceding papers discuss the use of DBS for the treatment of DOC. Hassler *et al.* (1969) stimulated the right internal globus pallidus and the left ventral anterior nucleus of the thalamus of one patient in "vigil coma" (vegetative state). It is unclear whether the reported behavioral arousal indicates actual functional improvement, reflexive stimulation artifacts, or confirmation bias on the part of the authors. Given the vague language and subtle behavioral changes (gaze movements, spontaneous hand movements, and unintelligible vocalizations), it is unlikely that the authors of this early study significantly improved the consciousness of the patient. On the other hand, Sturm *et al.* (1979) published a case report in which they stimulated the posterior part of the intralaminar nuclei of the thalamus in a patient presenting with "subcoma" after ischemic infarction of the midbrain. The patient is described as having "a degree of vigilance seeming to range just moderately below the level of consciousness" (Sturm *et al.*, 1979), and therefore, the term "subcoma" most likely corresponds to a modern diagnosis of MCS. After stimulation, the patient was able to respond to commands, communicate verbally, and be fed orally. This is an obvious early success of DBS in the treatment of a DOC, but we must consider this case with caution because there was no blinded comparison of stimulation on and off and only qualitative data were collected.

More recently, there have been open label studies of DBS of the mesencephalic reticular formation or the centromedian-parafascicularis nucleus complex of the thalamus in vegetative state patients. In one such study, Yamamoto *et al.* (2010) describe 8 of 21 VS patients who received DBS emerging to consciousness to obey verbal commands. However, this study is not controlled: the study has no randomized groups of DBS and placebo or even a randomized cross-over design using each patient as his or her own control. No information is given regarding selection criterial of the 21 DBS-treated patients (from a population of 107), and there is no indication whether any of these VS patients would be more accurately diagnosed as MCS. Additionally, these patients were implanted, stimulated, and showed improvement less than 20 months after initial injury. Considering this short time frame, spontaneous recovery, independent of DBS, cannot be excluded. These studies support the idea that DBS of the proper brain structures in an appropriate subpopulation of DOC patients can improve functionality and support emergence to consciousness, but it must be pointed out that steps need to be taken to ensure positive outcomes are not the result of confirmation bias. Randomized cross-over study designs and standard behavioral metrics of coma recovery should be utilized in all future clinical studies (Giacino, Fins, Aachado, & Schiff, 2012).

Figure 1.2 Functional nucleic groups of the Central Thalamus. Four groups of nuclei in the mouse central thalamus can be generally separated by their projections. The dorsal group of nuclei (PV — paraventricular, and IMD — intermediodorsal) projects to the ventral striatum, pre- and infralimbic cortices, and the amygdala. The lateral group (PC — paracentral, CL — central lateral, CM — anterior central medial) project to the dorsal striatum and the cingulate cortex. The ventral group (Re — reuniens, Rh — rhomboid, CM — posterior central medial) projects mainly to non-limbic cortical areas as well as the hippocampus. The posterior group (PF — parafascicular, centre médian — not present in mouse) projects to the striatum, and sensory and motor cortices. Figure adapted from Paxinos & Franklin (2001).

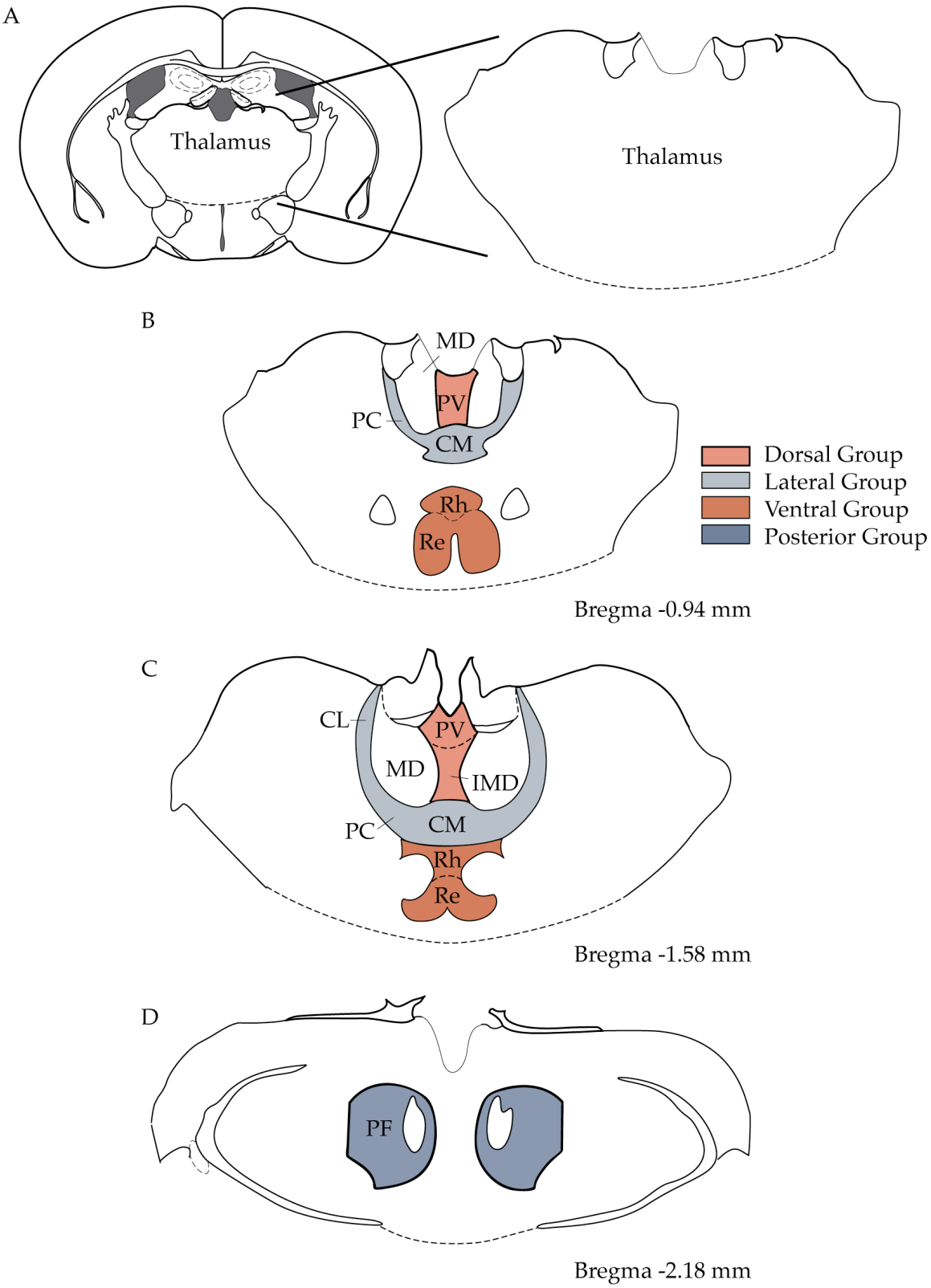
A
Thalamus
Thalamus
B
MD
PV
PC
CM
Rh
Re
Dorsal Group
Lateral Group
Ventral Group
Posterior Group
Bregma -0.94 mm
C
CL
PV
MD
IMD
PC
CM
Rh
Re
Bregma -1.58 mm
D
PF
Bregma -2.18 mm

Central Thalamus: Anatomy and DBS Target for MCS

Whereas the aforementioned studies of DBS in VS or MCS stimulate a part of the ascending arousal system (medullary reticular formation) or the nonspecific thalamic nuclei, the following rationale will focus on stimulation of the central thalamus (the nonspecific nuclei) for DOC.

The central thalamus (CT) encompasses the nonspecific nuclei of the thalamus, so called because of their lack of sensory specificity as well as their wide-ranging and diffuse projections. The CT can be divided into four groups of nuclei: dorsal, lateral, ventral, and posterior (see **Figure 1.2**). The dorsal group includes the paraventricular and intermediodorsal nuclei which project to the ventral striatum, the pre- and infralimbic cortices, and the amygdala. The lateral group consists of the paracentral, central lateral, and anterior central medial nuclei projecting mainly to the dorsal striatum and the cingulate cortex. The ventral group consists of the reuniens, rhomboid, and posterior central medial nuclei with spare projections to the striatum, mainly projecting to non-limbic cortical areas, and at least one, the reuniens, projects to the hippocampus. Finally, the posterior group of nuclei includes the parafasicular nuclei and the centre médian (not present as a separate nucleus in the mouse) which project primarily to the striatum as well as to sensory and motor cortices (Van der Werf, Witter, & Groenewegen, 2002).

The CT is uniquely poised for neuromodulation in the severely injured brain due to its neuroanatomical placement and role in regulating generalized arousal (Schiff, 2008). Anatomically located between the major ascending and basal forebrain arousal systems and the cortex, the CT is recruited to support overall cerebral activation and to maintain that activation during high arousal states (Schiff, 2008; see **Figure 1.3**). This level of cerebral activation is noticeably absent in the severely injured brain. Schiff (2009) theorizes that while MCS patients retain thalamo-cortical connections needed to support cerebral activation, they lack sufficient innervation from the arousal systems to sustain awareness. Therefore, CT/DBS in a severely injured brain should approximate this missing arousal input, allowing the CT to support cerebral activity and cognition.

GENERALIZED AROUSAL

Generalized arousal is a basic concept in neuroscience that has recently been codified into a definition that allows for systematic and methodical study. Intuitively, the concept of generalized arousal is a simple one: it is the difference between an awake animal or human and a resting one; a conscious, behaving, active animal or human, and one that is not (or cannot) respond to external stimuli. As reviewed in Quinkert *et al.* (2011), Pfaff developed an operational definition of generalized arousal as follows: an aroused animal displays 1) increased spontaneous motor activity, 2) increased sensory responsiveness, and 3)

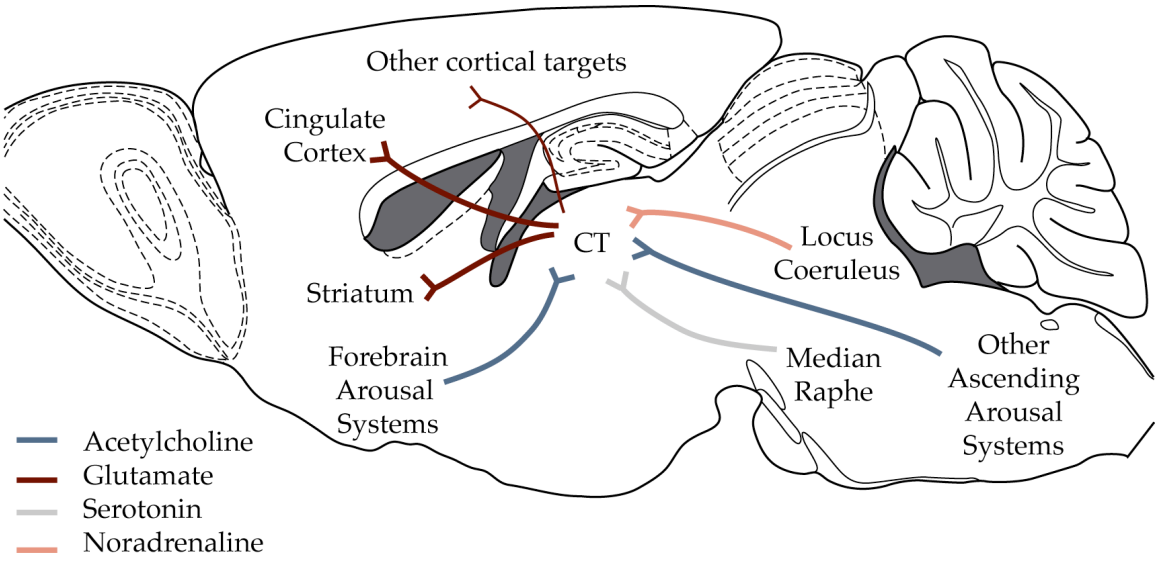

Figure 1.3 Projections to and from the Central Thalamus. The central thalamus receieves acetylcholinergic input from the ascending and forebrain arousal systems. It also receives noradrenergic input from the locus coeruleus and a serotonergic input from the median raphe. Central thalamic nuclei send glutamatergic projections mainly to the striatum and to various cortical areas including the cingulate cortex, pre- and infralimbic cortices, and non-limbic cortical targets. CT — central thalamus. Figure adapted from Paxinos & Franklin (2001).

increased emotional reactivity (Pfaff, 2006). **Table 1.2** summarizes the operational definition and requirements. Using these three dimensions of behavioral arousal (motor activity, sensory responsiveness, emotional reactivity), one can methodically observe this basic driving force of behavior.

Table 1.2 Operating Requirements of CNS Arousal Systems

Operational Definition
Provide alertness to sensory stimuli, body-wide, *all* sensory modalities Drive voluntary motor activity, *body-wide*, from fidgeting to running marathons Fuel emotional reactivity, positive *and* negative
Operational Requirements
Lability: 'Hair triggered', rapid, *not* sluggish Sensitivity: Especially to the momentary state of the organism Convergence: All sensory stimuli activate the same set of arousal subsystems, which, in turn, support each other Divergence: Activate cerebral cortex, autonomic nervous systems, and endocrine organs to initiate behavior Robustness: Does not fail. Survival of the organism depends on adequate CNS arousal

Table adapted from Quinkert *et al*. (2011).

Several lines of evidence exist that support this proposed primitive driving force of the brain: statistical, genetic, and mechanistic. Numerous behavioral experiments incorporating all three dimensions of the operational definition were analyzed using factor analysis; in these analyses, the most general, least specific factor, *i.e.*, generalized arousal, explained 30-45% of the variance in the data (Garey *et al.*, 2003). Insofar as generalized arousal is an inheritable trait, one can use the three dimensions of generalized arousal to breed for high and low arousal strains of mice, and the success of such an endeavor would also lend cre-

dence to the existence of generalized arousal (Weil, Zhang, Hornung, Blizard, & Pfaff, 2010).

While it has taken so long to write an operational definition, neuroanatomists have described the arousal circuits essential to driving and maintaining consciousness since the first half of the twentieth century. As maintaining arousal is necessary to the continued function of the organism, these neural circuits are widespread and redundant. This redundancy protects the arousal system from total failure; only bilateral focal damage to several of these pathways will induce prolonged unconsciousness.

The ascending arousal circuits that originate in the brainstem and project toward or into the forebrain have little capability of encoding specific stimuli, but form the basic drive that induces the cerebral cortex to action (see **Figure 1.3**). The descending arousal circuits, originating in the forebrain and projecting toward the brainstem and even to the spinal cord, prepare the body for action by influencing sensory excitability as well as activating autonomic nervous systems. More specifically, the locus coeruleus, part of the ascending arousal circuitry, is involved in emotional activation; it activates widespread, noradrenergic, mostly limbic, projections in response to emotionally salient stimuli (Aston-Jones, Rajkowski, Kubiak, Valentino, & Shipley, 1996). It also regulates circadian behavior patterns through an indirect afferent from the suprachiasmatic nucleus, the

primary circadian clock in mammals (Aston-Jones, Chen, & Yu, 2001). The serotonergic raphe nuclei project toward the forebrain, including cortical targets, and promote a quiet waking state associated with satiety, reduced appetitive behavior, and rhythmic behaviors such as grooming (Jones, 2003). The nucleus giganticellularis of the medullary reticular formation is unique in that it has both ascending and descending arousal-related projections. Additionally, this nucleus receives input regarding and responds to several sensory modalities, especially those that require immediate attention (Martin, Pavlides, & Pfaff, 2010). Through these connections, the nucleus giganticellularis is able to integrate salient arousing stimuli and coordinate signals sent to the forebrain, as well as to the spinal cord, in preparation for action (Pfaff, Martin, & Faber, 2012). These are short descriptions of only 4 of the interconnected circuits that control generalized arousal in the mammal brain.

This thesis will use the concept of generalized arousal and its operational definition to structure experiments using intact and brain injured mice and will test the effectiveness of DBS to increase generalized arousal. It is important to use generalized arousal to frame these experiments as it would be prohibitively difficult to develop a mouse model of a DOC and attempt to promote emergence to consciousness. Using the principles of generalized arousal, DBS can be studied

Figure 1.4 Incidence of Traumatic Brain Injury in the General Population and in the Military. Comparison of incidence rate of TBI in general and military populations (A). In the general population, comparison of incidence rate of TBI by sex (B) and cause of injury (C). In the military population, comparison of incidence rate of TBI by branch (D) and severity of injury (E). All graphs depict TBI incidence as a rate per 100,000 adults or active duty personnel. Data compiled from the CDC (2010), the Armed Forces Health Surveillance Center (2010), and Washington Headquarters Services: Directorate for Information Operations and Reports (2006).

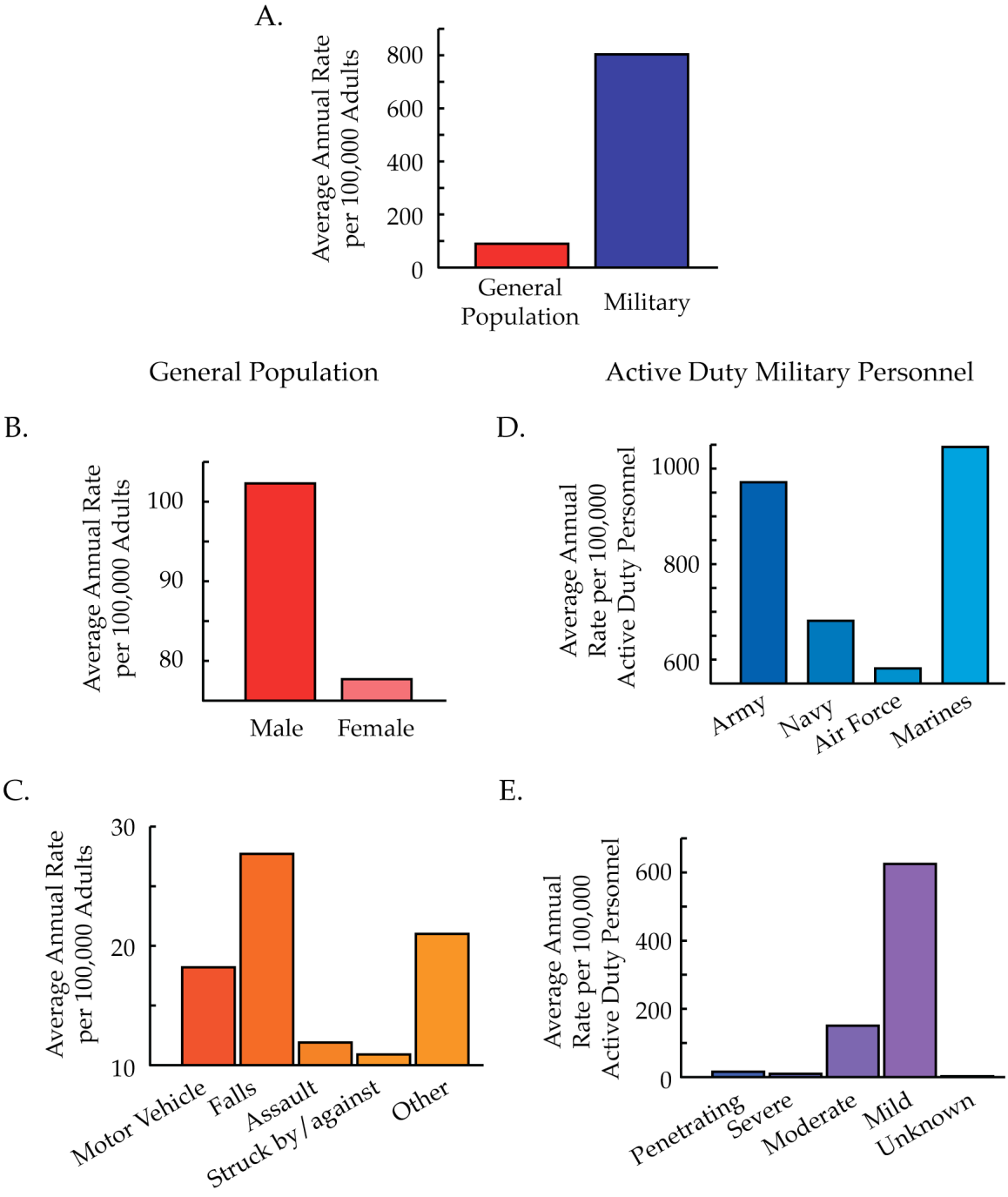
A.
Average Annual Rate per 100,000 Adults
800
600
400
200
0
General Population
Military
General Population
Active Duty Military Personnel
B.
Average Annual Rate per 100,000 Adults
100
90
80
Male
Female
D.
Average Annual Rate per 100,000 Active Duty Personnel
1000
800
600
Army
Navy
Air Force
Marines
C.
Average Annual Rate per 100,000 Adults
30
20
10
Motor Vehicle
Falls
Assault
Struck by/against
Other
E.
Average Annual Rate per 100,000 Active Duty Personnel
600
400
200
0
Penetrating
Severe
Moderate
Mild
Unknown

using brain-injured but conscious mice, and the conclusions of these experiments may then be applied clinically in DOC.

TRAUMATIC BRAIN INJURY

While many types of acquired brain injury may result in DOC, this thesis will focus on one type: traumatic brain injury (TBI). TBI is a common form of survivable brain injury attributable to rapid acceleration/deceleration or a blow to the head that can result, depending on severity, in a quickly healed concussion, sustained unconsciousness, or even brain death (Gaetz, 2004). An estimated 1.7 million TBIs occur in the US every year of which 52,000 patients die, 275,000 are hospitalized, and 1.4 million are treated and released from emergency departments. Additionally, TBI is a contributing factor of 30.5% of all injury-related deaths in the US (CDC, 2010). **Figure 1.4** summarizes the incidence of TBI from 2002-2006 in the general population and in the military (data compiled from the CDC, 2010; the Armed Forces Health Surveillance Center, 2010; and Washington Headquarters Services: Directorate for Information Operations and Reports, 2006). With the incidence of TBI so high, it is important to understand how TBI can affect the brain, and, importantly, how to ameliorate the consequences, both small and large.

Since TBI is such an important medical and societal concern, much research has been performed in the past 20 years into the pathology and mecha-

nisms of injury. The primary damage occurs in the moment of injury and can include lacerations of the scalp, fractures of the skull, surface contusions and lacerations of the brain, diffuse axonal injury, and intracranial hemorrhage (Graham, Adams, Nicoll, Maxwell, & Gennarelli, 1995). The secondary damage begins at the moment of injury, but does not manifest clinically until hours, days, or weeks later and can include damage due to increased intracranial pressure, ischemia, swelling, and infection (Graham, Adams, Nicoll, Maxwell, & Gennarelli, 1995). Since the recognition that these secondary processes are separate from the initial injury and the resolution of the medical community to avoid them if possible, there have been fewer fatalities after severe brain injury (Reilly, 2001). In addition to this knowledge of these injury processes, the medical community can also predict, to some extent, degree of neurological deficit based on degree of force that caused the initial injury as well as the extent of the primary brain damage. Lesser direct forces or acceleration/deceleration forces in a rostral/caudal orientation damage more restricted superficial areas of the brain and result in good recovery; on the other hand, larger direct forces or acceleration/deceleration forces in a lateral orientation damage more and deeper areas of the brain and can result in much more serious deficits and a higher likelihood of large-scale deafferentation and prolonged unconsciousness (Gaetz, 2004).

To test the effectiveness of various proposed treatments, animal models of TBI must be utilized. A host of animal models for TBI exist: controlled cortical impact, weight drop, fluid percussion, blast, diffuse, and many others (reviewed in Morales *et al.*, 2005). While each model has pros and cons, this thesis focuses on weight drop models because of their straightforward implementation, adjustability, and similarity to actual injury-causing phenomena. The weight drop model used in the following experiments is detailed in the next chapter. Briefly, an anesthetized mouse is placed under a weight suspended at a pre-selected height, and then the weight is dropped to impact the side of the skull. This is a basic protocol that utilizes an easily-constructed apparatus and is adjustable to fit many different animal species. The severity of the injury can also be adjusted by altering the mass of the weight and the drop height. The protocol itself closely parallels actual situations which result in TBI: whether the head strikes a surface or an object strikes the head, a hard surface and skull meet at medium-to-high velocity.

NEURAL CODING AND TEMPORAL PATTERNS

Assuming the mechanism of clinical action of DBS for MCS lies in substituting a missing input with an artificial one, the nature of the missing input needs to be determined before the artificial input can be logically designed. There are many theories as to the nature of neuronal input, or more precisely, the na-

ture of information transfer in neural systems. One hypothesis states that information can be encoded in the temporal patterns of neural spike trains (series of action potentials) and not strictly in a particular static parameter of those spikes (Wasserman, 1992; Kumar, Rotter, & Aertsen, 2010; Panzeri, Brunel, Logothetis, & Kayser, 2010).

A rich literature describes temporally-patterned neural responses, information theory analyses of temporally-patterned responses, physiological explanations for the presence (and possibly usage) of temporal patterns, and neural network models that utilize temporal patterns. Most descriptions of temporally-patterned neural responses come from various sensory systems; there are studies exploring temporal-pattern-sensitive neurons in visual (Mechler, Victor, Purpura, & Shapley, 1998; Reinagel & Reid, 2000), gustatory (Di Lorenzo, Leshchinskiy, Moroney, & Ozdoba, 2009; Glendinning, Davis, & Rai, 2006), olfactory (Laurent, Wehr, & Davidowitz, 1996; Lei, Christensen, & Hildebrand, 2004; Wehr & Laurent, 1999), auditory (Kozloski & Crawford, 2000; Malone, Scott, & Semple, 2010), tactile (Arabzadeh, Panzeri, & Diamond, 2006), and electro-sensing (Carlson, 2009) systems.

This thesis's current line of inquiry began with the observation of different robust temporal patterns resulting from different stimuli. Once these temporal patterns were observed, the question was posed: Are these temporal patterns

useful for transmitting information or do they represent noise around a meaningful average? One approach to answering this question is through the use of information theory. Informational theoretic analyses allow for calculation of the amount of information (generally in bits/second) transmitted by a neuronal signal, taking into account various parameters of that signal (Pfaff, 2006). In these analyses, more information is transmitted by the signal when temporal patterning of the signal is included; in some cases, the amount of information encompassed by temporal patterning is necessary for what the neuron or system does *in vivo* (Reinagel & Reid, 2000; Arabzadeh, Panzeri, & Diamond, 2006; Marsat & Pollack, 2005; Schnupp, Hall, Kokelaar, & Ahmed, 2006). Now that the idea of the importance of temporal patterning has taken hold, a growing body of evidence describes how receptors, neurons, and networks generate, and possibly use, temporal patterns (Sanchez, Gans, & Wenstrup, 2007; Williams & Stuart, 2000; Wu, Ma, & Kelly, 2004). In addition, neural network models of sensory systems emulate the complex characteristics of natural neural systems only when they include these temporal dynamics (Buonomano, 2000; Buonomano & Merzenich, 1995).

While most of the evidence for the usefulness of temporal patterns is indirect, a few groups use direct experimentation to reveal the response of a neural system to temporally-patterned input; two are listed here. First, Di Lorenzo *et al*.

(2009) used a conditioned aversion paradigm to test whether temporally-patterned stimulation of the nucleus tractus solitarius would elicit a taste perception with a particular quality. Using recordings from the nucleus tractus solitarius in behaving rats presented with quinine (a bitter tasting compound), the authors defined a temporal pattern of spike trains to simulate quinine. They found that conditioned aversion using their quinine-simulating temporal pattern generalized specifically to bitter taste stimuli. Additionally, conditioned aversion using randomized temporal patterns generalized to more than just bitter taste stimuli. They concluded that their subjects perceive a bitter taste when stimulated with their quinine-simulating temporal pattern. The second example, from Kimmel and Moore (2007), concluded that the frontal eye field in nonhuman primates is sensitive to temporal pattern of input in signaling saccadic eye movement (rapid voluntary movement). They found that an accelerating temporal pattern is most efficient at eliciting saccades; this temporal pattern was better than either a decelerating temporal pattern or a fixed interpulse interval pattern. In addition to these three temporal patterns (all with the same mean interpulse interval), the authors also used randomized temporal patterns; the random temporal patterns found to elicit saccades were, on average, accelerating, and those that were not found to elicit saccades were generally decelerating.

If temporal patterns can carry information, temporally-patterned DBS might be more effective for increasing arousal versus conventional fixed frequency stimulation. In fact, it has already been hypothesized that arousal systems depend on a specific mathematics of temporal patterning, nonlinear dynamics (Pfaff & Banavar, 2007), to ensure lability. A nonlinear dynamic (or chaotic) arousal system would have the advantage of being able to quickly amplify the smallest of perturbations, hypothetically resulting in a fast response to salient arousing stimuli. Additionally, various biological phenomena have been shown to take advantage of the benefits of several nonlinear dynamic equations (Cohen, 1995).

This thesis will explore the utility of temporally-pattered DBS by utilizing temporal patterns generated by one of two methods. Under the assumption that nonlinear dynamics are important to controlling arousal systems, a simple deterministic chaotic map, the logistic equation, was chosen to produce temporal patterns to use in DBS to increase generalized arousal. Additionally, a temporally-patterned control was included in some experiments. Since the logistic equation is deterministic, a true random number generator that is internally independent was chosen.

SUMMARY

This thesis will show that temporally-patterned deep brain stimulation (DBS) can modulate the increase of generalized arousal in intact mice and in a mouse model of traumatic brain injury (TBI). Importantly, this thesis will elucidate the likely benefits of temporally-patterned DBS and may lead to new practices in its clinical use. Chapter 2 will detail the methodology of all experiments. In Chapter 3, the effect of temporal pattern on DBS will be explored in hippocampal DBS of intact mice (these data published in Quinkert, Schiff, & Pfaff, 2010). Next in Chapter 4, central thalamic DBS (CT/DBS) will be explored first using 3 amplitudes, 4 frequencies, and standard temporal patterns, and then with the best amplitude/frequency pair and 3 temporal patterns (these data published in Quinkert & Pfaff, 2012). Chapter 5 will introduce a mouse model of TBI, and the response to temporally-patterned DBS in this model will be observed. In Chapter 6, olfactory responsiveness in intact and TBI mice, with and without DBS will be examined. Olfactory responsiveness was chosen to incorporate another dimension of the operational definition of generalized arousal into this thesis. Finally in Chapter 7, the overall results of this thesis, some caveats, and potential implications for clinical DBS will be discussed.

Chapter 2: Methods

ANIMALS

All experiments used male and female C57BL/6J mice, 6-9 weeks of age. During all experiments, mice were singly-housed on a reversed 12:12 hour light/dark cycle with lights on at 6 pm, with food and water available *ad libitum*. In stimulation experiments, mice were implanted bilaterally with monopolar electrodes (PlasticsOne) in the central thalamus (anterior/posterior: -1.70 mm, lateral: +/- 1.00 mm, depth: -3.00 mm, angle: 10° from vertical, coordinates relative to bregma) except where specified with ground wires placed on the surface of the skull near the burr holes. Some mice were also implanted with a subcutaneous transmitter (Data Sciences International) capable of transmitting single channel electroencephalogram (EEG). All surgical and injury procedures were done under ketamine/xylazine anesthesia (80/12 mg/kg, *i.p.*); analgesia (flunazine 5 mg/kg, *s.c.*) was given twice daily for 2 days after all survival surgeries as well as injury. All animal procedures were approved by the Rockefeller Institutional Animal Care and Use Committee.

STIMULATION CHARACTERISTICS

General Parameters

All stimulation was done using a four channel programmable stimulus generator (Multi Channel Systems). Stimulation consisted of symmetric biphasic

(negative phase first) square wave pulses with a total pulse width of 200 μs. Stimulation was always constant current, and amplitude of stimulation ranged from 75-150 μA. Frequency of stimulation ranged from 50-225 hz. Stimulation epochs were either 10 minutes of continous stimulation every 3-4 hours over the course of 1-3 days or 10 seconds of continuous stimulation spaced randomly (but not shorter than 1 hour apart) over the course of 4-5 days.

Temporal Patterns

Temporal patterns used in experiments are listed in **Table 2.1** and plotted as histograms in **Figure 2.1**. Two methods of generating temporal patterns were chosen to compare to conventional fixed frequency. One pattern generation method, based on the logistic equation, was chosen subsequent to our hypothesis that nonlinear dynamics may be important in the control of CNS arousal systems (Pfaff and Banavar, 2007). The second pattern generation method, based on a true random number generator, was chosen as a patterned control; based on independent true random numbers, the random temporal pattern was used to give perspective on the internally structured chaotic temporal pattern.

The generation of alternative temporal patterns is described as follows. The logistic equation, $X_n = R\, X_{n-1}\, (1 - X_{n-1})$, where X is the output at time n, has a constant modifier, R, that creates chaotic output at certain values. Output of the logistic equation was calculated to two or three thousand iterations with initial

Table 2.1 Temporal Patterns of Stimulation. Lists of interpulse intervals (μsec) for each temporal pattern used.

Nonlinear1	Nonlinear2	Chaotic	Random
11 660	32 260	12 900	7 300
29 780	3 440	1 380	4 460
13 840	12 000	4 800	14 180
31 880	29 860	11 940	8 820
7 100	11 580	4 640	12 940
21 880	29 400	11 760	12 960
30 120	13 020	5 200	11 300
12 840	30 840	12 340	2 320
31 060	8 420	3 360	9 880
9 880	24 500	9 800	9 480
	24 940	9 980	11 200
	24 080	9 640	1 520
	25 700	10 280	7 240
	22 560	9 020	6 220
	28 120	11 240	2 560
	16 620	6 640	11 200
	32 320	12 920	13 660
	3 160	1 260	7 800
	11 120	4 440	9 080
	28 840	11 540	8 620
	14 660	5 860	3 160
	31 900	12 760	1 700
	4 720	1 880	14 300
	15 800	6 320	1 800
	32 260	12 900	10 280
	3 400	1 360	10 600
	11 920	4 760	3 760
	29 780	11 920	10 220
	11 820	4 720	3 820
	29 660	11 860	7 020
	12 200	4 880	4 240
	30 080	12 040	13 140
	10 880	4 360	14 400
	28 520	11 400	5 860
	15 560	6 220	4 440
	32 200	12 880	5 540
	3 600	1 440	6 000
	12 520	5 000	5 620
	30 380	12 160	8 920
	9 900	3 960	11 600
	27 080	10 840	13 240
	19 340	7 740	3 600
	31 440	12 580	7 520
	6 360	2 540	13 580
	20 060	8 020	5 380
	30 900	12 360	10 200
	8 180	3 280	5 660
	24 020	9 600	11 000
	25 820	10 320	5 360
	22 300	8 920	5 240

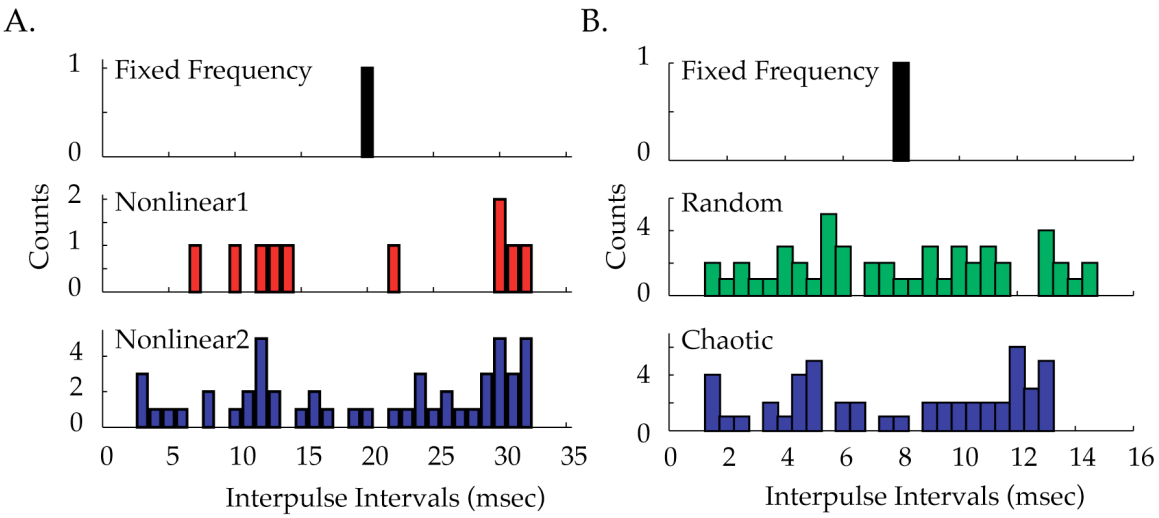

Figure 2.1 Histograms of Temporal Patterns of Stimulation. Histograms of interpulse intervals that make up each temporal pattern used in this thesis. Temporal patterns of stimulation for Chapter 3 (A), and Chapters 4 and 5 (B).

conditions to ensure chaotic behavior of the equation (R = 3.90 and X_0 = 0.2). The true random number generator used to generate temporal patterns takes atmospheric noise measurements to generate three thousand uniformly distributed numbers (Haar, 1998). To ensure that depolarization block did not occur, a minimum interpulse interval (IPI) was defined as 0.3 ms, and chaotic and random sequences were scaled to meet that minimum. For both sequences of numbers, a consecutive set of numbers was found such that the number of elements in the set divided by the sum of the scaled output equaled the desired average frequency. In this manner, four temporal patterns were defined: 1) 10 pulses from the logistic equation output, named 'Nonlinear1,' 2) 50 pulses from the logistic

equation output, named 'Nonlinear2,' 3) 50 pulses from the logistic equation output, named 'Chaotic,' and 4) 50 pulses from the true random number generator output, named 'Random.' To ensure the only difference in a mouse's response to stimulation was the temporal patterning of pulses, all patterns in a single experiment were identical with respect to pulse shape, pulse duration, amplitude, average frequency, and stimulation duration.

TRAUMATIC BRAIN INJURY MODELS

In choosing a traumatic brain injury (TBI) model, two factors were considered essential: 1) that the model result in a closed head injury and 2) that the model produce long-lasting deficits, long enough to ensure deficits after implantation surgery and recovery. Weight drop models were chosen because they fit the first criterion and because of their similarity to real injury causing phenomena; several were tested. Of the injury models tested, only one met the length of deficit criteria, multiple TBI (**Figure 2.2**). Multiple TBI uses a small pointed 20 g weight with a point diameter of 3 mm dropped from a height of 25 cm on the right side of a mouse's skull.

A Neurological Severity Screen (NSS) was adpated from Flierl *et al.* (2009) as a general indication of severity of injury and neurological deficit (**Figure 2.3**). This neurological screen is different from the screen developed by Arrieta-Cruz (2007). Arrieta-Cruz's neurological test included 28 tests each with possible

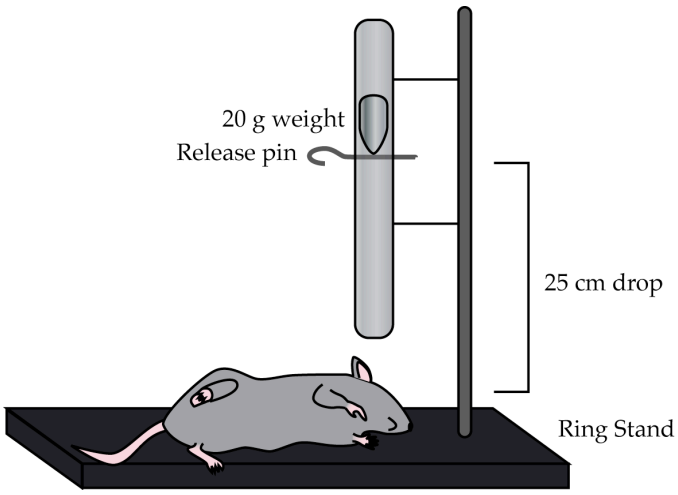

Figure 2.2 Diagram of Multiple TBI apparatus. A 20 g weight with a 3 mm diameter point is suspended 25 cm over the head of an anesthetized mouse. By pulling the release pin, the weight is dropped on the right side of the mouse's skull. The release pin is replaced, the weight reloaded, and additional drops are performed as necessary.

scores from 0-4; higher scores resulting from greater functionality and lower scores resulting from neurological injury. The NSS used here is slimmed down to only 10 tests that have binary scoring. Since the purpose of the NSS was not to fully characterize the neurological ability of the mice, and only to give some indication of severity of injury, the NSS was chosen for its speed, simplicity, and scoring system. Tests in the NSS are described in **Table 2.2** and detailed here. Two hours after injury, mice were placed in a circular open maze with a single small exit (**Figure 2.3.A**), and four tests were scored: 1) ability to exit circle within

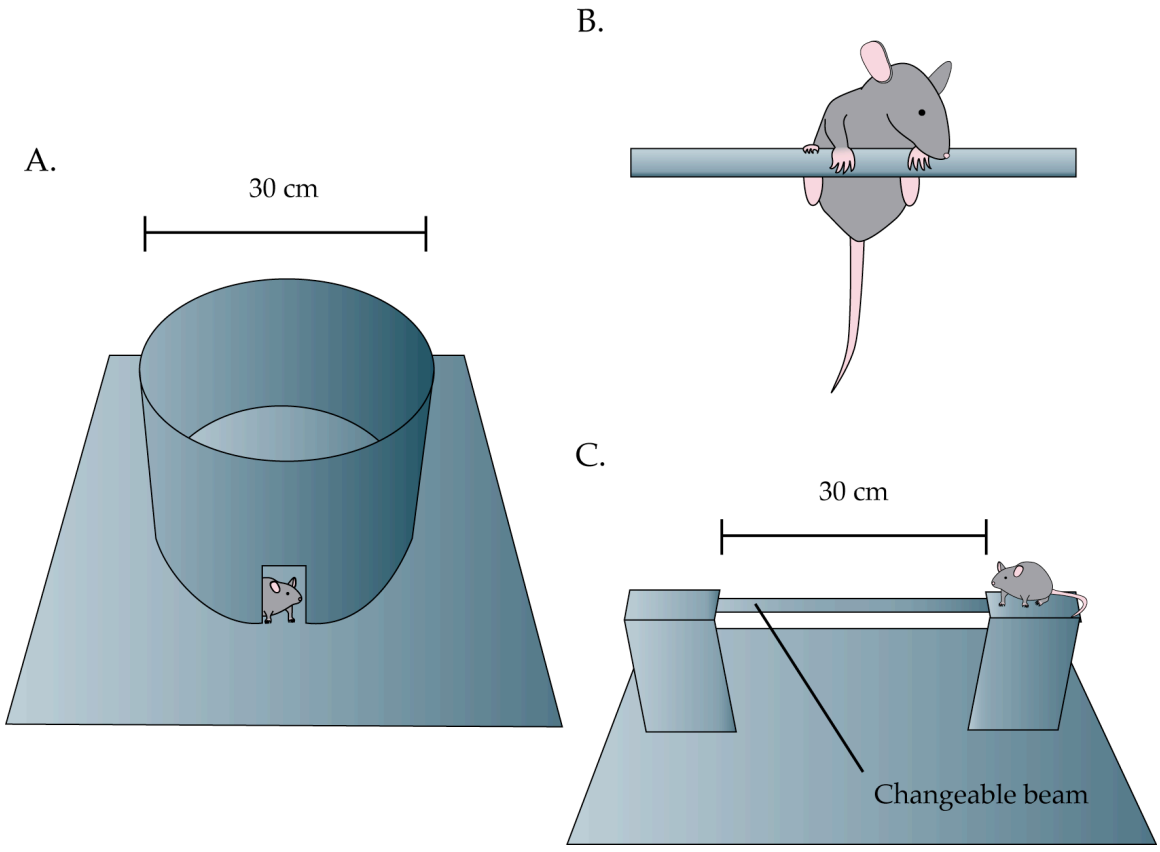

Figure 2.3 Diagrams of Neurological Severity Screen Tests. Circular open maze of 30 cm diameter (A). Mice must exit the maze within 3 minutes to pass this test. Mice are also observed in this maze for normal ambulation and spontaneous seeking behavior. An acoustic startle response is also tested. Illustration of a perching mouse (B). For balancing tests on both square and round rods, mice must attain this position and sustain it for 10 seconds to pass. Platform for functional walking tests (C). Mice must walk from one platform to the other over 3 cm, 2 cm, and 1 cm wide beams of 30 cm in length.

Table 2.2 Neurological Severity Screen Tests

Neurological Tests (in the order of performance)
Exit from 30 cm circle within 3 minutes
Straight walk
Startle reflex
Seeking behavior
Hind limb flex
Flat beam balance for 10 seconds
Round beam balance for 10 seconds
3 cm beam walk within 3 minutes
2 cm beam walk within 3 minutes
1 cm beam walk within 3 minutes

NSS tests are scored pass (0, normal behavior) or fail (1, abnormal behavior). The overall score is a sum of each test resulting in a score of 0 (normal) to 10 (high severity of injury).

three minutes, 2) ability to walk straight, 3) presence of acoustic startle (freezing or flinching in response to a sudden loud clap), and 4) spontaneous investigation of environment (seeking behavior). The mouse was then picked up by the tail and the reflexive hind limb flex was scored. The more difficult function tasks followed. Mice were placed on flat and round beams (0.5 cm width or diameter) and scored on their ability to perch on the beams (all four feet touching the beam) for at least 10 seconds (**Figure 2.3.B**). Finally, mice were placed on a simple platform with 3 cm, 2 cm, and 1 cm wide beams, each 30 cm long, and tested on whether they were able to walk across to get to another platform (**Figure 2.3.C**). Each test is scored pass-fail: failing receives a score of 1, succeding a score of 0. For each mouse, scores for all 10 tests are summed to produce an overall score; normal mice receive an overall score of 0 and the most severely injured mice receive an overall score of 10. All injured mice underwent NSS two hours post-injury.

DATA COLLECTION AND ANALYSIS BY CHAPTER

Chapter 3: Intact DBS of the Hippocampus

Mice were implanted in the hippocampus (n=19) and the central thalamus (n=3) as a control and then stimulated for 10 minutes every 3 hours only during the dark up to 12 times over the course of 3 days and were challenged with at least two of three temporal patterns (Fixed - FF, Nonlinear1 - NL1, Nonlinear2 -

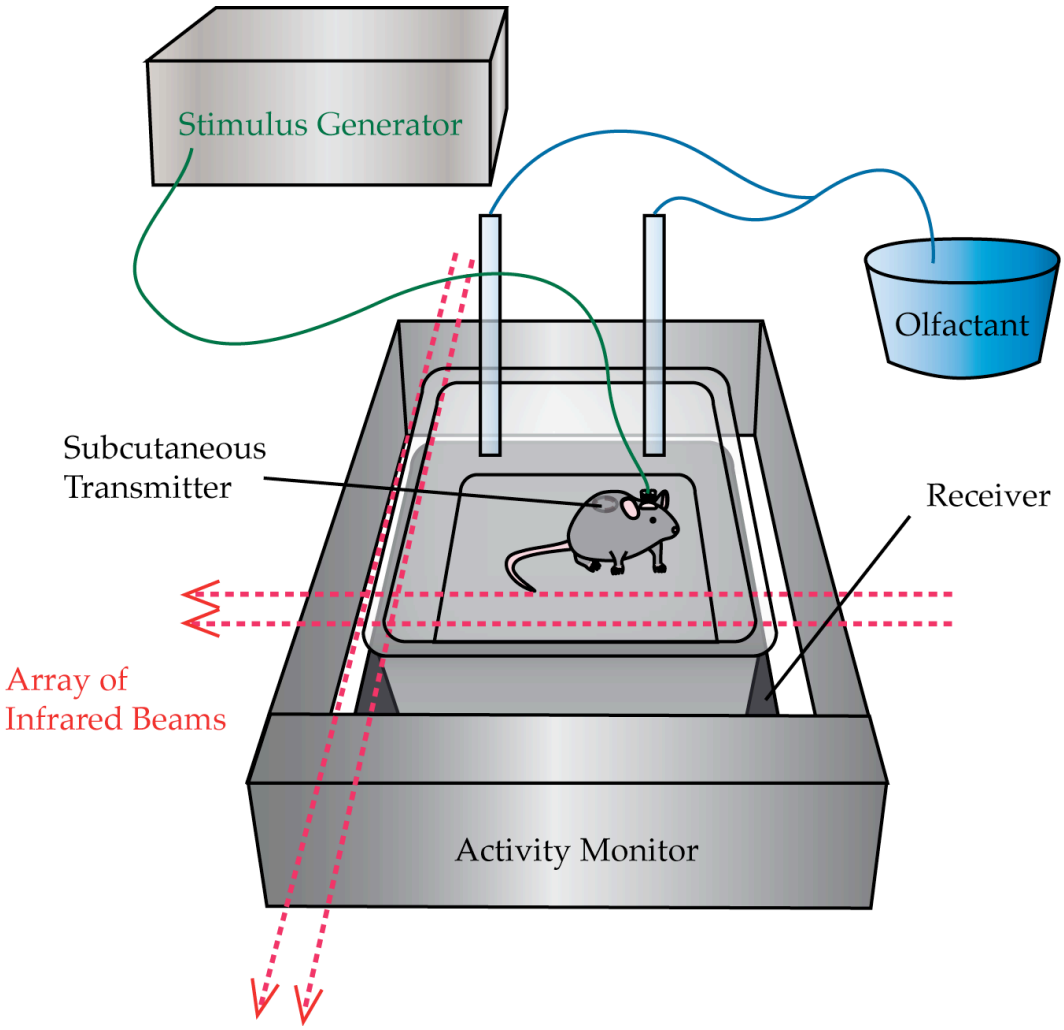

Figure 2.4 Diagram of basic data collection set up. All chapters utilize stimulus generator to deliver DBS and home cage activity monitor to monitor motor activity. Work described in Chapters 3 and 4 utilized the subcutaneous transmitter and receiver located under the cage to record single channel electroencephalogram (EEG). Work described in Chapter 6 utilized the olfactant delivery system which operates a compressed air valve to present the mouse with an odorant.

NL2). To account for possible order effects, DBS temporal patterns were counterbalanced for order in each mouse and between mice as much as possible. More specifically, for four epochs of stimulation in one day, an example of the order of stimulation a mouse would see is as follows: FF, NL1, NL1, FF. And for every mouse that started a given day with FF stimulation, another mouse started the day with NL1 stimulation.

Figure 2.4 shows a comprehensive diagram of the data collection setup used. Prior to the start of data collection, mice were plugged into the stimulus generator (Multichannel Systems). EEG was measured and collected by the DSI telemetry system, and home cage activity data were collected by a 3D infrared monitor (Accuscan Instruments). The three behavioral measures observed included whole body activity ("Activity Counts" or "Counts"), collected by the DSI transmitter and representing changes in field strength between the transmitter and receiver as the mouse moves; fidgeting movements ("Horizontal Activity" or "Hactv"), collected by the home cage Accuscan system and representing the number of infrared beams broken in the horizontal plane; and ambulation ("Total Distance" or "Totdist"), collected by the home cage Accuscan system and representing non-repeating beam breaks in the horizontal plane. These data measures were recorded as the sum of activity for 10 minutes prior to stimulation, 10 minutes during stimulation, and 10 minutes after stimulation. In addition, EEG spec-

tra were estimated for minute long recordings, 10 minutes before and 10 minutes after stimulation, using MATLAB's multitaper method, and spectral power was integrated from the following frequency bins: delta (0.5 - 4 hz), theta (4.5 - 8 hz), alpha (8.5 - 12 hz), beta (12.5 - 20 hz), and gamma (35 - 45 hz). These EEG waves were then reported as relative power, *i.e.,* the percent of power in each bin to the sum of the power in all five bins. Relative power of these frequency bins was not calculated during stimulation to avoid the confounding effects of stimulation artifacts. All data were normalized and recorded as the percent of measurements before stimulation.

To guarantee that our main conclusion did not depend on the exact nature of the statistics used, both standard parametric statistics as well as non-parametric statistics were performed. To test for DBS and temporal pattern effects, two-way ANOVA and, to confirm, non-parametric Friedman analyses were performed. For more detailed post-hoc analysis, t-tests with Bonferroni corrections and, to confirm, non-parametric Wilcoxon matched-pairs signed ranks tests were used. All inferences of significance utilized a minimum requirement of $p<0.05$. In addition to the statistics reported in Chapter 3, data were also systematically compared with respect to pulse amplitude, and this comparison yielded no significant results that might have influenced the results.

Chapter 4: Intact DBS of the Central Thalamus

Parametric Experiment

In this experiment, mice (n=10) were stimulated for 10 minutes for a maximum of 24 stimulations over the course of three days. To space stimulations evenly over the course of the study, stimulation epochs occurred every three hours. Three amplitudes (75, 100, and 125 μA) and four frequencies (50, 125, 175, and 225 hz) were tested. While amplitude was increased systematically over the three days in all mice, frequency was counterbalanced for order.

Temporal Pattern Experiment

Based on the motor activity data from the parametric experiment, the parameters of 125 hz and 100 μA were chosen for this temporal pattern experiment. In addition to our optimized fixed frequency pattern, two temporal patterns were chosen: Random and Chaotic. Mice (n=16) were stimulated for 10 minutes for a total of six stimulations over the course of one day. To space stimulations evenly over the course of that day, stimulation epochs occurred every four hours. Each mouse was challenged with all three temporal patterns, counterbalanced for order.

Data Collection and Statistical Analyses

Figure 2.4 shows a comprehensive diagram of the data collection setup used. During the course of each study, one channel EEG and three behavioral

data measures were collected. Two data collection systems were utilized; a 3D infrared beam home cage activity monitor (Accuscan Instruments) was used to collect motor activity data, and an implantable transmitter telemetry system (Data Sciences International or DSI) was used to collect EEG as well as motor activity data. The three behavioral measures observed included: 1) counts, 2) horizontal activity, and 3) total distance. EEG, collected by the DSI system, was divided into minute long epochs and its power spectra were estimated using the multitaper method. EEG waves were integrated over the following frequency bins: delta (0.5-4 hz), theta (4.5-8 hz), alpha (8.5-12 hz), beta (12.5-20 hz), and gamma (35-45 hz). EEG data are reported as the relative power of each frequency bin to the summed power in all five frequency bins. Data were reported for 10 minutes before, 10 minutes during (only for behavioral measures), and 10 minutes after each stimulation. Data collected during and after stimulation were normalized to data collected directly before stimulation. Because motor activity and EEG inherently change over the course of the light dark cycle, analyses were restricted to the half hour surrounding stimulation to avoid the intrinsic fluctuations of the outcome measures.

For statistical evaluation, each data measure was analyzed by multiple factor ANOVA and post-hoc two-tailed t-tests with Bonferroni corrections for multiple comparisons. Multiple factor ANOVA is a common method for deter-

mining the relative effects of multiple independent variables as well as their interactions on a single outcome measure. The factors included in our analyses were stimulation, stimulation parameters (amplitude and frequency in the Parametric experiment, temporal pattern in the Temporal pattern experiment), phase of the light/dark cycle, as well as any interactions between these factors. Since no significant interactions were found, these analyses were not included in the following for discussion. Despite obvious strong differences where the standard error of the means did not overlap, several post-hoc comparisons were not significant with Bonferroni-corrected t-tests. Even though these Bonferroni corrections were very conservative, we included them during our interpretation of the results.

Extensive analyses of data from both experiments were done to determine if any sex differences in response to stimulation exist. All differences found were small and inconsistent across data measures and between the two data sets; therefore, data presented in Chapter 4 are pooled from males and females.

Chapter 5: Multiple TBI and DBS

For injury experiments, mice were placed into a 3D home cage monitor (Accuscan Instruments) one week prior to injury, and home cage motor activity data were collected from this point until the end of the experiments. To determine rate of recovery, one set of mice (n=12) were left alone and observed 14

days post-injury. A second set of mice (n=14) were implanted bilaterally in the central thalamus two days post-injury and allowed to recover from surgery for an additional 4-6 days. After recovery, these mice were stimulated for 10 minutes every 4 hours over the course of one day.

Figure 2.4 shows a comprehensive diagram of the data collection setup used. During each study, two behavioral measures were collected: horizontal activity and total distance. To determine motor activity deficits, daily activity (sum over 24 hours) was calculated, normalized to average baseline activity, grouped by baseline, post-injury, or post-surgery (only stimulated mice), and averaged across mice. To determine any effects on circadian behavior, activity was summed over 12 hours, normalized to average total daily baseline activity, grouped by baseline, post-injury, or post-surgery (only stimulated mice), and averaged across mice. For analyses on the effects of stimulation, activity data directly surrounding the stimulation (10 minutes before, 10 minutes during, and 10 minutes after stimulation) were analyzed.

Both parametric and non-parametric statistical tests were used to avoid the bias inherent in the assumptions of parametric tests. Multiple factor ANOVA was used in addition to Friedman and Kruskal Wallis tests to analyze the effects of injury and surgery on daily motor activity as well as the effects of CT/DBS, light phase, and temporal pattern of stimulation on motor activity in the small

time frame analyzed. Post-hoc analyses were done using t-tests, Wilcoxon matched-pair signed ranks test, and Mann Whitney U tests as appropriate. As always, only p-values of 0.05 or less were considered significant.

Chapter 6: Sensory Responsiveness

Simultaneous Stimulus Delivery

During the first of two olfactory responsiveness experiments, intact (n=8) and multiple TBI (n=7) mice were placed in isolation boxes to reduce exposure to unintended external stimuli. During the experiment, mice were exposed to three experimental conditions: 1) a 10 second air puff containing benzaldehyde, an odorant that is known to strongly stimulate mitral cell activity in the olfactory bulb without a trigeminal component and smells like almonds, 2) a 10 second DBS epoch of 125 hz (fixed frequency) and 150 μA, and 3) 10 seconds of simultaneous olfactant air puff and DBS. The stimulus delivery system (Habitest system by Coulbourn Instruments) was programmed to wait for a 1 minute epoch of quiesence from the mouse and then to randomly deliver one of the three experimental conditions. A wait of random length between 60-120 minutes was programmed to occur between each stimulation. Data collection was automatically stopped after 20 trials of each experimental condition. **Figure 2.4** shows a comprehensive diagram of the data collection setup used.

Olfactory Stimulation Delayed after DBS

In the second olfactory responsiveness experiment, intact mice (n=7) were placed in isolation boxes to reduce exposure to unintended external stimuli. During the experiment, mice were exposed to an olfactory stimulus delayed after DBS. The stimulus delivery system was programmed to wait for a 1 minute epoch of quiescence from the mouse and then to randomly deliver 10 seconds of DBS (fixed frequency, 125 hz, 150 μA) or no stimulus. One minute later, an olfactory stimulus (benzaldehyde) was programmed to be delivered. A wait of random length between 60-120 minutes occurred between each experimental set. Data collection was automatically stopped after 20 trials of each experimental condition.

Statistical Analyses

Data collected by the stimulus delivery system characterized the status of the mouse as active or inactive. Raster plots of activity were generated for the time surrounding each experimental trial, and activity was averaged across trials for each experimental condition. Control data were collected by finding 1 minute epochs of inactivity during times in which no stimuluation occurred. Control data were averaged by randomly selecting 20 trials, averaging, and repeating this random selection 100 times to generate an average activity surrounding a 1 minute wait period. Averaged activity of all experimental conditons and control were

integrated over 10 seconds to smooth data before statistical analysis. These analyses included both parametric ANOVA and post-hoc t-tests as well as appropriate non-parametric tests (Friedman, Wilcoxon matched-pair signed-ranks, and Mann Whitney U tests). As always, a p-value of 0.05 or less was considered statistically significant for all tests.

BRAIN TISSUE PROCESSING

At the end of all behavioral studies, mice were euthanized following deep anesthesia, and their brains were dissected and freshly frozen. Fresh frozen brain tissue was sliced on a cryostat at 30 μm. To histologically confirm electrode placement, brain tissue slices from all stimulated mice were processed using an aceytlcholinesterase stain. All stimulated mice included in statistcal analyses were confirmed to have, at minimum, a unilateral hit in the brain region specified.

Chapter 3: Intact DBS in the Hippocampus

BEHAVIOR

Electrical Stimulation both in the hippocampus and the medial thalamus increased arousal-related motor activity as measured by fidgeting movements ("Horizontal Activity"), ambulation ("Total Distance"), and an independent measure of whole body movement ("Activity Counts"). However, the measured activity increases specifically depended on the temporal pattern within the pulse train of stimulation delivered to both structures, with different temporal patterns of pulses increasing activity during stimulation of hippocampus or medial thalamus. Moreover, specific temporal patterns of pulses showed differentiable patterns of effects across measured behavioral variables.

Hippocampal DBS

The temporal pattern of electrical pulses affected the magnitude of the behavioral result in several ways. With respect to activity counts, two-way ANOVA confirmed an effect of DBS ($F_{2,833} = 16.96$, $p<0.001$) and that responses to temporal pattern were significantly different ($F_{2,833} = 9.56$, $p<0.001$); see **Figure 3.1.A**. DBS also increased horizontal activity ($F_{2,323} = 24.23$, $p<0.001$) as well as total distance ($F_{2,316} = 14.43$, $p<0.001$). Temporal pattern of stimulation also significantly affected horizontal activity response ($F_{2,323} = 5.59$, $p<0.01$); see **Figure 3.1.B**.

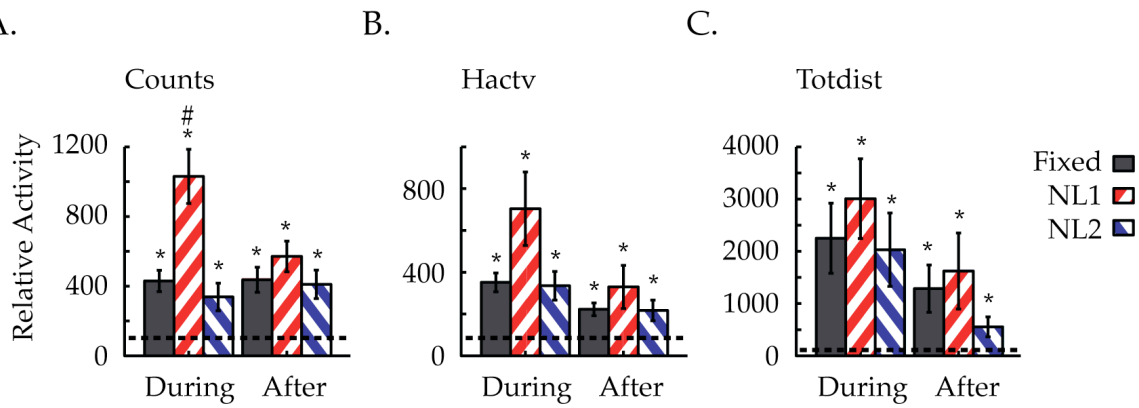

Figure 3.1 Hippocampal DBS: Behavior. Behavioral response to hippocampal DBS. Behavioral measures shown are: activity counts, "Counts" (A), horizontal activity, "Hactv" (B), and total distance, "Totdist" (C). Panels include 10 minutes of data during and 10 minutes of data after CT/DBS, all normalized to before stimulation. Data are presented as mean ± s.e.m. *p<0.05 compared to before; # p<0.05 compared to FF and NL2.

In general all three temporal patterns increased behavioral response to hippocampal DBS in all three behavioral measurements. As seen in Figure 3.1.A, FF (during: $t_{128} = 5.39$, $p<0.001$; after: $t_{132} = 4.68$, $p<0.001$), NL1 (during: $t_{49} = 5.97$, $p<0.001$; after: $t_{51} = 5.32$, $p<0.001$), and NL2 (during: $t_{77} = 2.99$, $p<0.01$; after: $t_{80} = 3.79$, $p<0.001$) increased activity counts during and after stimulation compared to before stimulation. Horizontal activity response to stimulation increased during and after FF stimulation (during: $t_{55} = 5.61$, $p<0.001$; after: $t_{55} = 4.03$, $p<0.001$),

during and after NL1 stimulation (during: $t_{26} = 3.43$, $p<0.01$; after: $t_{27} = 2.22$, $p<0.05$), and during and after NL2 stimulation (during: $t_{25} = 3.43$, $p<0.01$; after: $t_{27} = 2.01$, $p<0.05$); see **Figure 3.1.B**. As seen in **Figure 3.1.C**, total distance response to stimulation was also increased during and after FF stimulation (during: $t_{50} = 3.20$, $p<0.01$; after: $t_{54} = 2.62$, $p<0.05$), during and after NL1 stimulation (during: $t_{23} = 3.80$, $p<0.001$; after: $t_{26} = 2.36$, $p<0.05$), and during and after NL2 stimulation (during: $t_{26} = 2.75$, $p<0.05$; after: $t_{27} = 2.37$, $p<0.05$). It is clear that all three temporal patterns of stimulation in the hippocampus increased arousal-related motor activity in all three of the observed behavioral measures.

The magnitude of increase in behavior during and after stimulation depended on the temporal pattern of stimulation. While generally NL1 hippocampal stimulation increased behavior better than either FF or NL2 stimulation, only in one behavioral measure were these differences statistically significant. With regard to whole body movement (see **Figure 3.1.A**), NL1 stimulation increased activity counts during DBS greater than either FF ($t_{65} = -3.59$, $p<0.01$) or NL2 stimulation ($t_{75} = 3.96$, $p<0.01$). In short, temporal pattern of hippocampal stimulation affected the resulting behavioral increase; NL1 stimulation of the hippocampus increased arousal-related activity more than either other pattern.

Figure 3.2 Hippocampal DBS: behavior at high temporal resolution of one illustrative mouse. Motor activity behavior of one mouse at 3 temporal patterns of hippocampal DBS: A. Fixed Frequency (FF), B. Nonlinear1 (NL1), and C. Nonlinear2 (NL2). Activity counts ('counts') shown at 1 sample every 10 seconds, Horizontal activity ('Hactv') and Total distance ('Totdist') shown at 1 sample every 1 second. Grey boxes mark epochs of stimulation.

A.

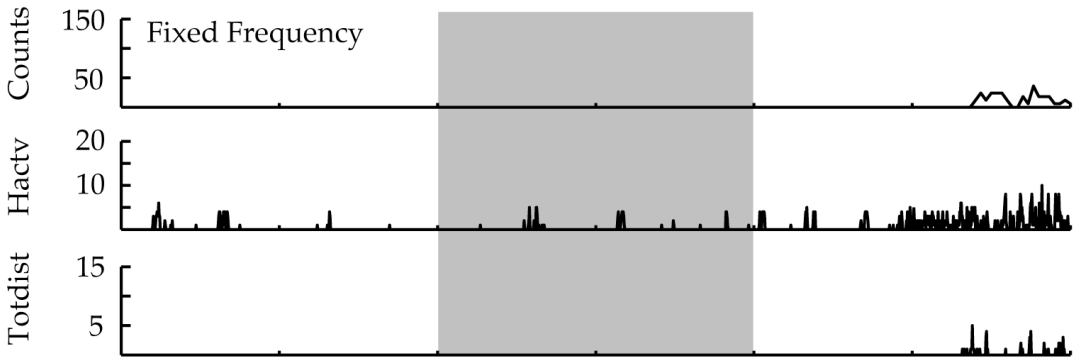
Fixed Frequency
Counts
150
50
Hactv
20
10
Totdist
15
5

B.

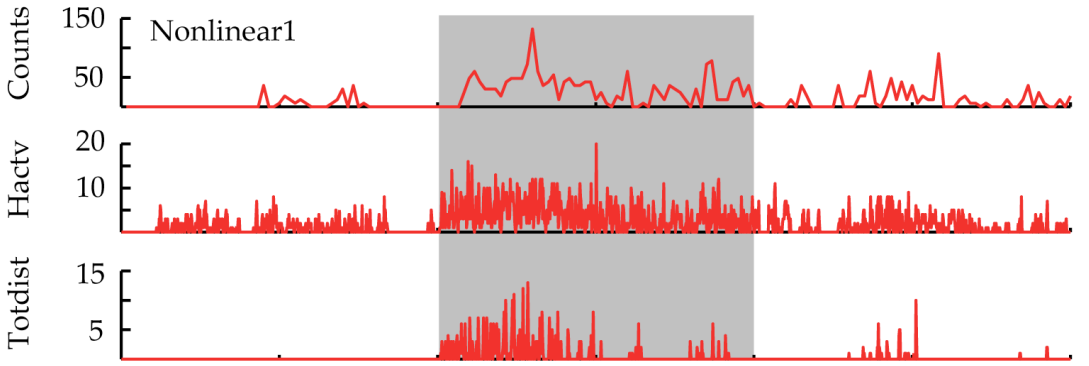
Nonlinear1
Counts
150
50
Hactv
20
10
Totdist
15
5

C.

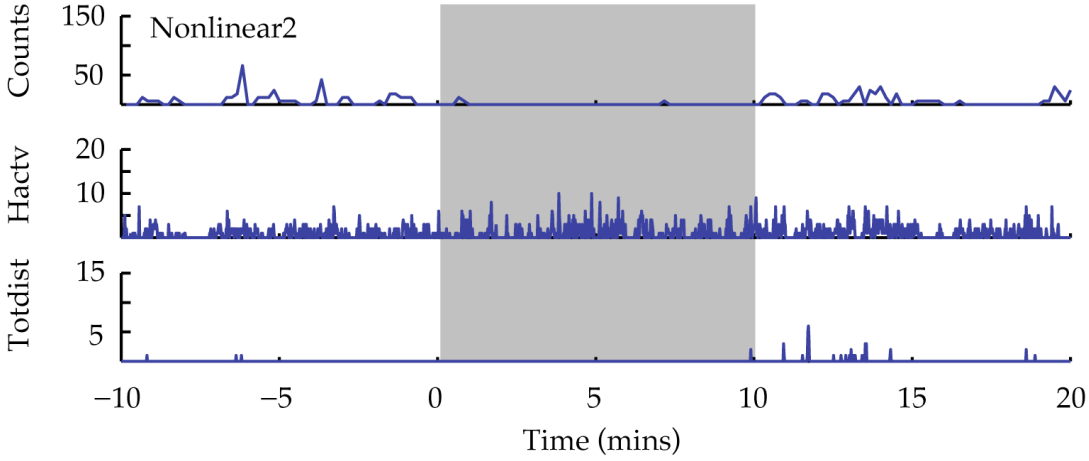
Nonlinear2
Counts
150
50
Hactv
20
10
Totdist
15
5
−10
−5
0
5
10
15
20
Time (mins)

Behavioral Description of One Illustrative Mouse

In addition to quantitative behavioral measurement, infrared cameras were used to videotape behavior of some mice during the course of the study for qualitative behavioral measurement. An ethological description of the behavior of one exemplary mouse is recorded here with its corresponding quantitative measurement shown in **Figure 3.2**.

In the ten minutes before FF hippocampal stimulation, the mouse sat in one corner of her cage, occasionally moving her head or scratching her ear, but spending most of the time sitting still. During FF stimulation, she continued to sit in one corner and did not move from this spot, but did spend slightly more time moving her head or scratching than before stimulation. After FF stimulation, she sat in her corner and moved only occasionally for the first six minutes. After that, she moved from her spot and walked along the edges of the cage; see **Figure 3.2.A** for quantitative measures of this stimulation.

Before NL1 stimulation, the mouse was sitting in the corner eating and occasionally drinking. She groomed occasionally, reared once, and pivoted in a circle in her corner once. During NL1 stimulation, the mouse walked quickly around the edges of her cage several times, stopping at the corners and the water spout to drink. After NL1 stimulation, the mouse again sat in one corner, but occasionally ventured to other corners as well as to the water spout. She did not

walk as much as during stimulation, but continued to move, drink, and eat while sitting; see **Figure 3.2.B** for quantitative measures of this stimulation.

Before NL2 stimulation, the mouse sat in one corner of the cage, moved her head often, took one to two steps away from her corner and returning, and pivoted in a circle 1-2 times. During NL2 stimulation, the mouse continued to sit in her corner and move, but did not walk around. She pivoted in a circle and moved her head to eat, but she did not walk away from her corner. After NL2 stimulation, she sat in her corner eating, and once walked only as far as the water spout before returning to the corner; see **Figure 3.2.C** for quantitative measures of this stimulation. As seen in **Figure 3.2** and from the above description, this mouse's behavioral activity dramatically increased during NL1 stimulation, but not during FF or NL2 stimulation.

Medial Thalamic DBS

Similar to hippocampal stimulation, medial thalamic stimulation increased behavioral activity in all three measures of behavior. An effect of stimulation was seen in activity counts ($F_{2,127} = 7.39$, $p<0.001$), horizontal activity ($F_{2,129} = 10.65$, $p<0.001$) and total distance ($F_{2,124} = 7.06$, $p<0.01$) using two-way ANOVA. The magnitude of increase in each behavioral measurement was also found to be significantly different depending on the pattern of stimulation. Activity count response was significant with respect to temporal pattern ($F_{2.127} = 4.39$, $p<0.05$) as

was horizontal activity response ($F_{2,129} = 5.41$, $p<0.01$) and total distance response ($F_{2,124} = 5.31$, $p<0.01$; see **Figure 3.3**).

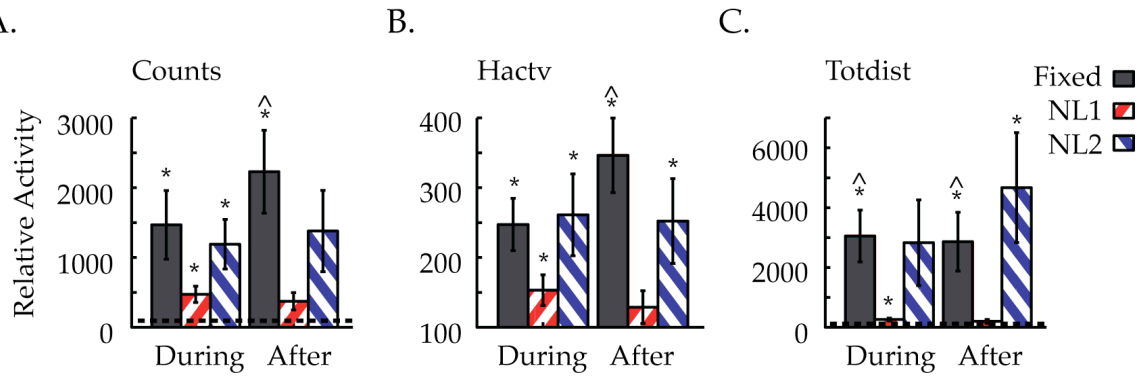

Figure 3.3 Medial Thalamic DBS: Behavior. Behavioral response to medial thalamic DBS. Behavioral measures shown are: activity counts, "Counts" (A), horizontal activity, "Hactv" (B), and total distance, "Totdist" (C). Panels include 10 minutes of data during and 10 minutes of data after CT/DBS, all normalized to before stimulation. Data are presented as mean ± s.e.m. *$p<0.05$ compared to before; ^ $p<0.05$ compared to NL1.

With all three types of stimulation, most behavioral measures were increased during and after stimulation. All temporal patterns of stimulation increased activity counts during stimulation (FF: $t_{19} = 2.78$, $p<0.05$; NL1: $t_{11} = 2.41$, $p<0.01$; NL2: $t_{10} = 3.06$, $p<0.05$) as well as trended or significantly increased activity after stimulation (FF: $t_{20} = 3.59$, $p<0.01$; NL1: $t_{11} = 2.20$, $p = 0.0505$; NL2: $t_{11} =$

2.20, p = 0.0503; see **Figure 3.3.A**). With regard to horizontal activity, all temporal patterns of stimulation increased activity during stimulation (FF: t_{19} = 3.92, p<0.01; NL1: t_{11} = 2.41, p<0.05; NL2: t_9 = 2.74, p<0.05), and FF (t_{23} = 4.61, p<0.01) and NL2 (t_{11} = 2.51, p<0.05) stimulation increased activity after stimulation (see **Figure 3.3.B**). Finally in total distance, FF (t_{19} = 3.41, p<0.01) and NL1 (t_{11} = 3.36, p<0.01) stimulation increased activity during stimulation while FF (t_{21} = 2.82, p<0.05) and NL2 (t_{11} = 2.49, p<0.05) stimulation increased activity after stimulation (see **Figure 3.3.C**). Despite not every behavioral measure increasing during and after every temporal pattern of stimulation, in general medial thalamic stimulation also increased arousal-related motor activity.

Unlike hippocampal stimulation, where NL1 stimulation elicited the largest behavioral responses, NL1 stimulation of the medial thalamus generated the smallest behavioral response increases during and after stimulation in all three behavioral measures. As seen in **Figure 3.3.A**, activity count response to NL1 stimulation was less than FF after stimulation (t_{22} = 3.06, p<0.05). NL1 stimulation increased horizontal activity less than FF after stimulation (t_{30} = 3.72, p<0.01; see **Figure 3.3.B**). Regarding Total distance in **Figure 3.3.C**, NL1 increased behavioral response less than FF during (t_{19} = 3.22, p<0.05) and after (t_{21} = 2.71, p<0.05) stimulation. While temporal pattern of medial thalamic stimulation also affects resulting behavioral response, the specific response of medial thalamic stimula-

tion to different temporal patterns is not the same as hippocampal stimulation. Interestingly, with DBS in medial thalamus, FF gave larger increases in arousal-related behavior than NL1.

EEG

In addition to behavioral effects, electrical stimulation altered the relative power of wave forms in specific frequency bins of the electroencephalogram (EEG) with both hippocampal stimulation and medial thalamic stimulation. While stimulation of both brain regions elicited EEG changes, the specific responses to the different patterns of stimulation were different for each brain region.

Hippocampal DBS

EEG spectral content was altered with hippocampal stimulation in general, but showed few differences among temporal patterns of stimulation. By two-way ANOVA, two of five frequency bins showed significant relative power differences after stimulation, and only one frequency bin showed any differences between temporal patterns used. Theta waves, on average, decreased after stimulation ($F_{1,546} = 5.91$, $p<0.05$), and a significant interaction effect was found between stimulation and temporal pattern ($F_{2,546} = 4.50$, $p<0.01$; see **Figure 3.4.B**). Beta waves also decreased after stimulation ($F_{1,559} = 7.47$, $p<0.01$, see **Figure 3.4.D**). Looking more closely, theta waves were decreased after NL1 ($t_{46} = -2.14$, $p<0.05$)

and NL2 (t_{72} = -3.06, $p<0.01$) stimulation compared to before (see **Figure 3.4.B**), and beta waves were decreased after NL1 (t_{50} = -2.21, $p<0.05$) and NL2 (t_{76} = -3.05, $p<0.01$) stimulation compared to before (see **Figure 3.4.D**). Additionally, NL2 stimulation significantly decreased theta waves more than FF stimulation (t_{140} = 3.08, $p<0.01$), but no other differences between temporal patterns were found to be significant (see **Figure 3.4.B**).

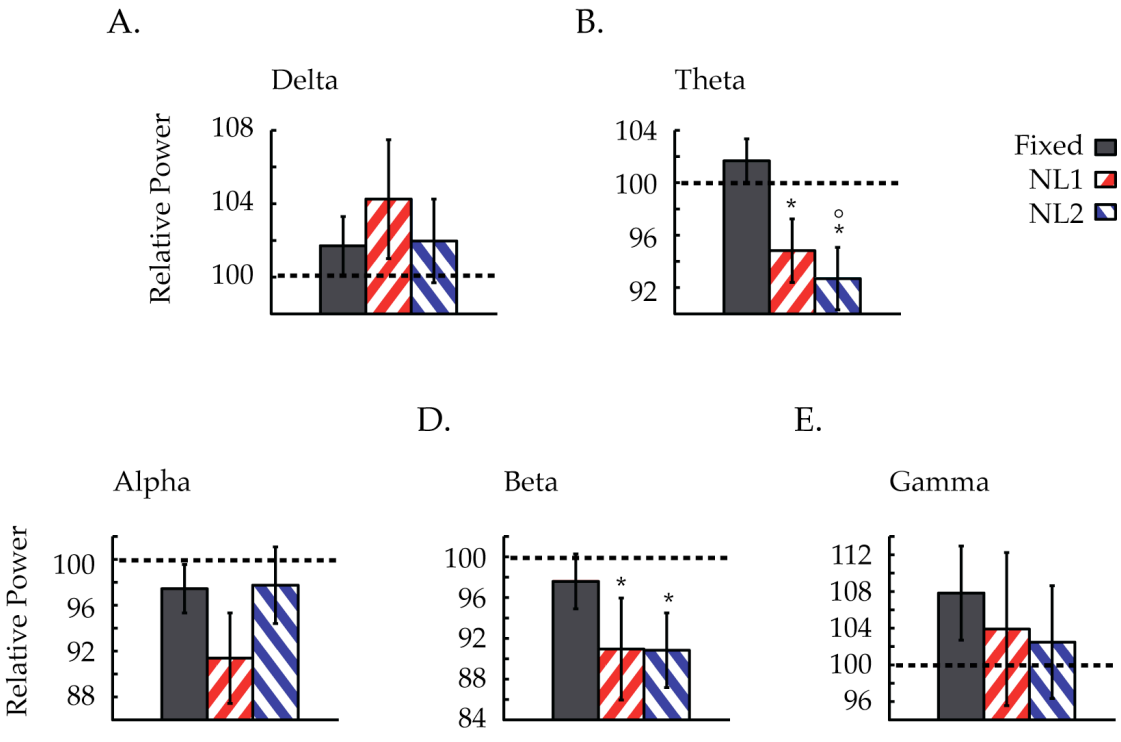

Figure 3.4 Hippocampal DBS: EEG. EEG response to hippocampal DBS. EEG waves are defined by the following frequency bins: delta (0.5-4 hz), theta (4.5-8 hz), alpha (8.5-12 hz), beta (12.5-20 hz), and gamma (35-45 hz). Panels include 10 minutes of data after CT/DBS, normalized to before stimulation. Data are presented as mean ± s.e.m. *$p<0.05$ compared to before; °$p<0.05$ compared to FF.

Medial Thalamic DBS

Paralleling hippocampal stimulation, medial thalamic stimulation led to a change in relative power of frequency bands of the EEG with only a few differences between different temporal patterns of stimulation. Three of five frequency bins showed a significant effect of stimulation by two-way ANOVA. Delta waves increased after stimulation ($F_{1,81} = 13.67$, $p<0.001$; see **Figure 3.5.A**). On average, theta ($F_{1,84} = 19.77$, $p<0.001$; see **Figure 3.5.B**) and beta ($F_{1,83} = 10.76$, $p<0.01$; see **Figure 3.5.D**) waves decreased after stimulation. Only one frequency bin showed a significant effect of pattern: gamma ($F_{2,85} = 4.73$, $p<0.05$; see **Figure 3.5.E**).

Upon more detailed post-hoc analysis, FF stimulation generated the greatest effect on the EEG. In delta waves, FF stimulation, unlike NL1 and NL2 stimulation, increased relative power compared to before stimulation ($t_{19} = 3.44$, $p<0.01$; see **Figure 3.5.A**). With regard to theta waves, both FF ($t_{20} = -3.65$, $p<0.01$) and NL1 ($t_9 = -3.10$, $p<0.05$) stimulation decreased relative power (see **Figure 3.5.B**). In beta waves, only FF stimulation significantly decreased relative power ($t_{22} = -3.89$, $p<0.001$; see **Figure 3.5.D**). Finally in gamma waves, not only is FF stimulation the only temporal pattern to significantly increase relative power compared to before ($t_{20} = 3.07$, $p<0.01$), FF stimulation increases gamma power significantly more than NL1 stimulation ($t_{30} = 3.42$, $p<0.001$; see **Figure 3.5.E**).

There were no other significant differences between different temporal patterns of stimulation.

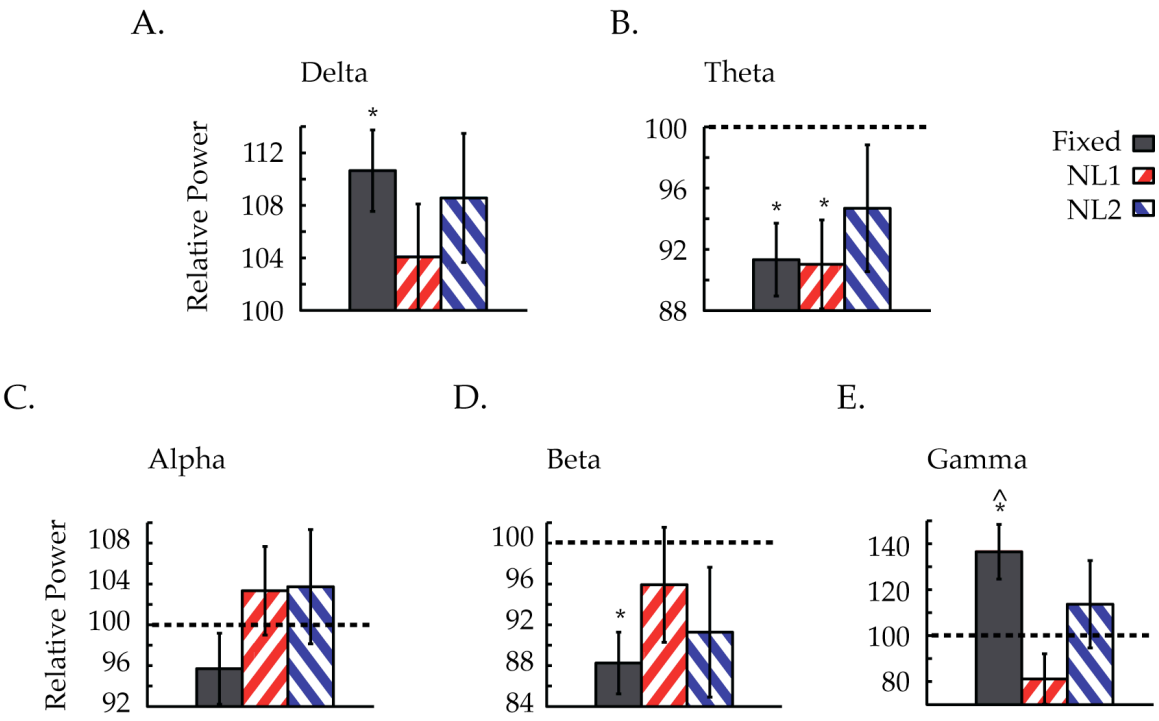

Figure 3.5 Medial Thalamic DBS: EEG. EEG response to medial thalamic DBS. EEG waves are defined by the following frequency bins: delta (0.5-4 hz), theta (4.5-8 hz), alpha (8.5-12 hz), beta (12.5-20 hz), and gamma (35-45 hz). Panels include 10 minutes of data after CT/DBS, normalized to before stimulation. Data are presented as mean ± s.e.m. *$p<0.05$ compared to before; ^ $p<0.05$ compared to NL1.

DISCUSSION

Findings

Behavior

In this chapter, we conclude that temporal patterning of pulses in DBS affects arousal-related motor behavior. With stimulation in two different brain regions, increases in motor activity during and after stimulation were modulated by the temporal pattern of stimulation. In the hippocampus, NL1 stimulation increased arousal-related behavior more than either FF or NL2. In the medial thalamus, stimulation with either FF or NL2 produced significantly more activity increases than NL1. We see that not only does temporal pattern make a difference, but also that the response to temporal pattern is different in each DBS target. This difference between brain regions likely depends on the physiology of the target of stimulation and its function within the particular neuronal circuit of interest.

EEG

EEG spectral response to temporal pattern of DBS was surprising. While there was little evidence of a difference in response to temporal pattern, we found a general effect of DBS. Most interestingly, we found a consistent increase in delta power after DBS. In conjunction with the increases seen in behavioral activity, this seemed paradoxical. Why should an EEG wave associated with sleep

increase in power at the same time as an increase in behavioral activity? There might be many possibilities to explain such a phenomenon; below we propose three.

One possibility to explain this surprising increase in delta power is that it has some relation to the phenomenon of "alpha-delta arousals," usually seen in human brains as intrusions into Non-Rapid Eye Movement sleep (Kryger, Roth, & Dement, 2000). Recordings of EEG during sleep also reveal brief arousals that include large amplitude low frequency waves in a pattern often called "K-complexes." Whether or not our unpredicted finding can be explained by those observations in human brain remains an open question. Secondly, another possibility is that our unexpected delta effect is a rebound phenomenon. In order to test that idea, stimulating using epochs of varying lengths would be required to find out whether very short trains could arouse the mouse without the hypothetical rebound in the EEG. Finally, from a mechanistic point of view, there is the possibility that our increased delta power reflect apical dendritic potentials of the pyramidal cells and other subthreshold events that we measure as low frequency summated potentials (Doi *et al.*, 2007), recruited by DBS. Which of these or other interpretations of our surprising EEG result are actually correct remain to be determined.

Literature

When these data were published, they comprised the first example of temporally-patterned DBS that increased its effectiveness. Prior to this, Birdno *et al*. (2008) published a report stating that irregularly-patterned DBS in tremor patients decreased effectiveness. Since then, several papers have explored the usefulness of temporally-patterned DBS in both clinical and pre-clinical contexts; here, three are mentioned. Cota and colleagues (2009) compared standard and patterned stimulation in a rat model of epilepsy. They found that patterned DBS differentially modulated seizure behavior; specifically, a randomized temporal pattern of stimulation increased the dosage necessary to produce seizure behavior compared to conventional DBS, *i.e.*, the randomized temporal pattern was the more effective anticonvulsant. Alternatively, So and colleagues (2011), found that irregularly-patterned DBS reduced effectiveness of stimulation in a rat model of Parkinson's disease; pathological circling behavior was maximally reduced with standard high frequency DBS compared to standard low frequency or irregular high frequency DBS. Baker and colleagues (2011), also investigated temporal pattern of DBS in an animal model of Parkinson's disease. In a non-human hemiparkisonian model, standard, irregular, bursting, and oscillating temporal patterns were tested. In these experiments, standard, irregular, and bursting DBS improved performance in a reach and retrieval task equally, and oscillating DBS

was less effective at improving performance. Importantly, while the bursting DBS was equally as effective as standard DBS at improving performance, it also reduced the current necessary to produce improvement. Finally, Birdno and colleagues (2011) published another more detailed study into the effects of temporally-patterned DBS on clinical tremor suppression: only those temporal patterns with long pauses reduced effectiveness in tremor suppression. Together, the data presented above and the articles mentioned here stress the importance of exploring temporal pattern of stimulation. Even if the only benefit is to reduce current necessary to produce clinical effectiveness, it is important to examine the affect of different temporal patterns of DBS and how they impact desired outcomes.

Caveats

The magnitude of the effect of temporal patterning of DBS was not always the same. Three considerations can be brought to bear, for explaining this variability. First, from comparisons among data sets, we suspect that the background level of excitability of the mouse may differentially affect arousal responses to different temporal patterns. Second, in some of the data, greater behavioral effects NL1 occurred during the 10 minutes immediately after DBS, whereas in other experiments, the NL1 effect was maximal (compared to FF) during DBS. Third, since these experimental subjects were female mice, it is important to note

that the largest difference between NL1 and FF results were obtained in ovariectomized mice as estrogens are know to affect arousal level (Riberio, Pfaff, & Devidze, 2009). This may be because of the consideration raised above, namely, the importance of the background level of excitability of the test mice influence the magnitude of the NL1 effect. In addition to response variability, we also note that all of the observations we report here were made during the dark part of the daily light cycle, and thus that observations following DBS during the light part of the cycle might differ.

Outlook

While our data show that temporal patterning can be used to modulate CNS arousal in response to DBS, the dynamics of that patterning, as it affects behavioral response, have not yet been comprehensively explored. One consideration for future studies will be approaches based on randomness. This would require special consideration since some random generators are not truly random and are themselves nonlinear dynamic equations. In contrast, a full exploration of pure randomness in this experimental setting will require constructing new families of pulse trains based either on the mathematics of Poisson processes, in which timings of individual pulses are determined in a manner independent of one another (Snyder & Miller, 1991), or on the mathematics of random sequences, their randomness proven by the inability to compress them into shorter repeating

sequences (Martin-Löf, 1966). In addition, besides the logistic equation, there are several other equations that generate deterministic chaos (Cohen, 1995), and they might be explored as well. Finally, it must also be recognized that our two non-linear temporal patterns were generated from the same equation, but resulted in different behavioral and EEG responses. Understanding exactly how these dynamics influence the CNS arousal system will be essential to finding the optimal temporal pattern for maximizing behavioral arousal responses.

Chapter 4: Intact DBS in the Central Thalamus

PARAMETRIC EXPERIMENT

In addition to looking for differences caused by the stimulation itself, we investigated differences caused by amplitude of stimulation, frequency of stimulation, and light phase during which stimulation occurred. All mice included in these analyses were confirmed with at least unilateral placement in the central thalamus (**Figure 4.1.B-D**).

Behavior

First and foremost, we found an effect of central thalamus DBS (CT/DBS) in all three behavioral measures (Counts: $F_{2,100} = 14.23$, $p<0.001$; Hactv: $F_{2,902} = 32.33$, $p<0.001$; Totdist: $F_{2,914} = 5.66$, $p<0.01$; see **Figure 4.2**). CT/DBS increased motor activity, decreased theta waves in the EEG, and increased alpha, beta, and gamma waves in the EEG. These data replicate our finding that CT/DBS increases generalized arousal.

Amplitude effects

ANOVA analyses also revealed an effect of amplitude, when all other factors are held constant, in all three behavioral measures (Counts: $F_{2,1000} = 15.68$, $p<0.001$; Hactv: $F_{2,902} = 7.83$, $p<0.001$; Totdist: $F_{2,914} = 5.13$, $p<0.01$; see **Figure 4.2**). Comparing individual amplitudes, 125 μA stimulation increased activity counts greater than either 75 μA (during: $t_{197} = -3.06$, $p<0.01$; after: $t_{200} = -3.15$, $p<0.01$) or

Figure 4.1 Histology: Diagram of electrode placements in coronal section. A. Coronal figure at bregma - 1.70 mm of whole mouse brain and close up of the thalamus. Electrode placements indicated by black dots. To be included in analysis, mice must have at least one hit within the central thalamus. Parametric experiment mice: close up on just the thalamus at B. bregma - 1.70 mm, C. bregma - 1.94 mm, and D. bregma -2.06 mm. Temporal Pattern experiment mice: close up on just the thalamus at E. bregma - 1.70 mm, F. bregma - 1.94 mm, and G. bregma -2.06 mm. Abbreviations for thalamic nuclei include CL (central lateral thalamic nucleus), PC (paracentral thalamic nucleus), CM (central medial thalamic nucleus), MD (mediodorsal thalamic nucleus), PF (parafascicular thalamic nucleus).

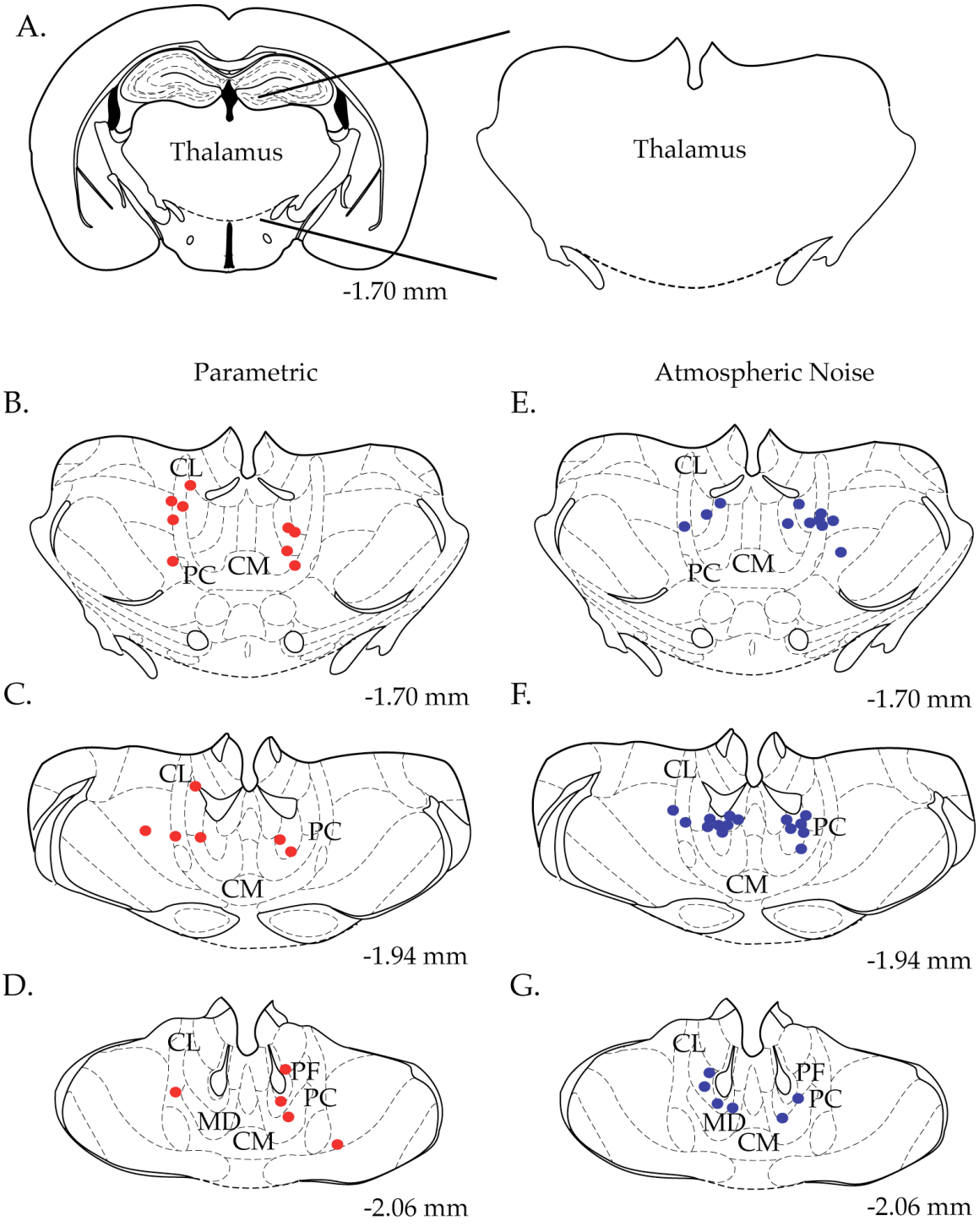
A.
Thalamus
Thalamus
-1.70 mm
Parametric
Atmospheric Noise
B.
CL
PC
CM
E.
CL
PC
CM
C.
-1.70 mm
F.
-1.70 mm
CL
PC
CM
CL
PC
CM
-1.94 mm
-1.94 mm
D.
G.
CL
PF
PC
MD
CM
CL
PF
PC
MD
CM
-2.06 mm
-2.06 mm

Figure 4.2 Parametric Experiment: Behavior. Behavioral response to amplitude (A. B. and C.), frequency (D. E. and F.), and light phase (G. H. and I.) of CT/DBS. Three behavioral measures are shown: activity counts (whole body movement), horizontal activity (fidgeting), and total distance (ambulation). Panels include 10 minutes of data during and 10 minutes of data after CT/DBS, all normalized to before stimulation. Data are presented as mean ± s.e.m. * $p<0.05$ compared to before, ° $p<0.05$ compared to 75 μA, ^ $p<0.05$ compared to 100 μA, # $p<0.05$ compared to dark phase.

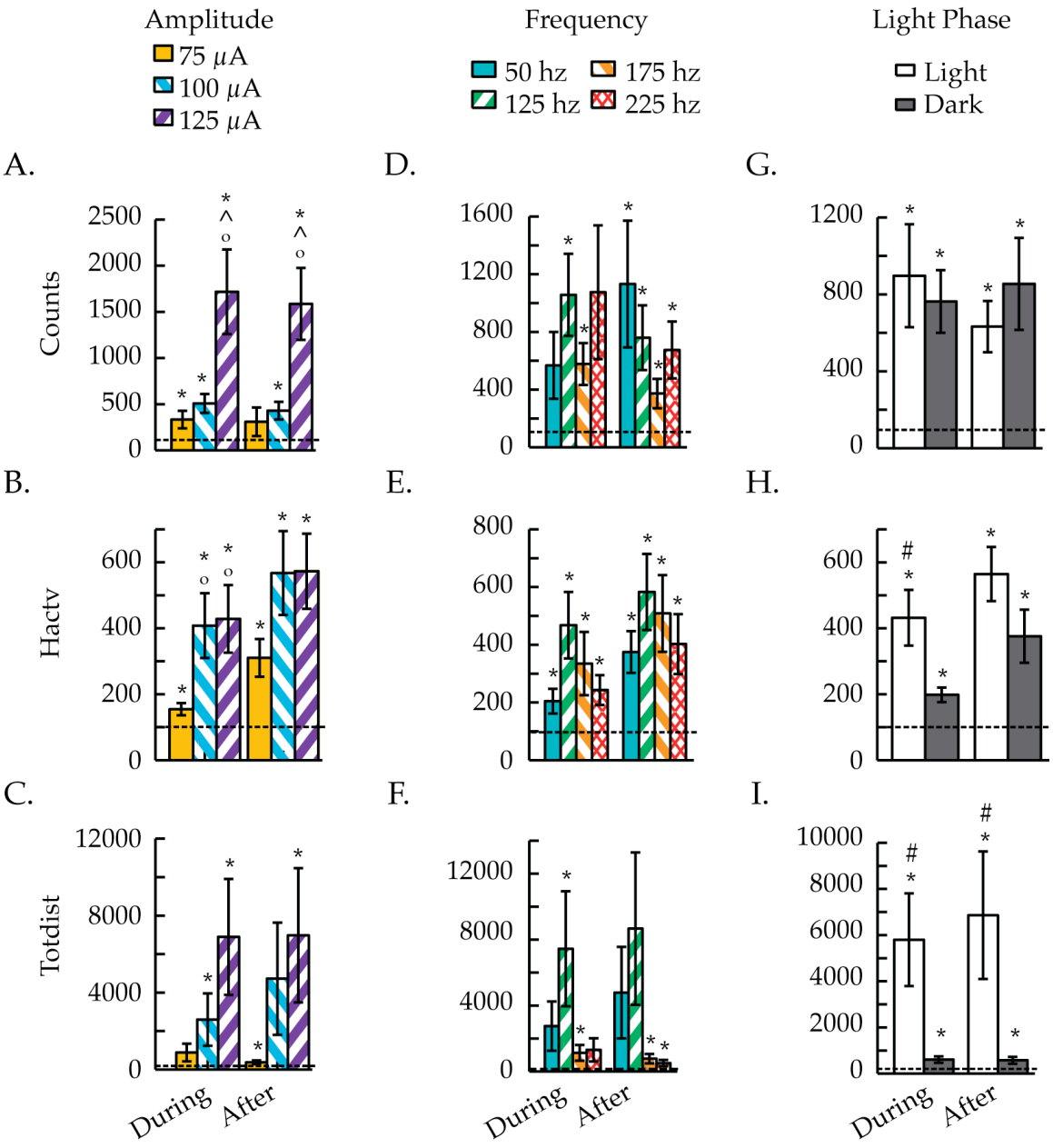
Amplitude
75 μA
100 μA
125 μA
Frequency
50 hz
125 hz
175 hz
225 hz
Light Phase
Light
Dark
A.
B.
C.
D.
E.
F.
G.
H.
I.
Counts
Hactv
Totdist
During
After

100 μA (during: t_{202} = -2.72, $p<0.05$; after: t_{202} = -3.03, $p<0.01$) during and after stimulation (see **Figure 4.2.A**). Looking at horizontal activity, 75 μA stimulation increased motor activity less than 100 μA (t_{178} = -2.76, $p<0.05$) or 125 μA (t_{175} = -2.90, $p<0.05$) during stimulation (see **Figure 4.2.B**). Confirming an effect of stimulation, all amplitudes increased all three behavioral measures during and after stimulation compared to before.

Frequency effects

Investigation of the frequency of stimulation led to the determination there was a significant effect of frequency in two of behavioral measures (Hactv: $F_{3,902}$ = 3.70, $p<0.05$; Totdist: $F_{3,914}$ = 5.98, $p<0.001$; see **Figures 4.2.E-F**). Despite this overall effect of frequency, none of the Bonferroni-corrected t-tests showed significant differences between individual frequencies. Comparing response during and after stimulation to before, 125 hz stimulation increased motor activity in activity counts during (t_{196} = -4.00, $p<0.001$) and after (t_{196} = -3.50, $p<0.01$; see **Figure 4.2.D**) stimulation, horizontal activity during (t_{184} = -4.12, $p<0.001$) and after (t_{184} = -4.72, $p<0.001$; see **Figure 4.2.E**) stimulation, and total distance during (t_{187} = -2.66, $p<0.05$; see **Figure 4.2.F**) stimulation. High temporal resolution raw behavioral data for all four frequencies in one illustrative mouse can be found in **Figure 4.3**.

Daily light phase effects

In addition to the various parameters of stimulation manipulated above, we found that the light phase during which stimulation occurred had an effect, holding all other factors constant, on response to DBS in two behavioral measures (Hactv: $F_{1,902} = 14.03$, $p<0.001$; Totdist: $F_{1,914} = 16.07$, $p<0.001$; see **Figures 4.2.H-I**). Motor activity increased with light phase stimulation more than dark phase stimulation in horizontal activity during stimulation ($t_{257} = 2.82$, $p<0.01$; see **Figure 4.2.H**) and total distance during ($t_{263} = 2.49$, $p<0.01$) and after stimulation ($t_{264} = 2.20$, $p<0.05$; see Figure 4.2.I).

EEG

By ANOVA, we found an effect of CT/DBS in three of five EEG wave s (Alpha: $F_{1,780} = 18.55$, $p<0.001$; Beta: $F_{1,793} = 14.44$, $p<0.001$; and Gamma: $F_{1,775} = 28.32$, $p<0.001$, see **Figure 4.4**). In addition to increasing motor activity seen above, CT/DBS decreased alpha and beta waves and increased gamma waves in the EEG. While the decrease in alpha and beta waves was not expected, the increase in gamma waves is concurrent with our previous finding that CT/DBS increases generalized arousal.

Amplitude effects

In the ANOVA analyses of EEG waves, an effect of amplitude, holding all other factors constant, was found in one of five EEG waves (Beta: $F_{2,793} = 6.07$,

Figure 4.3. Parametric Experiment: behavior at high temporal resolution of one illustrative mouse. Motor activity behavior of one mouse at 4 frequencies of stimulation, 100 μA, in the light phase. A. 50 hz, B. 125 hz, C. 175 hz, D. 225 hz. Activity counts ('Counts') shown at 1 sample every 10 seconds, Horizontal activity ('Hactv') and Total distance ('Totdist') shown at 1 sample every 1 second. Grey boxes mark epochs of stimulation.

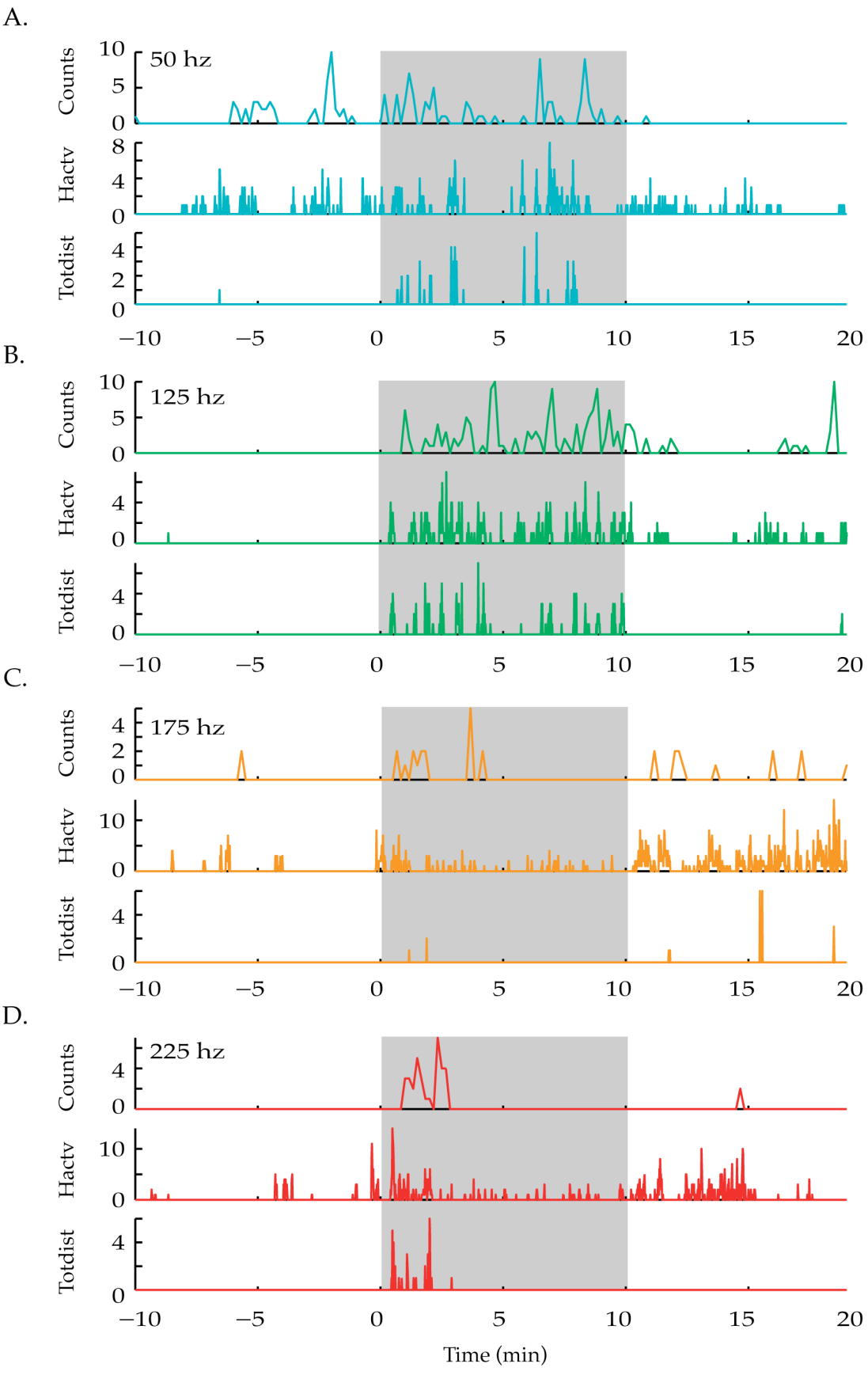
A.
50 hz
Counts
Hactv
Totdist
B.
125 hz
Counts
Hactv
Totdist
C.
175 hz
Counts
Hactv
Totdist
D.
225 hz
Counts
Hactv
Totdist
−10
−5
0
5
10
15
20
Time (min)

Figure 4.4 Parametric Experiment: EEG. EEG response to amplitude (A. B. C. D. and E.), frequency (F. G. H. I. and J.), and light phase (K. L. M. N. and P.) of CT/DBS. EEG waves are defined by the following frequency bins: delta (0.5-4 hz), theta (4.5-8 hz), alpha (8.5-12 hz), beta (12.5-20 hz), and gamma (35-45 hz). Panels include 10 minutes of data after CT/DBS, normalized to before stimulation. Data are presented as mean ± s.e.m. * $p<0.05$ compared to before, # $p<0.05$ compared to dark phase.

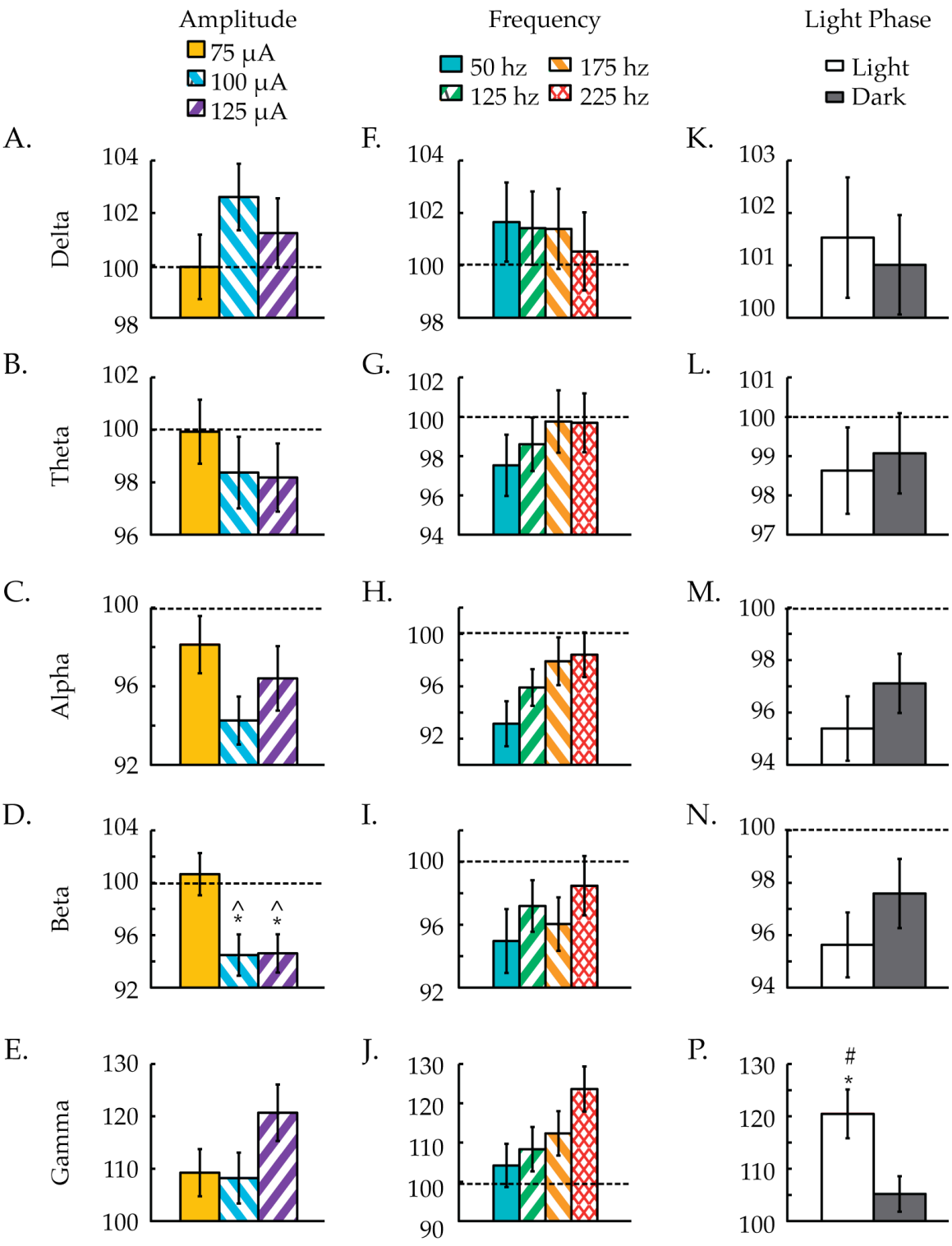
Amplitude
75 µA
100 µA
125 µA
Frequency
50 hz
175 hz
125 hz
225 hz
Light Phase
Light
Dark
A.
B.
C.
D.
E.
F.
G.
H.
I.
J.
K.
L.
M.
N.
P.
Delta
Theta
Alpha
Beta
Gamma
104
102
100
98
96
92
130
120
110
90
103
101
99
97
94
^
*
#

$p<0.01$, see **Figure 4.4.D**). In more detail, beta waves were decreased compared to before stimulation with two amplitudes of stimulation (100 μA: $t_{138} = 3.51$, $p<0.01$; 125 μA: $t_{124} = 3.69$, $p<0.01$). Additionally, both 100 μA ($t_{275} = 2.74$, $p<0.05$) and 125 μA ($t_{260} = 2.78$, $p<0.05$) were significantly different from 75 μA DBS. These data suggest that greater current has a greater effect on the mouse. To avoid negative side effects of injecting too much current into the brain, we decided on the conservative choice of 100 μA for future studies.

Frequency effects

There were no frequency effects, holding all other factors constant, in the ANOVA analyses of the 5 EEG waves (see **Figure 4.4.F-J**).

Daily light phase effects

In ANOVA analyses of EEG waves, light phase of stimulation had a significant effect on response to stimulation in one EEG wave band (Gamma: $F_{1,775} = 9.492$, $p<0.001$; see **Figure 4.4.P**). Gamma waves increased more with stimulation in the light phase than in the dark phase ($t_{333} = 2.66$, $p<0.01$). Additionally, response of gamma waves in the light was greater compared to before DBS ($t_{177} = -4.41$, $p<0.001$). These data coincided with previous observations that increases to arousal due to stimulation are larger in the light than the dark.

TEMPORAL PATTERN EXPERIMENT

In the analysis of the temporal pattern experiment, we looked for differences caused by the stimulation itself and investigated differences caused by pattern of stimulation and light phase during which stimulation occurred. All mice included in these analyses were confirmed with at least unilateral placement in the central thalamus (**Figure 4.1.E-G**).

Behavior

As with the Parametric data set, we found a significant effect of stimulation in all three behavioral measures (Counts: $F_{2,453} = 21.47$, $p<0.001$; Hactv: $F_{2,513} = 15.19$, $p<0.001$; Totdist: $F_{2,504} = 12.56$, $p<0.001$; see **Figure 4.5**) and four of the EEG waves (Delta: $F_{1,271} = 8.76$, $p<0.01$; Theta: $F_{1,258} = 13.29$, $p<0.001$; Beta: $F_{1,258} = 5.57$, $p<0.05$; Gamma: $F_{1,261} = 8.25$, $p<0.01$; see Figure 4.5). Again, we replicate findings here and elsewhere that CT/DBS increases generalized arousal as measured by motor activity and EEG response.

Temporal pattern effects

ANOVA analyses also revealed an effect of temporal patterning, while all other factors remain constant, in two behavioral measures (Counts: $F_{2,453} = 8.56$, $p<0.001$; Hactv: $F_{2,513} = 6.44$, $p<0.01$; see **Figures 4.5.A-B**). While an overall effect of pattern was found, only one post-hoc comparison between patterns was significant. Random stimulation increased activity counts significantly more than

Figure 4.5 Temporal Pattern Experiment: Behavior. Behavioral response to temporal pattern (A. B. and C.) and light phase (D. E. and F.) of CT/DBS. Three behavioral measures are shown: activity counts (whole body movement), horizontal activity (fidgeting), and total distance (ambulation). Panels include 10 minutes of data during and 10 minutes of data after CT/DBS, all normalized to before stimulation. Data are presented as mean ± s.e.m. * $p<0.05$ compared to before, # $p<0.05$ compared to chaotic.

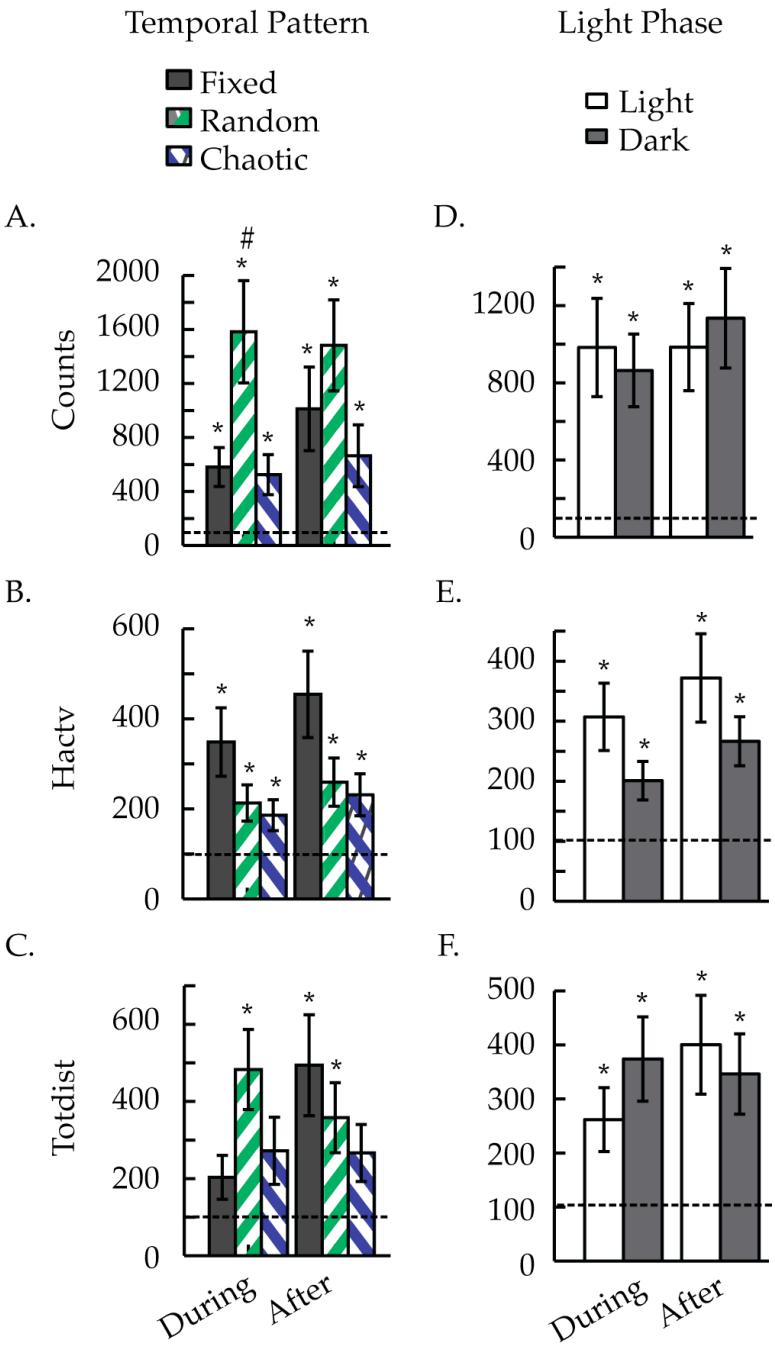
Temporal Pattern
Fixed
Random
Chaotic
Light Phase
Light
Dark
A.
B.
C.
D.
E.
F.
Counts
Hactv
Totdist
2000
1600
1200
800
400
0
600
200
100
300
500
#
*
During
After

Figure 4.6 Temporal Pattern Experiment: behavior at high temporal resolution of one illustrative mouse. Motor activity behavior of one mouse at 3 temporal patterns of stimulation, 100 μA, in the light phase. A. Fixed, B. Random, and C. Chaotic. Activity counts ('Counts') shown at 1 sample every 10 seconds, Horizontal activity ('Hactv') and Total distance ('Totdist') shown at 1 sample every 1 second. Grey boxes mark epochs of stimulation.

A.

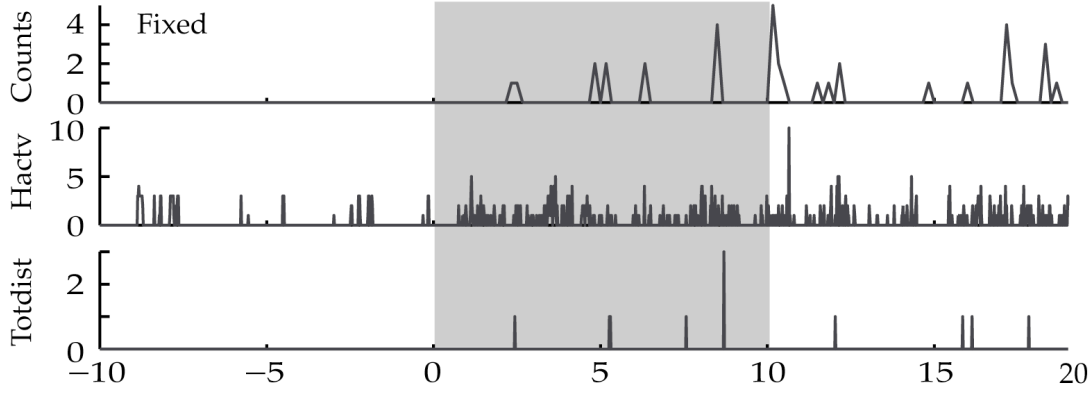
Fixed
Counts
Hactv
Totdist
4
2
0
10
5
0
2
0
−10
−5
0
5
10
15
20

B.

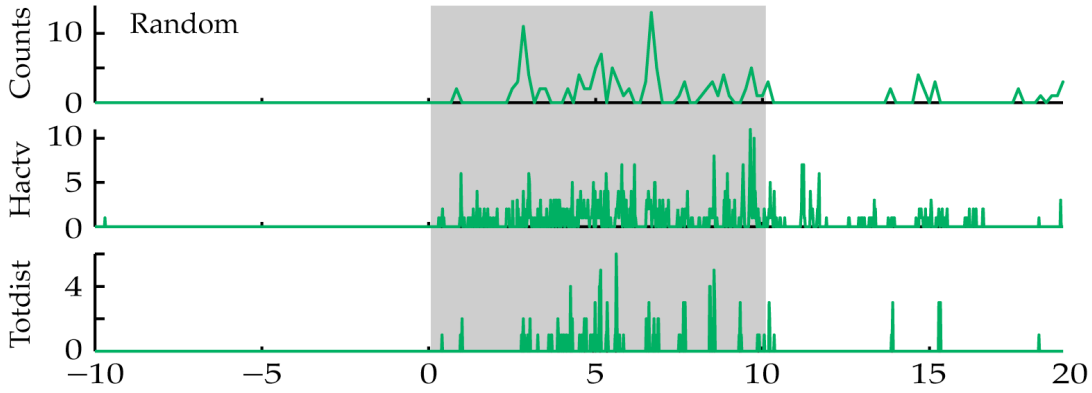
Random
Counts
Hactv
Totdist
10
0
10
5
0
4
0
−10
−5
0
5
10
15
20

C.

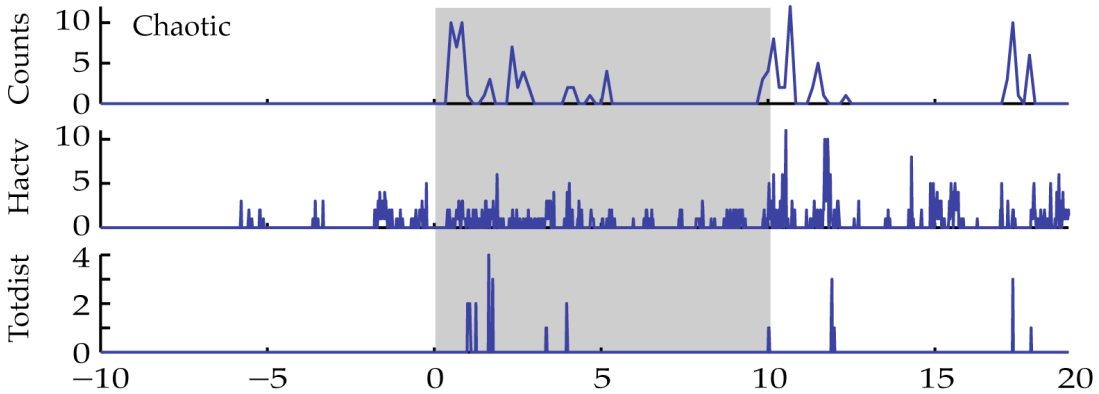
Chaotic
Counts
Hactv
Totdist
10
5
0
10
5
0
4
2
0
−10
−5
0
5
10
15
20

Chaotic during stimulation (t_{96} = 2.52, p<0.05; see **Figure 4.5.A**). Comparing response during and after stimulation to before, all patterns increased motor activity compared to before in activity counts during (Fixed: t_{103} = -3.83, p<0.001; Random: t_{113} = -4.39, p<0.001; Chaotic: t_{105} = -2.35, p<0.01) and after stimulation (Fixed: t_{104} = -3.38, p<001; Random: t_{114} = -4.56, p<0.001; Chaotic: t_{106} = -2.76, p<0.05; see **Figure 4.5.A**), horizontal activity during (Fixed: t_{116} = -3.33, p<0.01; Random: t_{121} = -2.93, p<0.05; Chaotic: t_{116} = -2.55, p<0.05) and after stimulation (Fixed: t_{115} = -3.79, p<0.01; Random: t_{121} = - 3.10, p<0.01; Chaotic: t_{116} = -2.86, p<0.05; see **Figure 4.5.B**), and total distance during (Random: t_{120} = -3.87, p<0.001) and after stimulation (Fixed: t_{114} = -3.12, p<0.01; Random: t_{119} = -3.02, p<0.01; see **Figure 4.5.C**). High temporal resolution raw behavioral data for all three patterns in one illustrative mouse can be found in **Figure 4.6**.

EEG

Using ANOVA, we found a significant effect of stimulation in two of the EEG waves (Theta: $F_{1,261}$ = 9.15, p<0.01; and Gamma: $F_{1,265}$ = 9.37, p<0.01; see **Figure 4.7**).

Temporal pattern effects

In the EEG analysis, there was no overall effect of pattern in any of the EEG waves, but in comparing responses after DBS to before, one significant difference emerged. Chaotic DBS increased gamma waves after stimulationg (t_{44} =

-2.55, $p<0.05$; see **Figure 4.7.E**). Conservative Bonferroni-corrected post hoc analyses reveal few significant differences between specific temporal patterns.

Daily light phase effects

An effect of daily light phase was found in two of the EEG waves (Theta: $F_{1,271} = 4.24$, $p<0.05$; Alpha: $F_{1,258} = 6.49$, $p<0.05$; see **Figure 4.7.G-H**). This general effect was confirmed by post-hoc t-tests comparing light to dark in theta waves ($t_{125} = -2.55$, $p<0.05$, see **Figure 4.7.G**) and almost reached criterion for significance in alpha waves ($t_{124} = -1.96$, $p=0.0521$, see **Figure 4.7.H**) after stimulation. In both theta ($t_{62} = 4.09$, $p<0.001$) and alpha ($t_{60} = 2.31$, $p<0.05$) waves, show greater decreases compared to before stimulation during the light phase. This recapitulates our result that higher relative responses to stimulation occur during the light phase.

Figure 4.7 Temporal Pattern Experiment: EEG. EEG response to temporal pattern (A. B. C. D. and E.) and light phase (F. G. H. I. and J.) of CT/DBS. EEG waves are defined by the following frequency bins: delta (0.5-4 hz), theta (4.5-8 hz), alpha (8.5-12 hz), beta (12.5-20 hz), and gamma (35-45 hz). Panels include 10 minutes of data after CT/DBS, normalized to before stimulation. Data are presented as mean ± s.e.m. * $p<0.05$ compared to before, # $p<0.05$ compared to dark phase.

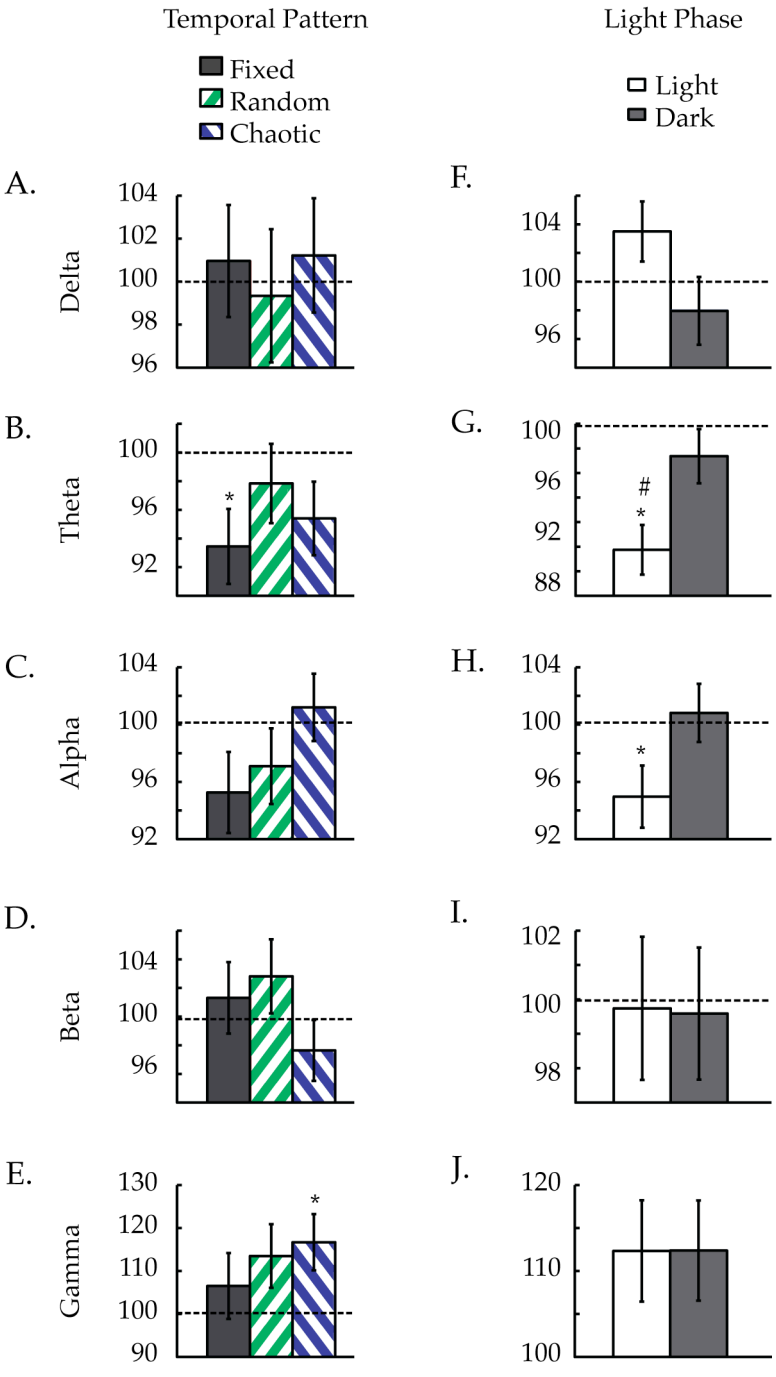
Temporal Pattern
Fixed
Random
Chaotic
Light Phase
Light
Dark
A.
Delta
104
102
100
98
96
F.
104
100
96
B.
Theta
100
96
92
*
G.
100
96
92
88
#
*
C.
Alpha
104
100
96
92
H.
104
100
96
92
*
D.
Beta
104
100
96
I.
102
100
98
E.
Gamma
130
120
110
100
90
*
J.
120
110
100

DISCUSSION

Findings

Behavior

Considering the behavioral results of both experiments presented above, we conclude that generalized arousal as measured by spontaneous motor activity can be increased by CT/DBS. This increase can be modulated by various parameters of stimulation. Amplitude of DBS increases behavioral response in an expected way; more current yields a concomitant increase in motor activity. Behavioral responses to various frequencies of DBS also differ, but in this particular circumstance the differences between the specific frequencies chosen were not significant. Light phase during which DBS occurs can also affect degree of increase in behavior; larger increases during and after stimulation occur during the light phase and are most likely due to the low baseline activity during the light. Most importantly we have found that temporal pattern of stimulation affects behavioral response to CT/DBS. This effect of temporal pattern in behavioral response to DBS replicates our previous findings (Quinkert, Schiff, & Pfaff, 2010) that temporal patterning makes a difference.

Our behavioral data revealed an overall effect of temporal pattern, but only one specific significant difference in the Bonferroni-corrected post-hoc analysis and only in the activity counts behavioral measure. In that instance,

Random CT/DBS increased motor activity during stimulation more than Chaotic. This result is unexpected. Since it has been theorized that nonlinear dynamics play a role in controlling arousal systems (Pfaff & Banavar, 2007), we hypothesized that Chaotic CT/DBS would increase arousal more than either Fixed or Random; instead we see that Random does better. At the moment, it is unclear why one temporal pattern did better than another in one behavioral measure. Given that our results ran counter to our expectations, it might be that some singular undefined characteristic of the Random temporal pattern was responsible for the temporal pattern's success instead of theoretical method by which it was generated.

EEG

EEG responses to DBS were as expected. In both experiments, EEG waves changed significantly with CT/DBS. Some of these changes were in a direction consistent with an increase in arousal. Theta waves, associated with sleep and quiet wakefulness (Niedermeyer, 2005b), decreased with CT/DBS, while gamma waves, associated with wakefulness and higher cognitive functions such as attention (Niedermeyer, 2005a), increased with CT/DBS. Responses of delta, alpha, and beta waves, on the other hand, are confusing under the assumption that CT/DBS increases generalized arousal. Degree of response to DBS was modulated by amplitude of stimulation and temporal pattern of stimulation, but these changes

were small and often not significant. Differences between response to various frequencies of stimulation were negligable. EEG response to DBS during the two phases of the light cycle were also different; changes after DBS were larger in the light phase than in the dark. We assume these larger responses during the light phase are due to the nocturnal nature of mice; since mice are often quiescent during the light phase, they respond more dramatically to an arousing stimulus then.

Literature

Due to the novelty of this work, there is only a handful of articles, reporting work done in varying contexts, to compare our results to. CT/DBS has been investigated in intact rats (Shirvalkar, Seth, Schiff, & Herrera, 2006), brain injured rats (Mair & Hembrook, 2008), macaque monkeys (Smith *et al.*, 2009), mice (Quinkert, Schiff, & Pfaff, 2010), and one human case study (Schiff *et al.*, 2007). Concurrent with what we observe here, CT/DBS increased motor activity or enhanced performance on a cognitive task in all of these studies; however, none of the work mentioned above explored the importance of temporal pattern of stimulation. Shirvalkar and colleagues (2006) showed increased early action gene expression in cortical and basal ganglia regions as well as enhanced performance on a novel object recognition task with CT/DBS in intact rats. In a DMTP rat model, Mair and Hembrook (2008) showed enhanced working memory with

CT/DBS. Smith *et al.* (2009) used bayesian statistical methods to analyze the effect of CT/DBS on a sustained attention task in macaque monkeys. This method was also used to further analyze data collected from the human case study of CT/DBS in a MCS patient. It was confirmed that CT/DBS helped facilitate functional recovery in this patient (Schiff *et al.*, 2007; Smith *et al.*, 2009). These studies represent the body of evidence that CT/DBS can increase arousal and enhance cognition, but there are still questions to explore such as what stimulation parameters, including pattern, are best and how do these parameters need to be adjusted, patient to patient.

Caveats

Like many behavioral studies with multiple subjects, especially mice, these experiments show a large variability. Three potential sources of variance are considered: baseline activity level, exact electrode placement, and sex differences. First, it is clear that baseline activity level does influence response to stimulation. Mice respond differentially to stimulation in the light and dark; responses during the light phase, when mice are more often quiescent, are relatively larger than those during the dark phase. Fluctuations of baseline activity on a smaller scale are likely causes of intra-subject variability. Second, small variations in electrode placement might affect inter-subject variability. These small position differences change the electrical field of stimulation and which

specific neurons are influenced by this field. These changes might alter the efficiency of stimulation as well as the magnitude of response during and directly after stimulation. Finally, we observed small, inconsistent sex differences as mentioned in Chapter 2 (page 39). While these differences were not statistically significant, it is likely they affected inter-subject variability once the data from males and females were pooled.

Conclusions

Here we have presented more evidence that temporal patterning of DBS can affect the magnitude of desired responses. While a comprehensive exploration of temporal patterns in DBS is outside the scope of this paper, possible avenues to continue this work would be to investigate 1) longer sequences of pulses that would presumably permit still more entropy, 2) specific local characteristics of the temporal patterns presented here to determine why Random was better than Chaotic, 3) other deterministic chaotic equations, and 4) playbacks or temporal patterns recorded from central thalamus or from arousal systems that project to the central thalamus. Additionally, it stands to reason that because we found that temporal patterns of CT/DBS are important in modulating motor activity and EEG response, temporal patterns of stimulation might modulate desired responses to DBS in other, medically important contexts. More research is needed into how neuronal circuits of interest function in normal and diseased

states as well as how DBS can be used to effect desired changes in these circuits. This is essential to the future of DBS therapy because the more we know about diseased neuronal circuits and how DBS affects them, the better able we will be to logically choose stimulation parameters and design DBS regimes. Choosing a stimulation regime for a specific disorder or set of symptoms will be much more efficient than the current method for finding stimulation parameters, by trial and error.

Chapter 5: Multiple TBI and DBS

Mouse Model of Multiple TBI

To ensure long lasting deficits, several traumatic brain injury (TBI) models were tested. The final model chosen, multiple TBI (described in Chapter 2, page 36), results in neurological and motor actvity deficits that last 11-14 days without compromising gross dark-light behavior. Briefly, anesthetized mice were placed under the TBI apparatus and a 20 g weight was dropped from 25 cm onto the right side of the mouse's head up to 5 times.

Neurological Severity Screen

Each injured mouse underwent a neurological severity screen (NSS) 2 hours post injury. The NSS is described in detail in Chapter 2 (page 36), and each test is summarized briefly in **Table 5.1**. In this set of mice (n=12), NSS scores ranged from 3-6 with an average overall score of 4.75±0.28. This average score is significantly different from 0 (t_{11} = 17.05, $p<0.001$; signed rank = 0, $p<0.001$). These data show that neurological deficits can be generated by this mouse model of traumatic brain injury, multiple TBI.

Motor Activity Deficits

In addition to neurological deficits, multiple TBI can also generate deficits in the motor aspect of arousal. A timeline of daily activity in one illustrative injured mouse can be found in **Figure 5.1.B-C**. Motor activity was summed over 24

Table 5.1 Neurological Severity Screen following Multiple TBI

Neurological Tests (in the order of performance)	**Number of mice that Failed**	**Total of mice Tested**
Exit from 30 cm circle within 3 minutes	4	12
Straight walk	0	12
Startle reflex	4	12
Seeking behavior	0	12
Hind limb flex	0	12
Flat beam balance for 10 seconds	4	12
Round beam balance for 10 seconds	10	12
3 cm beam walk within 3 minutes	11	12
2 cm beam walk within 3 minutes	12	12
1 cm beam walk within 3 minutes	12	12

NSS tests are scored pass (0, normal behavior) or fail (1, abnormal behavior). The range of overall scores (*i.e.*, number of tests failed) was 3-6 and the overall score average was 4.75±0.28.

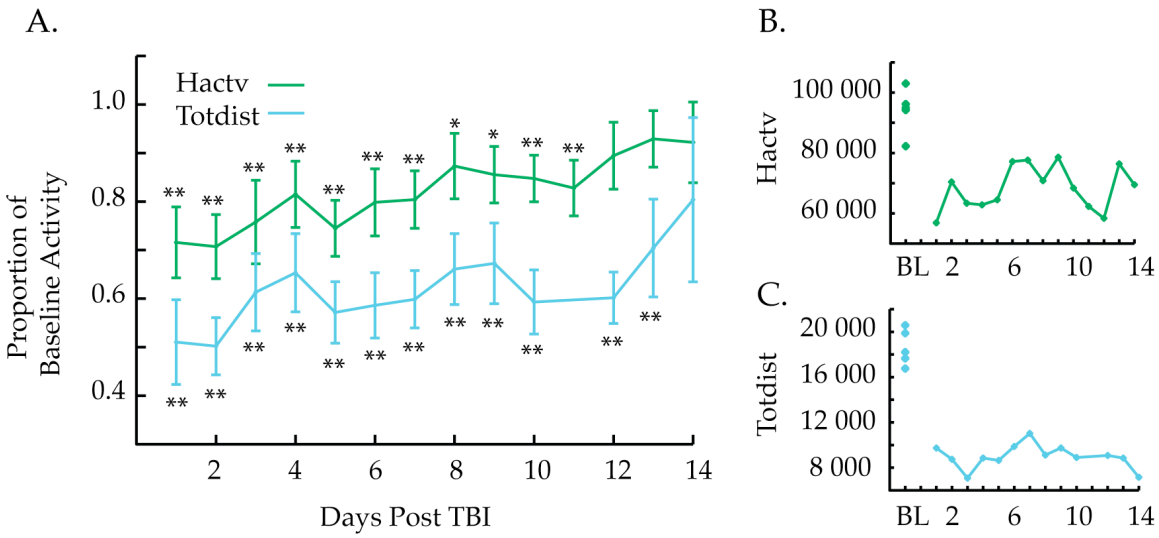

Figure 5.1 Motor Activity Deficits following Multiple TBI. Normalized average daily acitivity (A) for two motor activity measures (horizontal activity — blue; total distance — green) up to 14 days after injury, represented as mean ± s.e.m. of n=12 mice. Timeline of raw daily activity in one injured mouse for horizontal activity (B) and total distance (C) up to 14 days after injury. * $p<0.05$; ** $p<0.01$. BL — baseline.

hours, and these sums were normalzied to the average activity of a 5 day baseline observed prior to injury. Normalized daily activity was averaged across mice (n=12), and this average timeline can be found in **Figure 5.1.A**. To avoid the biases present in the assumptions of parametric statistical tests, appropriate non-parametric tests were also used to confirm results of parametric tests. T-tests, and to confirm Wilcoxon matched-pair signed-ranks tests, were used to determine

whether motor activity deficits were significantly different from baseline. Significant deficits in two measures of motor activity occurred on the day after injury: horizontal activity (t_{11} = -3.47, $p<0.01$; signed rank = 6, $p<0.01$) and total distance (t_{11} = -4.39, $p<0.001$; signed rank = 5, $p<0.01$). These significant deficits lasted for several days after injury.

Recovery without Intervention

As this is a closed head injury, it is expected that injured mice will begin to heal and recover functionality over the course of the experiment. As expected, deficits decrease and motor activity aproaches pre-injury baseline levels at around 11-14 days post injury. In one of the two data measures, horizontal acitivity, deficits were significantly different from baseline up to day 12 using non-parametric statistics (signed rank = 21, $p<0.05$) or up to day 11 using parametric t-tests (t_{11} = -2.89, $p<0.01$). With total distance, deficits were significanlty different from baseline up to day 14 for non-parametric (signed rank = 14, $p<0.05$) or up to day 13 for parametric t-tests (t_{11} = -3.18, $p<0.01$). These data show that multiple TBI can generate motor activity deficits that last 11-14 days post injury.

Preserved Nocturnal Behavior Pattern

In addition to overall locomotion, activity over the course of the light/dark cycle was observed to determine whether multiple TBI hindered dark-light behavior as well as reduced overall motor activity. Activity was summed over 12

hours, and these sums are presented as a proportion of average total daily baseline activity. Dark-light behavior of one illustrative injured mouse can be found in **Figure 5.2.C-D**. Normalized 12 hour data were grouped into baseline and post injury and then averaged across mice. These averages can be found in **Figure 5.2.A-B**. Notice that even after injury, activity in the dark is increased over activity in the light, *i.e.*, nocturnal behavior pattern is preserved.

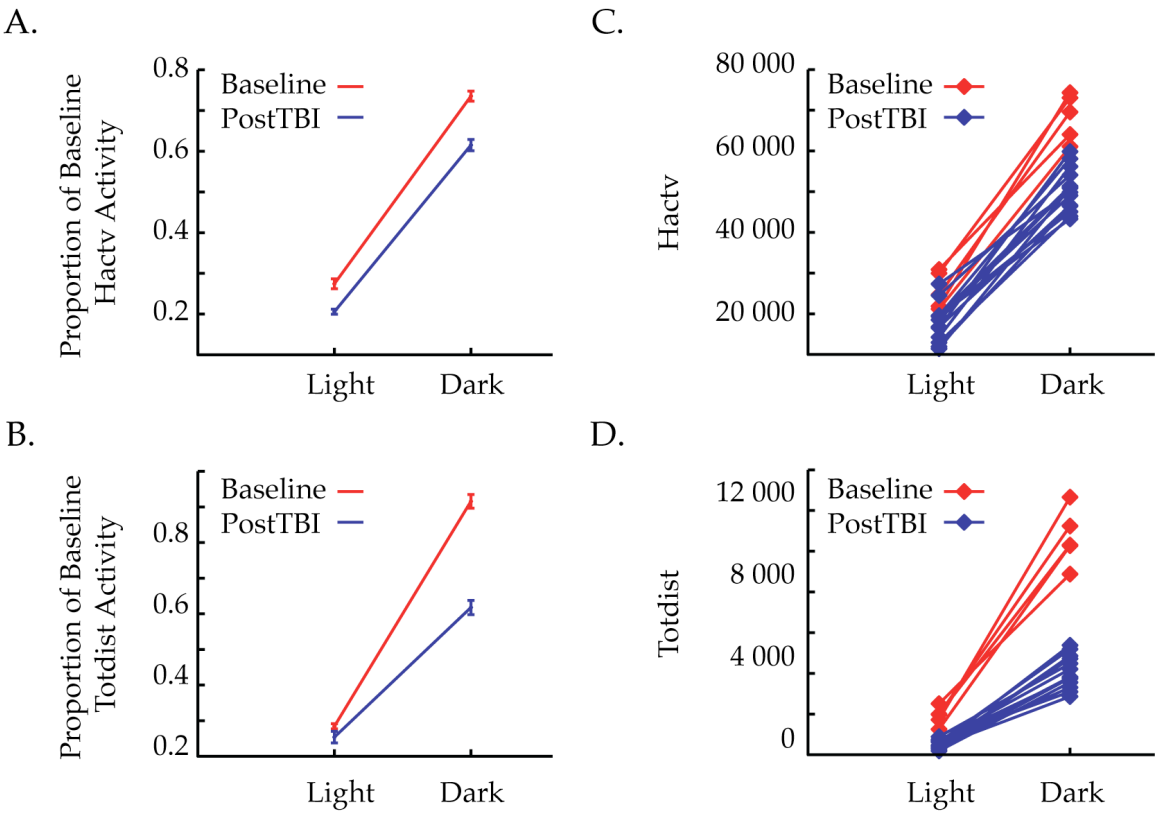

Figure 5.2 Preserved Nocturnal Behavior Pattern following Multiple TBI. Normalized average dark-light behavior for horizontal activity (A) and total distance (B), represented as mean ± s.e.m. of n=12 mice. Dark-light behavior in same illustrative mouse as **Figure 5.1** for horizontal activity (C) and total distance (D).

DEEP BRAIN STIMULATION FOLLOWING MULTIPLE TBI

In the previous section, a mouse model of closed head injury, multiple TBI, was described. The deficits caused by this model of TBI are long-lasting enough for experiments that include electrode implantation surgery and subsequent recovery from surgery. With a brain injury model that results in sufficiently long-lasting deficits, the effects of deep brain stimulation on brain-injured mice can be tested. Here, the effect of DBS on injured mice is tested.

Neurological and Motor Activity Deficits

Neurological and motor activity deficits for this set of mice is confirmed in **Table 5.2** and **Figure 5.3**. In this set of mice (n=14), the range of NSS overall scores was 3-10, and the average overall score was 7.3±0.8 (**Table 5.2**). This average score is significantly different from 0 (t_{12} = 12.73, $p<0.001$; signed rank = 0, $p<0.001$). To determine motor activity deficits, daily summed and normalized data were grouped as follows: baseline, post injury (PostTBI), and post surgery (PostSx). These grouped data were averaged across mice (n=14). Averaged deficits can be seen in **Figure 5.3.A-B**, and raw daily activity in one illustrative injured and stimulated mouse can be found in **Figure 5.3.C-D**. Motor activity deficits after injury as well as after surgery were significantly different from baseline using t-tests as well as Wilcoxon signed ranks test. In horizontal activity, post injury was significantly less than baseline activity (t_{18} = -9.66, $p<0.001$; z = -3.82,

Table 5.2 Neurological Severity Screen following Multiple TBI, later stimulated.

Neurological Tests (in the order of performance)	**Number of mice that Failed**	**Total of mice Tested**
Exit from 30 cm circle within 3 minutes	9	14
Straight walk	11	14
Startle reflex	10	14
Seeking behavior	3	14
Hind limb flex	2	14
Flat beam balance for 10 seconds	13	14
Round beam balance for 10 seconds	14	14
3 cm beam walk within 3 minutes	12	14
2 cm beam walk within 3 minutes	13	14
1 cm beam walk within 3 minutes	13	14

NSS tests are scored pass (0, normal behavior) or fail (1, abnormal behavior). The range of overall scores (*i.e.*, number of tests failed) was 3-10 and the overall score average was 7.3±0.8.

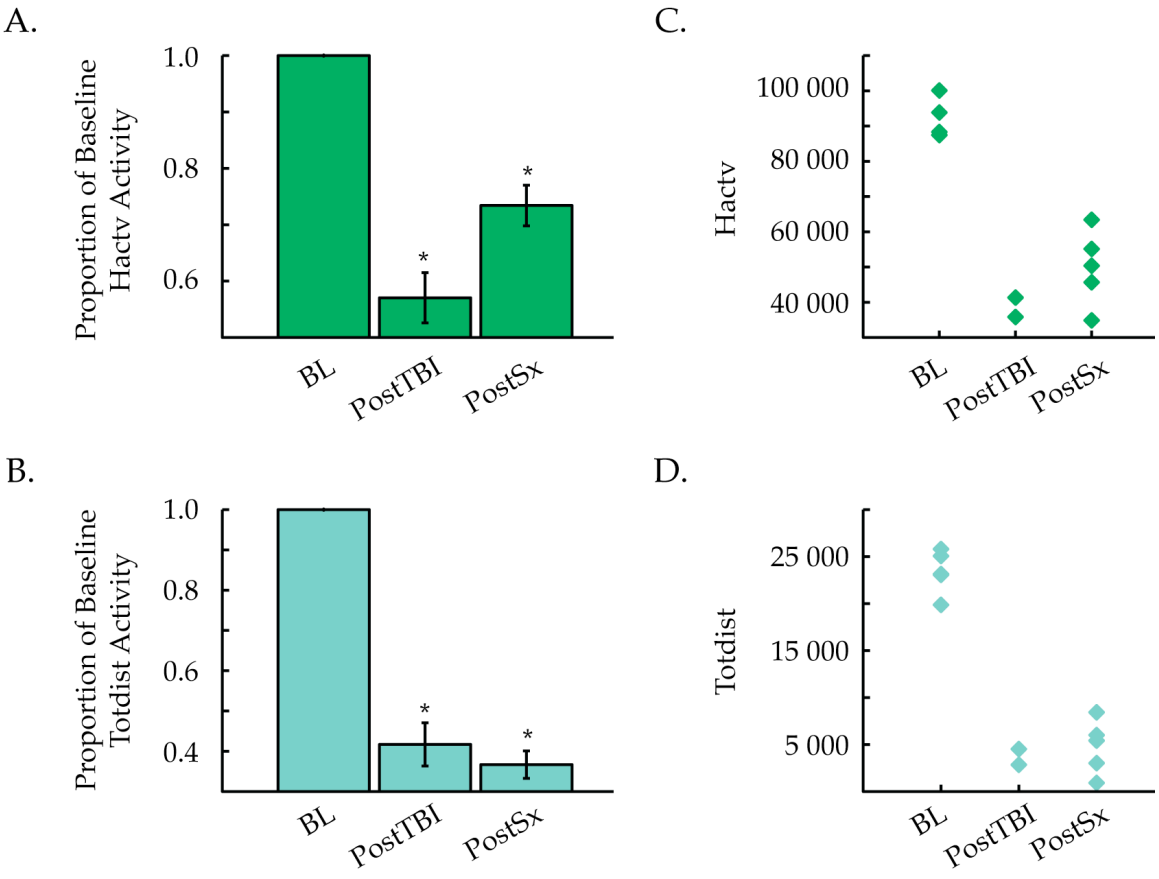

Figure 5.3 Motor Activity Deficits following Multiple TBI. Normalized, grouped, average daily activity for horizontal activity (A) and total distance (B), represented as mean ± s.e.m. of n=14 mice that were later stimulated. Grouped raw daily activity in one injured and stimulated mouse for horizontal activity (C) and total distance (D). * $p<0.001$. BL — baseline, PostSx — post surgery, PostTBI — post injury.

$p<0.001$) and post surgery was significantly less than baseline (t_{75} = -7.38, $p<0.001$; z = -6.20, $p<0.001$). In total distance, post injury was significantly less than baseline (t_{18} = -10.88, $p<0.001$; z = -3.82, $p<0.001$) and post surgery was significantly less than baseline (t_{75} = -18.51, $p<0.001$; z -7.51, $p<0.001$). Notice that the magnitude of motor activity deficit in these mice is larger than can be seen in **Figure 5.1**. For recovery without intervention mice, motor activity deficits immediately after injury were 70% and 50% of baseline for the two data measures while injured and stimulated mice had motor activity deficits of 55% and 40%. This is to be expected; multiple TBI, stimulated mice had a higher average NSS score, *i.e.*, a higher severity of injury, than recovery without intervention mice. It is logical to expect higher motor activity deficits with correspondingly higher severity of injury.

In addition to neurological and motor activity deficits, these mice (n=14) also display preserved nocturnal behavior pattern (**Figure 5.4**). Again, 12 hour summed and normalized data were grouped into baseline, post injury, or post surgery and then averaged across mice. This average can be found in **Figure 5.4.A-B** and raw data from one illustrative injured and stimulated mouse can be found in **Figure 5.4.C-D**. As with the recovery without intervention data set, activity in the dark is increased over activity in the light, *i.e.*, dark-light behavior is preserved.

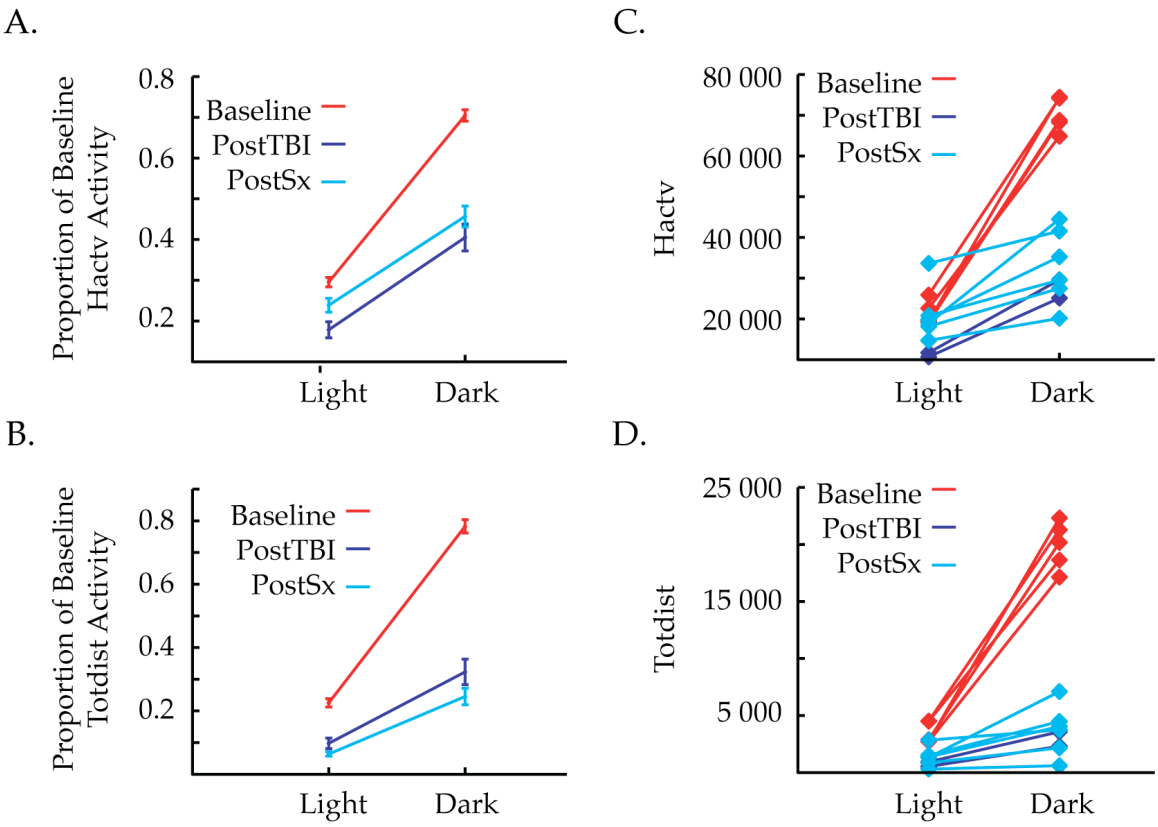

Figure 5.4 Preserved Nocturnal Behavior Pattern following Multiple TBI, Stimulated mice. Normalized, grouped, average dark-light behavior for horizontal activity (A) and total distance (B), represented as mean ± s.e.m. of n=14 mice that were later stimulated. Grouped raw dark-light behavior in same illustrative mouse as **Figure 5.3** for horizontal activity (C) and total distance (D). BL — baseline, PostSx — post surgery, PostTBI — post injury.

Effects of Deep Brain Stimulation

In the previous two chapters, DBS has been shown to increase arousal as measured by motor activity in intact mice. Here, the effects of DBS on brain-

injured mice have been tested. Mice were implanted bilaterally in the central thalamus (A: -1.70 mm, L: +/- 1.00 mm, D: -3.00 mm) and only those with at least one histologically confirmed hit were included in statistical analyses. A diagram of electrode placements can be found in **Figure 5.5**.

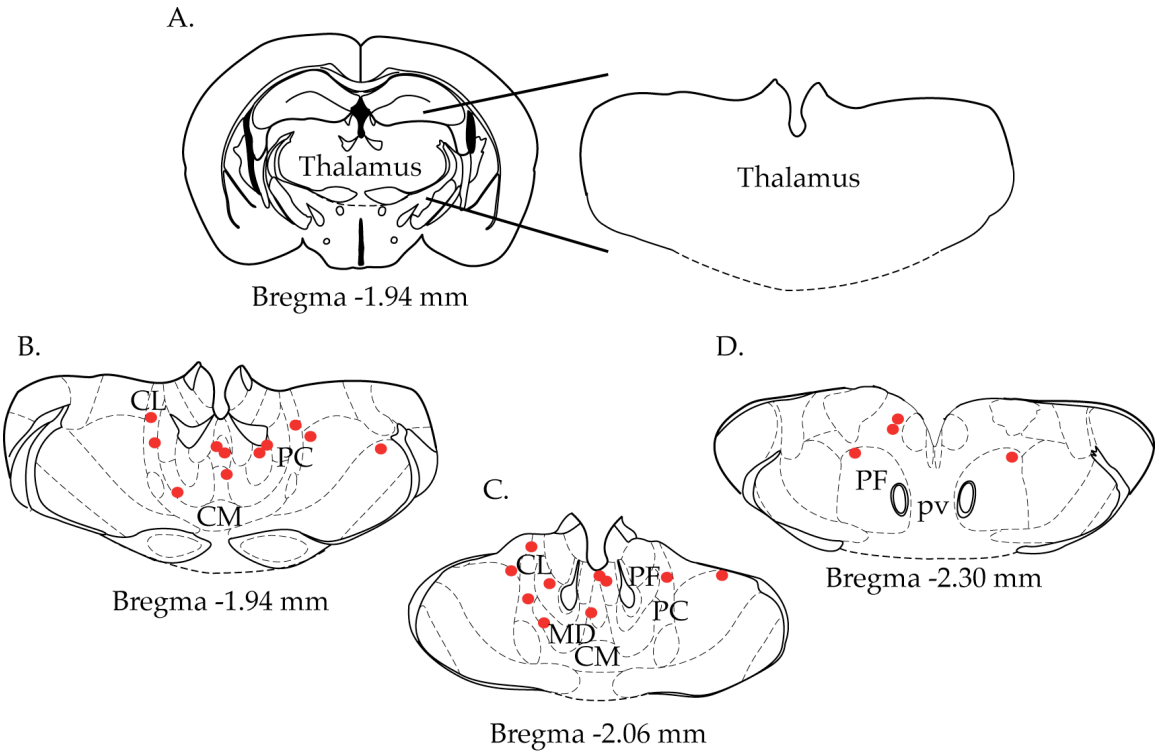

Figure 5.5 Electrode Placements of Multiple TBI, Stimulated mice. Cornal section of mouse brain at Bregma -1.94 mm and zoomed in image of thalamus for reference (A). Placements are represented as red dots on coronal sections at Bregma -1.94 mm (B), -2.06 mm (C), and -2.30 mm (D). Placements of n=14 mice. Diagrams adapted from Paxinos and Franklin (2001).

Motor activity, as measured by horizontal activity and total distance, increases during and after stimulation in brain injured mice. Data presented here represent sums of activity 10 minutes before, 10 minutes during, and 10 minutes after stimulation with activity during and after stimulation normalized to activity before stimulation. These normalized sums are then averaged across mice (n=14, 4-6 stimulations per mouse) and analyzed using parametric and non-parametric statistics to determine the effects of the stimulation, light phase of stimulation, and temporal pattern of stimulation. While an overall effect of stimulation by multi-factor ANOVA is seen in both horizontal activity ($F_{2,415}$ = 3.26, $p<0.05$, **Figure 5.6.A**) and total distance ($F_{2,342}$ = 3.69, $p<0.05$, **Figure 5.6.B**), there were no overall effects of light phase (**Figure 5.6.C-D**) or temporal pattern of stimulation (**Figure 5.6.E-F**). ANOVA analyses did uncover a significant interaction effect between temporal pattern and stimulation in horizontal activity ($F_{4,415}$ = 4.20, $p<0.01$). Using non-parametric analyses, an effect of stimulation as well as a lack of effect of light phase or temporal pattern were confirmed. The balanced Friedman test uncovered a significant effect of stimulation in horizontal activity (χ^2 = 17.67, $p<0.001$) and total distance (χ^2 = 22.97, $p<0.001$). While these data are not completely congruous with previous stimulation data collected in intact mice, these data do replicate the findings that DBS can increase motor activity and that the temporal pattern of stimulation can make a difference.

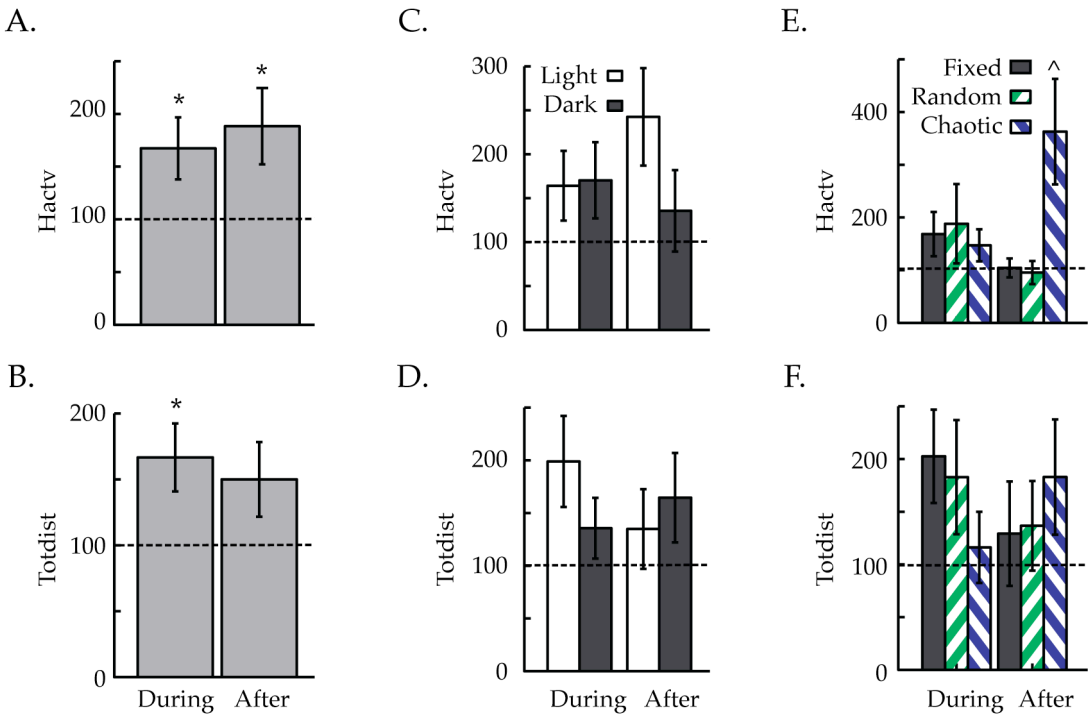

Figure 5.6 DBS following Multiple TBI increases Motor Aspect of Arousal. Response to stimulation in horizontal activity (A) and total distance (B). Differential response to stimulation in the dark and light in horizontal activity (C) and total distance (D). Differential response to temporal patterns of stimulation in horizontal activity (E) and total distance (F). Data are presented as mean ± s.e.m. of n=14 mice (4-6 stimulations per mouse). Data represent 10 minutes before, 10 minutes during, and 10 minutes after stimulation. Data during and after stimulation are normalized to data before stimulation. * $p<0.05$ compared to before stimulation, ^ $p<0.05$ compared to other temporal patterns.

In looking more closely at post-hoc analyses, the effect of stimulation is confirmed and the interaction effect between temporal pattern and stimulation seen in horizontal activity is explained. Using t-tests and Mann-Whitney U tests, horizontal activity is increased during ($t_{140} = 2.29$, $p<0.05$; $z = -3.03$, $p<0.001$) and after ($t_{139} = 2.44$, $p<0.05$; $z = -4.54$, $p<0.001$) stimulation compared to before stimulation, and total distance is increased during ($t_{105} = 2.58$, $p<0.05$; $z = -4.06$, $p<0.001$) and after ($z = -4.58$, $p<0.001$) stimulation compared to before stimulation. Comparing temporal patterns of stimulation, only after chaotic stimulation is horizontal activity increased compared to fixed ($t_{48} = -2.54$, $p<0.05$) and random ($t_{50} = -2.61$, $p<0.05$) stimulation using Bonferroni-corrected t-tests. This difference was not confirmed with non-parametric statistical tests. Despite the lack of strong differences between all three temporal patterns, these data suggest that temporal pattern makes a difference in CT/DBS.

In addition to normalized averaged data, raw motor activity of one illustrative injured and stimulated mouse is shown in **Figure 5.7**. The three stimulations represented in this figure occured during the dark. Notice the very little movement registered by the total distance data measure. This is much less than similar plots for intact mice (see **Figures 4.3** and **4.6** on page 79 and 87). As total distance is a measure of ambulation, it is possible that these injured mice are moving (as evidenced by horizontal activity), but have decreased motivation to

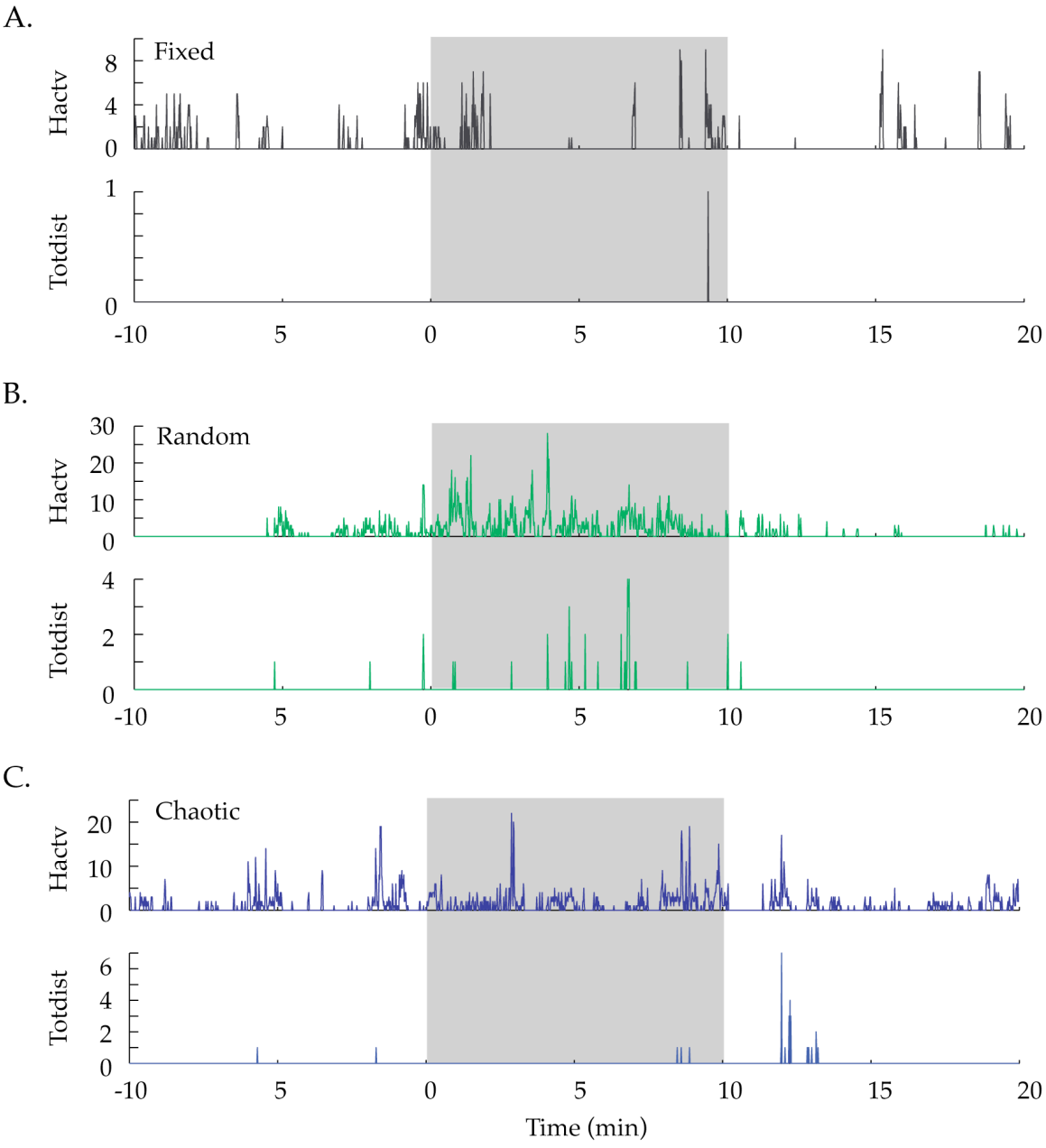

Figure 5.7 Motor Activity Response to DBS in one Multiple TBI mouse. Response to fixed (A), random (B), and chaotic (C) stimulation in one mouse during the dark. Data are presented at a sampling frequency of 1 hz. Grey boxes denote epochs of stimulation.

walk within their cages thereby staying in relatively the same spot. This has implications for the high variability inherent in these data, and this implication will be discussed below.

DISCUSSION

Findings

Here, a modified closed head injury model, multiple TBI, is described that results in acute neurological deficits, motor activity deficits lasting 11-14 days post injury, and preserved nocturnal behavior pattern. These data also show that CT/DBS can increase the motor aspect of arousal in this traumatic brain injury model. These data also suggest that temporal pattern of stimulation makes a difference as evidenced by the interaction effect of temporal pattern and stimulation. While differences between the three temporal patterns are not strong for all time points (during and after stimulation), chaotic stimulation does increase horizontal activity after stimulation more than either fixed or random stimulation. Temporal patterning of CT/DBS can modulate its effect in this mouse model of TBI.

Literature

Little is published in the pre-clinical or clinical literature on the use of DBS in brain injured patients or animal models of brain injury. Zhang and colleagues (2011) studied the effect of DBS on molecular changes after cerebral ischemia in

rats, and they found that stimulation of the olfactory bulb after injury reduced the expression of a molecule thought to inhibit axonal growth, reduced infarct volume, and improved neurological function. In a second study in rats, Liu and colleagues (2012) found that stimulation of the cerebellar fastigial nucleus after cerebral ischemia promoted the expression of a DNA repair molecule as well as improved performance on a functional motor task. The data presented here support these articles with more evidence that DBS can ameliorate deficits caused by acquired brain injury.

Caveats

Home cage motor activity data are inherently variable especially with brain injured mice. Sources of variability include endogenous variability over the course of a single day, over the course of the injured mouse's recovery, and from mouse to mouse. Inter-mouse variability can be caused by inherent differences between mice, differences in injury severity, differences in injury locus, and differences in electrode placement. This multifaceted variability can make it difficult to uncover trends or statistical differences between groups of treatments. To mitigate some of this inherent variability, the effect of stimulation has only been analyzed on a very small timeframe surrounding that stimulation, and these analyses have included normalization to the behavior of the mouse directly prior to stimulation. But this treatment of the data does not completely remove the

variablity. In a particularly vexing example, there was absolutely no movement in one data measure before, during, or after stimulation in one quarter of all stimulations. These non-responding events had to be removed from analysis because they obliterated any and all significant difference of stimulation when included. It has already been hypothesized that these non-responding events are caused by the injured mouse's decreased motivation to walk. As the only other ways to reduce variability include absolute control over the injury mechanism and electrode implantation, all studies going forward must be done with the understanding that these experiments are inherently variable and the data collected are inherently complex.

Conclusions

This chapter discusses the development of a mouse model of TBI that results in closed head injury that resembles concussion and with motor activity deficits that last up to two weeks. The most promising conclusion from these data is that CT/DBS can be used to increase the motor aspect of arousal in a mouse model of multiple TBI. Despite a lack of strong statistical differences between all three temporal patterns tested, the data collected here suggest that temporal pattern of CT/DBS in a mouse model of TBI can make a difference in magnitude of increases in motor activity. The data presented here are promising and suggest that DBS can help an injured brain maintain arousal.

Chapter 6: Sensory Responsiveness with DBS

DBS has been shown to increase generalized arousal as measured by motor activity. Since the operational definition of generalized arousal is not confined to only motor activity, the effects of DBS on sensory responsiveness were explored. Under the assumption that DBS increases generalized arousal, it was hypothesized that DBS paired with a sensory stimulus would increase sensory responses over and above the response to sensory stimulus alone. In these experiments, the sensory modality chosen was olfaction. The olfactory system of mice is highly responsive, and there is a body of data suggesting ease of manipulation of generalized arousal using olfactory stimuli. The olfactant chosen for all underlying experiments was benzaldehyde, known to activate olfactory bulb mitral cells without concomitant trigeminal activation.

SIMULTANEOUS STIMULUS DELIVERY

In this first experiment, mice (both intact and injured) were presented with three stimuli: olfactory, DBS, and simultaneous olfactory stimulation and DBS. Mice were implanted bilaterally in the central thalamus, and diagrams of electrode placement for intact and injured mice can be found in **Figure 6.1**. Once implanted, mice were placed in isolation boxes to reduce exposure to unintended external stimuli for the duration of the study. A more detailed description of methodology can be found in Chapter 2 (page 47).

Figure 6.1 Diagram of electrode placements for Intact and Injured mice. Coronal section of mouse brain at Bregma -1.94 mm and zoomed in image of thalamus for reference (A). Placements in intact mice (n=8) are represented as red dots on coronal sections at Bregma -1.94 mm (B), -2.06 mm (C), and -2.30 mm (D). Placements in injured mice (n=7) are represented as blue dots on coronal sections at Bregma -1.94 mm (E), -2.06 mm (F), and -2.30 mm (G). Diagrams adapted from Paxinos and Franklin (2001).

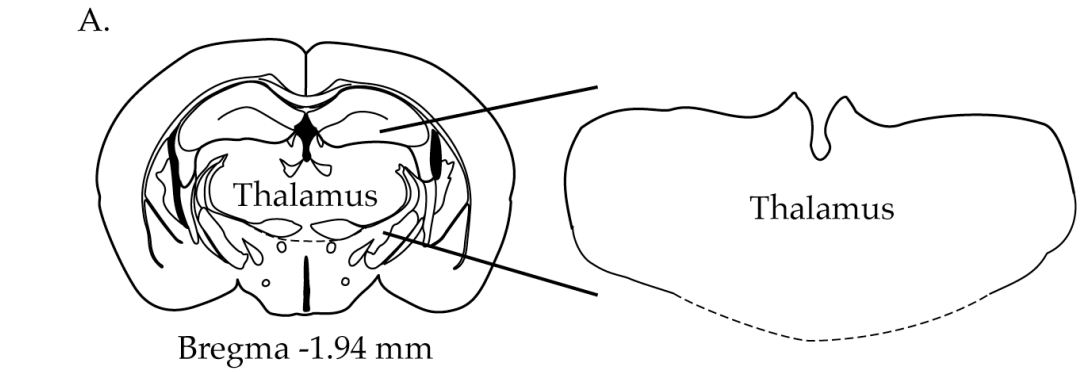

Intact

Injured

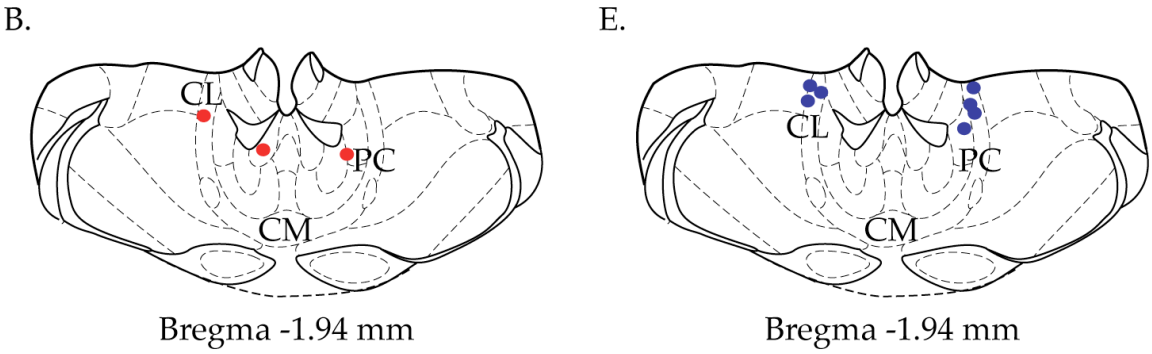

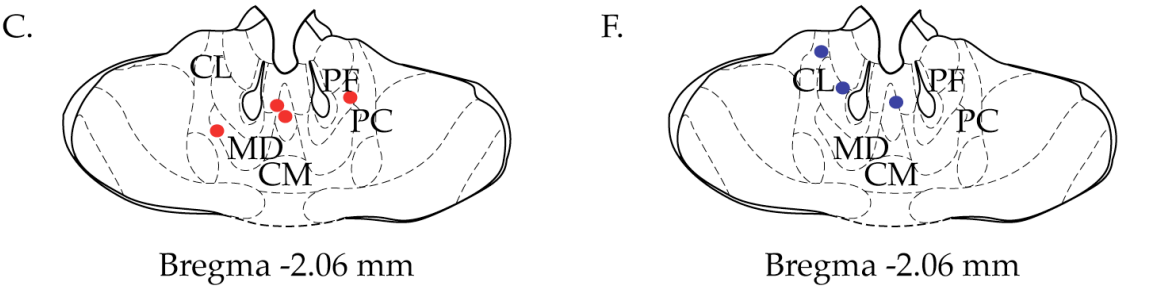

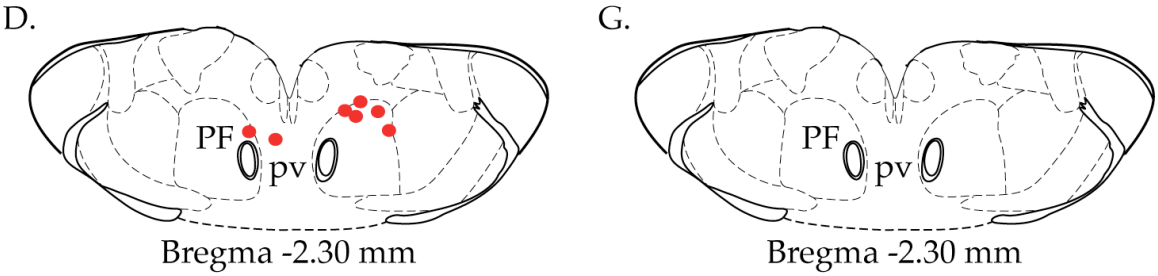

Olfactory Responsiveness in Intact mice

Responses to stimuli in intact implanted mice (n=8) were as expected. Raster plots of response to the three stimuli and a control activity in one illustrative intact mouse can be found in **Figure 6.2**. In each raster plot, black lines denote motor activity and white spaces denote inactivity. Each row in each raster plot represents a single trial of a given stimulus type. Notice that for each raster trial there is 1 minute of spontaneous activity followed by 1 minute of inactivity. After this inactivity, the stimulus is presented (represented by colored rectangles above the raster plots: red — olfactory, blue — DBS, purple — simultaneous olfactory and DBS or 'Both'). The control raster plot is a random selection of epochs during which there was no stimulation as well as at least one minute of inactivity. For each mouse, raster plots were collapsed into an average response to each stimulus, these averages were integrated every 10 seconds, and these integrated averages were averaged across mice (n=8). This integrated average response can be seen in **Figure 6.3.A**. These data showed a strong immediate response to olfactory stimulation both with and without concurrent DBS that slowly tapered over the course of 1.5-5 minutes (**Figure 6.3.A**). DBS, on the other hand, produced a delayed increase in activity that presented at 2.5-3 minutes and lasted an addition 1-2 minutes.

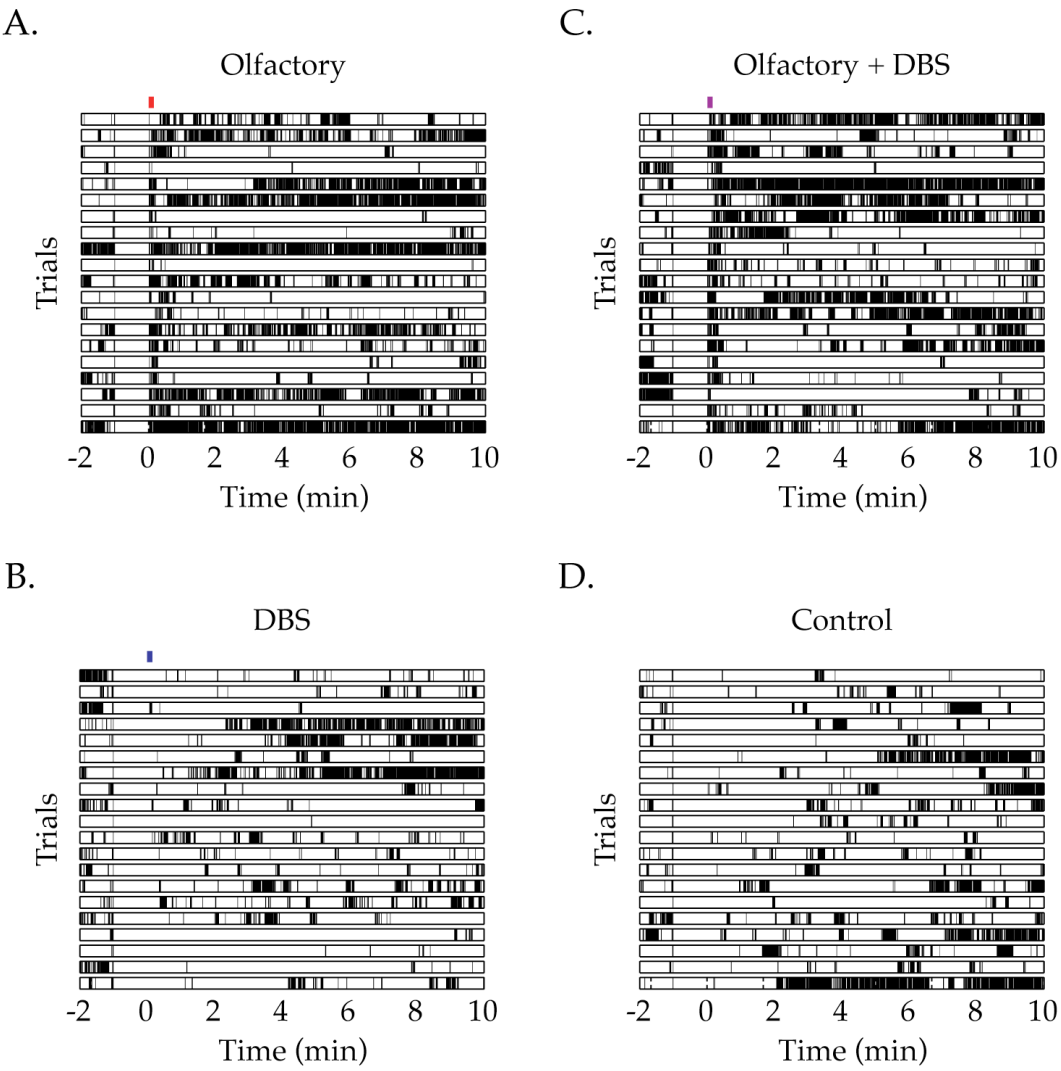

Figure 6.2 Raster plots of activity in one illustrative intact mouse. Black lines represent activity, white areas represent inactivity. Each row represents a single trial of an olfactory stimulus (A), DBS (B), a simultaneous olfactory and DBS (C), and 20 randomly chosen control epochs with no stimulation (D). Stimulation delivery is denoted by colored boxes at the top of raster plots; blue denotes DBS, red denotes an olfactory stimulus, and purple denotes simultaneous DBS and olfactory stimulation.

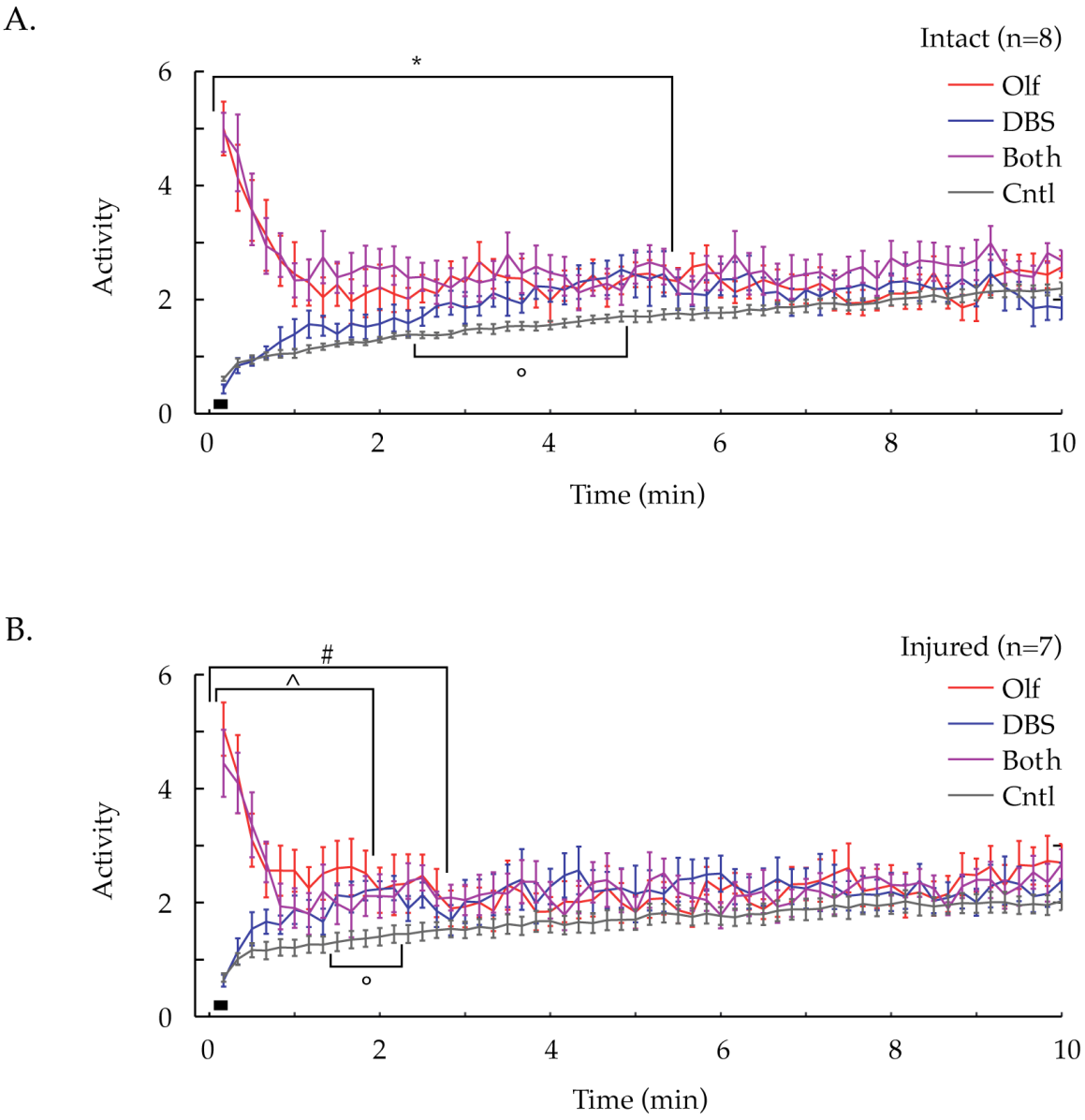

Figure 6.3 Response to olfactory stimulation and DBS in intact and injured mice: comparison of stimulation types. Activity response to olfactory, DBS, simultaneous olfactory and DBS stimulation, and non-stimulated controls averaged across intact mice (n=8, A) and injured mice (n=7, B). Stimulation denoted by black rectangles. *p<0.05 Olfactory and Both compared to control; °p<0.05 DBS compared to control; #p<0.05 Both compared to control; ^ p<0.05 Olfactory compared to control.

In the statistical analysis of these data, ANOVA uncovered an effect of stimulation ($F_{3,840}$ = 134.85, p<0.001), an effect of time ($F_{29,840}$ = 2.23, p<0.001), and an effect of the interaction of stimulation and time ($F_{87,840}$ = 3.92, p<0.001, **Figure 6.3.A**). Friedman analyses confirmed these results. To uncover more detail about these effects, Bonferroni-corrected post-hoc t-tests and Wilcoxon matched-pair signed-ranks tests were performed. Response to olfactory and simultaneous olfactory and DBS were larger than control activity at the time of stimulation until 5.17 minutes after stimulation (Olf: t_9 = 2.96, p<0.05; Both: t_8 = 2.98, p<0.05). Response to DBS was larger than control activity from 2.67 minutes after stimulation (t_8 = 2.65, p<0.05) to 4.38 minutes after stimulation (t_9 = 2.99, p<0.05). At no time point was olfactory response alone significantly different from response to simutaneous olfactory and DBS, *i.e.*, no additional activity response is seen when olfactory stimulus and DBS are paired.

Olfactory Responsiveness in Injured Mice

Response to stimuli in multiple TBI mice (n=7) were similar to that seen in intact mice. NSS scores of these mice are described in **Table 6.1**, and on average, injured mice had a severity score of 7.29±0.78. Rasterplots of activity response to stimuli in one illustrative injured mouse can be found in **Figure 6.4**. Again, black denotes activity, and white denotes inactivity; stimulation epochs are denoted by colored rectangles. Upon examination of the averaged data (**Figure 6.3.B**), a

Table 6.1 Neurological Severity Screen following Multiple TBI, sensory study

Neurological Tests (in the order of performance)	Number of mice that Failed	Total of mice Tested
Exit from 30 cm circle within 3 minutes	6	7
Straight walk	7	7
Startle reflex	5	7
Seeking behavior	4	7
Hind limb flex	0	7
Flat beam balance for 10 seconds	6	7
Round beam balance for 10 seconds	7	7
3 cm beam walk within 3 minutes	5	7
2 cm beam walk within 3 minutes	5	7
1 cm beam walk within 3 minutes	6	7

NSS tests are scored pass (0, normal behavior) or fail (1, abnormal behavior). The range of overall scores (*i.e.*, number of tests failed) was 3-6 and the overall score average was 7.29±0.78.

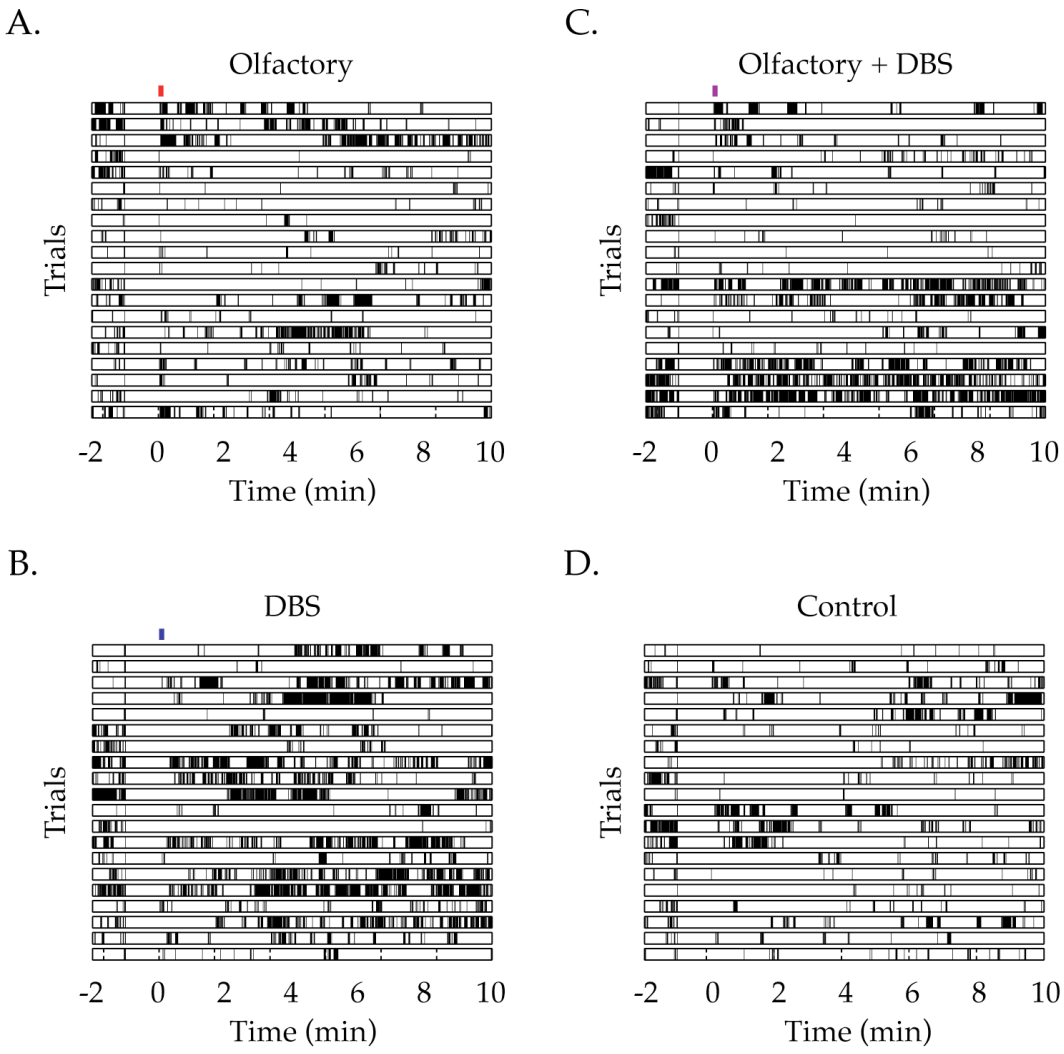

Figure 6.4 Raster plots of motor activity in one illustrative injured mouse. Black lines represent activity, white areas represent inactivity. Each row represents a single trial of an olfactory stimulus (A), DBS (B), a simultaneous olfactory and DBS (C), and 20 randomly choosen Control epochs with no stimulation (D). Stimulation delivery is denoted by colored boxes at the top of raster plots; blue denotes DBS, red denotes an olfactory stimulus, and purple denotes simultaneous DBS and olfactory stimulation.

strong response to olfactory stimuli, with or without concurrent DBS, is seen. This response dies off over the course of 1-2.5 minutes. Also seen is a slow, less intense DBS response; this response to DBS shows up after about a minute and dies off after another minute.

Parametric statistical analysis (ANOVA) uncovered an effect of stimulation ($F_{3,720} = 54.82$, $p<0.01$), an effect of time ($F_{29,720} = 1.57$, $p<0.05$), and a significant interaction effect between stimulation and time ($F_{87,720} = 2.85$, $p<0.01$, **Figure 6.3.B**). Nonparametric Friedman analyses confirmed these results. Bonferroni-corrected t-tests and nonparametric Wilcoxon matched-pair signed-ranks tests were used to uncover more detail about these data. Response to olfactory stimulation was significantly greater than control activity from the time of stimulation to 1.83 minutes after stimulation ($t_8 = 2.70$, $p<0.05$). Response to simutaneous olfactory stimulus and DBS was significantly greater than control activity from the time of stimulation to 2.67 minutes after stimulation ($t_{12} = 2.97$, $p<0.05$). Response to DBS appears at 1.50 minutes after stimulation ($t_{12} = 3.45$, $p<0.01$) and lasts until 2.17 minutes after stimulation ($t_{11} = 3.06$, $p<0.05$). There were no significant differences at any time point between olfactory stimulation response alone and response to simutaneous olfactory stimulation and DBS. Contrary to expectation, simutaneous stimulation of olfactory and DBS did not increase activity response greater than olfactory stimulation alone.

Comparison of Olfactory Responsiveness in Intact and Injured Mice

While the pattern of responses to stimuli in intact and injured mice was similar, there were distinct differences. Both intact and injured mice showed a strong immediate response to olfactory stimuli whether or not it was paired with DBS, but in intact mice, the decay of this response lasted roughly 5 minutes while in injured mice the response disappeared much more quickly, disappearing by 3 minutes after stimulation. DBS response was also different between the two groups; in intact mice, response to DBS appeared at around 2.5 minutes and lasted 2-3 minutes. However in injured mice, response to DBS appeared much more quickly, at 1-1.5 minutes, even if it did not last as long. While ANOVA did not reveal an overall difference between intact and injured mice, it did reveal an interaction effect of injury status and stimulation type ($F_{3,1647} = 9.62$, $p<0.001$). In **Figure 6.5**, direct comparisons of response to each stimulation type in intact and injured mice can be found (these are the same data as **Figure 6.3**). Notice that while the timing of responses as compared to control in each set is different, the variability of responses precludes the direct comparison of intact and injured response to the same stimulation from being significantly different except when it comes to DBS. DBS response was greater and more quickly seen in injured mice compared to control (**Figure 6.5.B**). This difference first appeared at 0.67 minutes after stimulation ($t_9 = -2.49$, $p<0.05$) and lasted until 2.00 minutes after

Figure 6.5 Response to olfactory stimulation and DBS: comparison of intact and injured mice. These data are the same as plotted in **Figure 6.3**. Activity response to olfactory (A), DBS (B), simultaneous olfactory and DBS stimulation (C), and non-stimulated controls (D) averaged across intact mice (n=8) and injured mice (n=7). Stimulation denoted by colored rectangles; red — olfactory, blue — DBS, purple — simultaneous olfactory and DBS. *$p<0.05$ intact compared to injury.

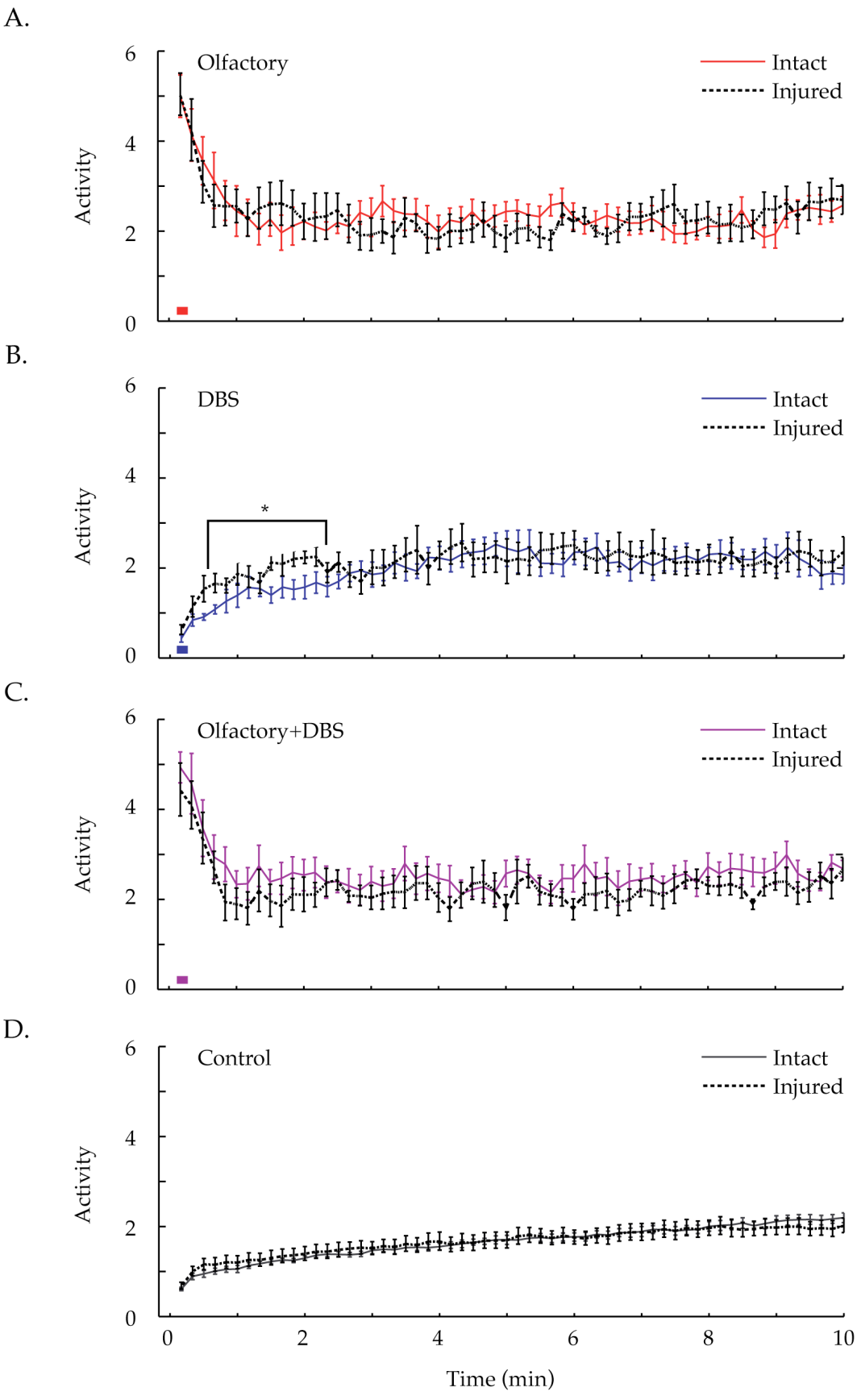
A.
Olfactory
Intact
Injured
Activity
6
4
2
0
B.
DBS
Intact
Injured
*
Activity
6
4
2
0
C.
Olfactory+DBS
Intact
Injured
Activity
6
4
2
0
D.
Control
Intact
Injured
Activity
6
4
2
0
0
2
4
6
8
10
Time (min)

stimulation (t_{11} = -2.26, $p<0.05$). Injured mice responded more strongly and more quickly to DBS than intact mice.

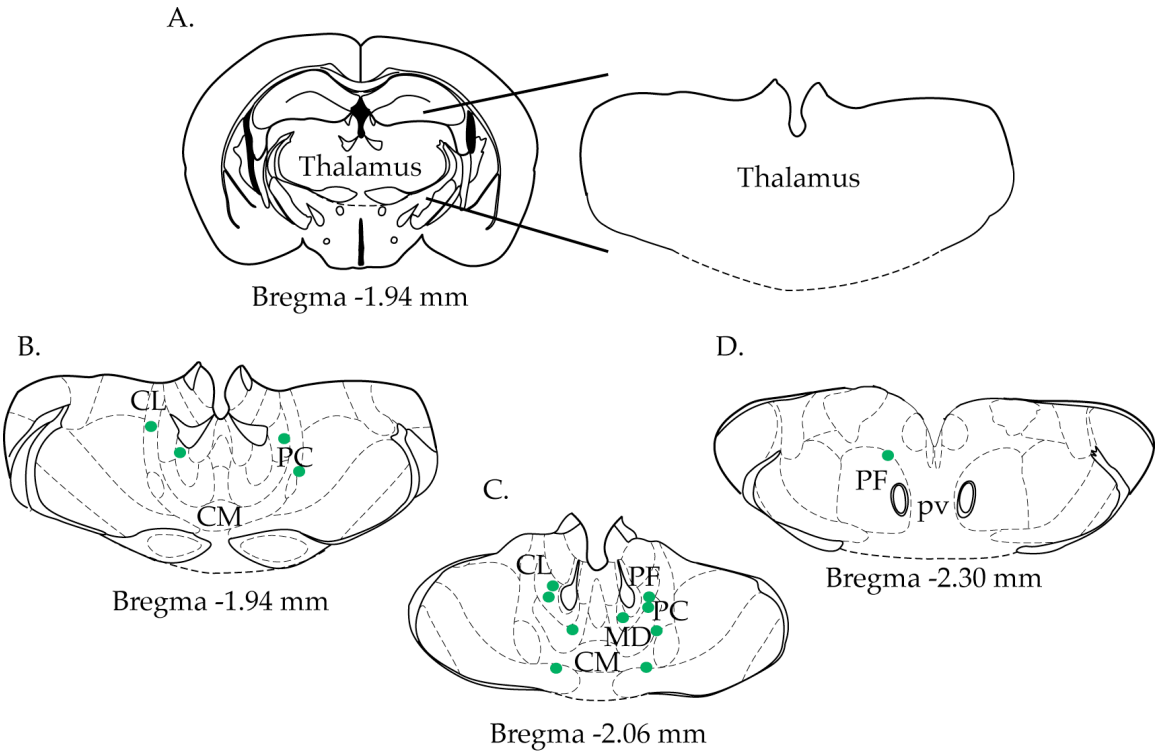

Figure 6.6 Diagram of electrode placements for mice in olfactory delayed after DBS experiment. Coronal section of mouse brain at Bregma -1.94 mm and zoomed in image of thalamus for reference (A). Placements are represented as green dots on coronal sections at Bregma -1.94 mm (B), -2.06 mm (C), and -2.30 mm (D). Placements of n=7 mice. Diagrams adapted from Paxinos and Franklin (2001).

OLFACTORY STIMULATION DELAYED AFTER DBS

With a lack of additive response of olfactory stimulation and DBS when presented concurrently, it may be that DBS needs to be presented first in order to facilitate greater response to olfactory stimulation. Since it took a few minutes for the response to DBS to be seen, it make take several minutes to increase generalized arousal and subsequently increase sensory responsiveness. To test this, a paradigm with an olfactory stimulation delayed after DBS was designed. A detailed description of the methodology can be found in Chapter 2 (page 47). Briefly, intact mice (n=7) were implanted bilaterally in the central thalamus, and diagrams of electrode placement for olfactory delayed after DBS mice can be found in **Figure 6.6**. Once implanted, mice were placed in isolation boxes to reduce unintended external stimuli during the study. Mice were then presented with either a 10 second DBS followed by an olfactory stimulus or no DBS followed by an olfactory stimulus. Each experimental pair was presented 20 times to each mouse. Raster plots of response to these experimental conditions in one illustrative mouse can be found in **Figure 6.7**. Black denotes activity, and white denotes inactivity; stimulation epochs are denoted by colored rectangles: red — olfactory, blue — DBS. Notice 1 minute of spontaneous activity and 1 minute of inactivity followed by initial DBS/NoDBS, and after another 1 minute, the olfactant presentation.

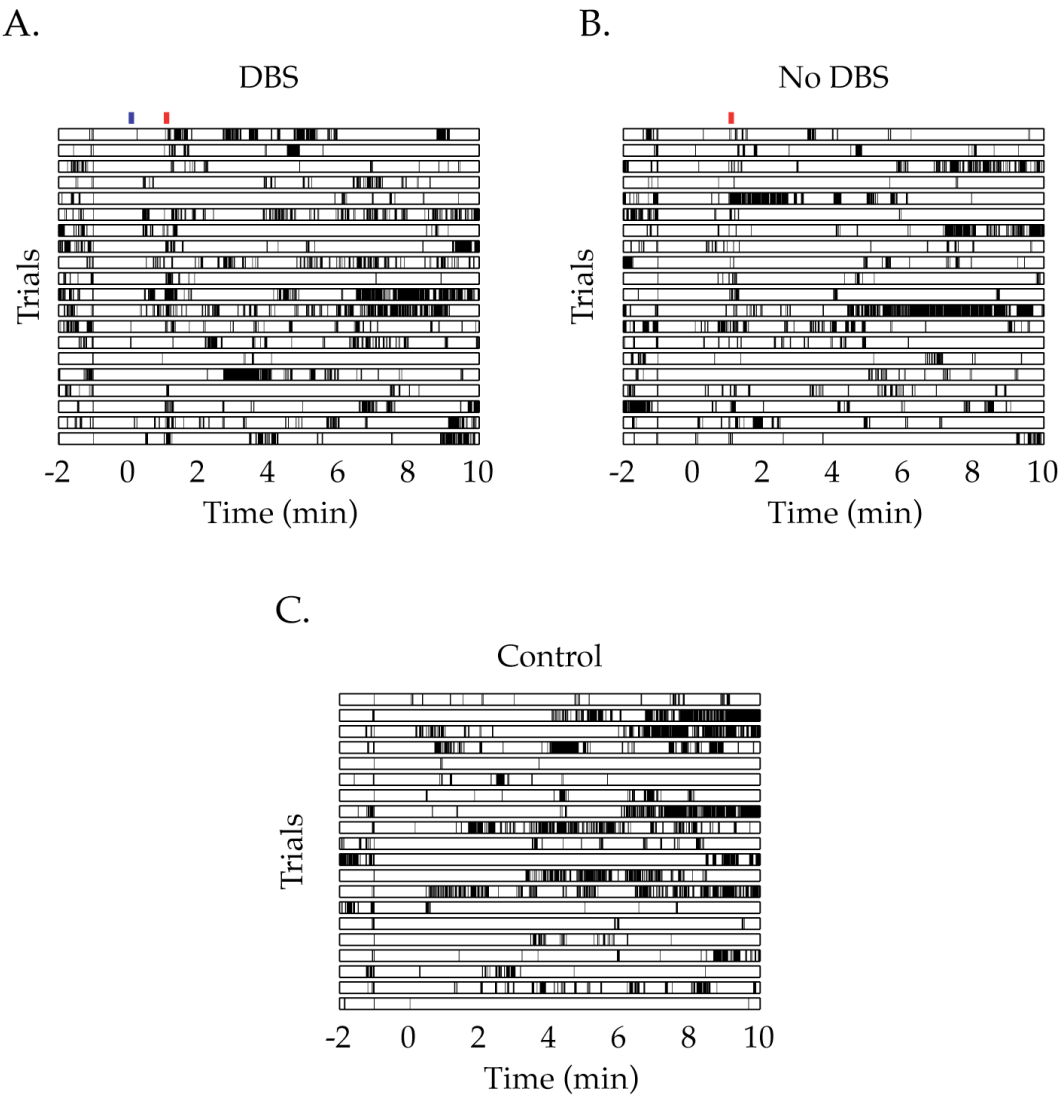

Figure 6.7 Raster plots of motor activity in one illustrative mouse in olfactory delayed after DBS experiment. Black lines represent activity, white areas represent inactivity. Each row represents a single trial of DBS followed by an olfactory stimulus (A), No DBS followed by an olfactory stimulus (B), and 20 randomly choosen Control epochs with no stimulation (C). Stimulation delivery is denoted by colored boxes at the top of raster plots; blue denotes DBS, red denotes an olfactory stimulus.

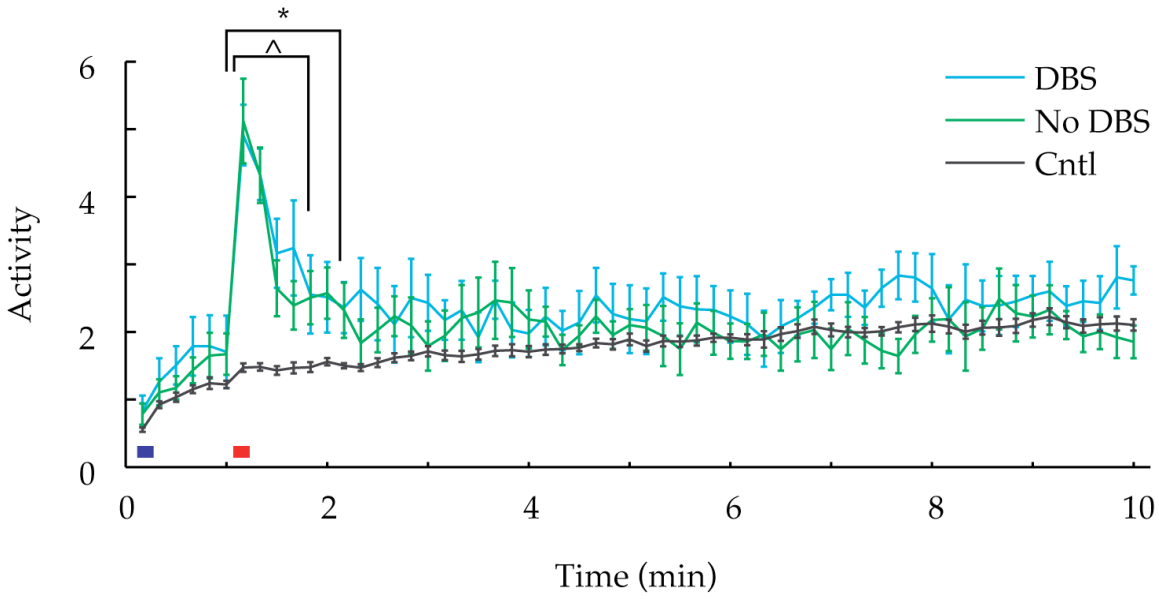

Figure 6.8 Response to olfactory stimulation and DBS in olfactory delayed after DBS experiment. Activity response to DBS and olfactory stimulation averaged across mice (n=7). Stimulation denoted by colored rectangles; red — olfactory, blue — DBS. *p<0.05 DBS compared to control; ^p<0.05 NoDBS compared to control.

Statistical analyses using ANOVA uncovered an effect of stimulation ($F_{2,540}$ = 51.44, p<0.001), time ($F_{29,540}$ = 8.78, p<0.001), and an interaction effect between stimulation and time ($F_{58,540}$ = 1.83, p<0.001, **Figure 6.8**). These results were confirmed using nonparametric Friedman analyses. To uncover further details, post-hoc t-tests and nonparametric Wilcoxon matched-pair signed-ranks tests were performed. In the first minute after initial DBS/NoDBS, there were no differences between control, DBS, or NoDBS. Response to olfactory stimulation with NoDBS priming was strong and lasted from the time of stimulation (t_6 = 5.80, p<0.001) to

0.83 minutes after olfactory stimulation ($t_6 = 2.66$, $p<0.05$). Response to olfactory stimulation with DBS priming was also strong and lasted from the time of stimulation ($t_6 = 7.58$, $p<0.001$) to 0.50 minutes after olfactory stimulation ($t_6 = 2.50$, $p<0.05$). There were no significant differences between response with DBS priming and with NoDBS priming. Even with an olfactory stimulus delayed 1 minute after DBS, there was no additive response to olfactory stimulation and DBS.

DISCUSSION

Findings

In all experiments, a strong immediate response to a pleasant food-like olfactant and a smaller slow response to DBS were seen. In both the simultaneous presentation experiment and olfactory delayed after DBS experiment, there was no evidence for the additive effect of DBS on response to an olfactory stimulus. However, the timing of response to DBS may play an important roll in the facilitation of an olfactory response, and more work is needed to determine the proper timing of such a stimulation regime. Also the differences between response to DBS in intact and injured mice suggest that using intact mice for such an experiment might not have been the most beneficial. Since injured mice show a stronger and quicker response to DBS than intact mice, they might be more likely to show a facilitation of olfactory response with DBS if appropriate timing of stimulation can be discovered.

Literature

This is no body of work looking at how DBS effects olfaction in any animal model. There are a few anecdotes and papers in the clinical literature relating DBS, especially of the motor thalamus and subthalamus, to olfaction. Here, response to olfactory stimuli was used as a behavioral surrogate of generalized arousal with the hypothesis that DBS of the central thalamus would increase the magnitude of sensory responses indirectly by increasing generalized arousal. There are no papers that touch on this topic or hypothesis in either the preclinical or clinical literature.

Caveats

As with virtually all behavioral experiments, high variability between and within subjects can obscure any positive results. In the simultaneous delivery experiment, the sensitivity to baseline behavioral levels was mitigated by waiting for the mouse to be in a state of quiescence for 1 minute. With the olfactory delayed after DBS experiment, this consistent low baseline is lost because of the desired timing of stimulation. Other sources of variability include differences in exact electrode placement. In brain injured mice, differences in severity and locus of brain injury may also contribute to variability in mouse response to DBS.

Another consideration to take into account is the sensory stimulation paradigm used. The olfactory stimuli presented in this experiment are not pure

olfactant only stimuli. The stimulus delivery apparatus includes a regulator that clicks, and the smell is delivered through air being pushed over a container of the olfactant. The mouse surely hears the click and the whoosh of air before smelling the olfactant. The length of time the olfactant lingers in the cage is also an uncontrolled variable. Due to these practicalities, these experiments may not be comparable to more controlled physiological studies of olfaction; however, this stimulation paradigm does produce differential behavioral responses to different types of stimulation without habituation.

Conclusions

These experiments show strong immediate responses to an olfactory stimulus, benzaldehyde, and small slow responses to DBS. While it was expected that olfactory stimulation and DBS presented together would produce even larger responses than olfactory stimulation alone, there is no strong evidence that DBS increases response to this olfactant. Studies replicating this work with variable timing for delay between DBS and olfactory stimuli are needed to ensure that this is truly a negative result.

Chapter 7: Discussion

This thesis describes previously unexplored pre-clinical work into an application of deep brain stimulation (DBS) to increase generalized arousal and to treat motor activity deficits in traumatic brain injury (TBI). The effectiveness of DBS to increase generalized arousal was measured by observing spontaneous motor activity as well as olfactory responsiveness. A small set of frequencies, amplitudes, and temporal patterns of stimulation were explored. Both intact mice and a mouse model of TBI were tested. Below, the conclusions of this work are described, the implications of the work to the larger literature are considered, and caveats associated with the conclusions and the limitations of this work are discussed. Finally, the broad clinical implications are explored.

MAJOR FINDINGS

The data presented in this thesis show that DBS of the central thalamus increases generalized arousal as measured by motor activity in both intact mice and a mouse model of TBI. All temporal patterns, amplitudes, frequencies, and light phases of stimulation tested in this thesis have been shown to increase motor activity during and directly after DBS. This result holds true for both male and female mice and for both uninjured and multiple TBI mice. Central thalamic DBS (CT/DBS) may also increase generalized arousal as measured by olfactory responsiveness, but the data presented in Chapter 6 (page 115) are not statisti-

cally significant. More work will conclusively determine whether CT/DBS potentiates olfactory responsiveness. Finally, the data presented in Chapters 3, 4, and 5 demonstrate that temporal pattern of DBS (targeting the hippocampus and central thalamus) modulates the magnitude of the resulting response.

FUTURE DIRECTIONS

The experiments exploring the effect of DBS on motor activity and olfactory responsiveness were designed using the framework of the operational definition of generalized arousal. As described in the introduction, generalized arousal has three dimensions: motor, sensory, and emotional, *i.e.*, an aroused animal has greater spontaneous motor activity, greater sensory responsiveness, and greater emotional reactivity. Further experiments can look into the effect of various epochs of DBS on motor activity as well as investigate how long the increase in motor activity lasts once DBS is turned off. As mentioned in the previous section, olfactory responsiveness to DBS should be explored using different delay times between stimulation and olfactant to determine whether DBS can potentiate olfactory responsiveness. These experiments could also be repeated using neurophysiologically distinct sensory modalities to ensure that DBS is affecting generalized arousal and not a specific sensory process. To incorporate the last dimension of generalized arousal, the effect of DBS on emotional behaviors should also be explored. Does DBS accelerate the timing or increase the fre-

quency of male sexual behaviors? Can DBS exacerbate the freezing and risk assessment behaviors of an innate fear paradigm? Can DBS affect anxiety-like behaviors? Answering these questions to incorporate the emotional dimension of generalized arousal will benefit research into the arousal effects of DBS.

CT/DBS is also hypothesized to enhance cognition by inducing the CT to recruit cortical neurons to support cognitive load. Experiments into the effects of CT/DBS on cognitive tasks would determine whether CT/DBS could benefit not only DOC patients, but also conscious TBI patients with cognitive deficits. Reversal learning tasks are useful for this idea because they require not only learning and memory, but also adaptability to the changing demands of the task: once the mouse learns the specified goal, that goal is switched and the mouse must then reverse the previous memory and learn the new goals.

Maternal behavior is also an intriguing motivated behavior to explore. In mice, all females, even virgins who have never been pregnant, have an instinct to retrieve and care for pups. Experience, hormones, and epigenetic changes are known to influence this behavior. Exploring how TBI alters maternal behavior ties together the motivational or emotional dimension of arousal, the cognitive deficits associated with brain injury, and the neuroprotective effects of estrogens. If deficits in the behavior paradigm exist in TBI mice, CT/DBS could be used to

rescue those deficits through its influence on generalized arousal as well as cognition.

MATHEMATICAL EXPLORATION

The rich detail and sizable complexity of the described behavioral data led to the collaboration of the author with experts for further mathematical exploration. Dr. Daniel Keenan, Professor of Statistics at the University of Virginia, was kind enough to lend his expertise in the processing and analyzing of the motor activity data presented in Chapter 4 (page 71). We wanted to discern statistically whether the increase in motor activity seen was induced by the DBS or whether it was a coincidental behavioral fluctuation; additionally we were interested in characterizing the pattern of movement during the light and dark, with and without stimulation. Dr. Keenan deconvolved the data of each mouse into zero-, one-, and two-dimensional movement, and from his analyses we concluded that 1) one-dimensional movement did not vary with light phase or with stimulation, 2) that two-dimensional movement was more prevalent in the dark phase compared to the light phase and with stimulation compared to without it, and 3) stimulation during the light phase initiated a pattern of movement more often seen during the dark phase. Importantly, this last conclusion supports the idea that DBS does not create an altered state with only an artifactual increase in motor activity, instead DBS induces a natural pattern of movement.

Additionally, to determine whether electrode placement variation can explain a portion of the behavioral variation, we have contacted Dr. Chris Butson, Associate Professor of Neurology and Neurosurgery at the Medical College of Wisconsin. In the future, he will model the neuronal effect of DBS in the mouse brain using the coordinates for each subject's electrode placement. Using the results of this model, he will then analyze the behavioral data to discover whether exact electrode placement could explain a portion of the variability in the data.

LITERATURE

The data presented in this thesis add to the literature describing the utility of temporal patterns in a neural system. Many groups have described temporal pattern-sensitive neurons in sensory systems; used informational theoretic analysis to calculate the information contained in temporal patterns; discovered how receptors, neurons, and networks generate temporal patterns; and modeled how complex neural systems use temporal patterns. The experiments in this thesis join a smaller body of literature into the direct manipulation of temporally-patterned stimulation; the two articles mentioned in the introduction used temporal patterns to manipulate taste sensation and elicit saccades.

In the literature of therapeutic DBS in clinical and pre-clinical contexts, there are a few papers exploring the utility of temporally-patterned DBS. While exploring the effectiveness of patterned DBS to reduce tremor in patients, Birdno

et al. (2008) found that irregular patterns were less effective at tremor reduction than conventional patterns. In a rat model of PD, So and colleagues (2011) found that pathological behavior was maximally reduced with conventional DBS compared to temporally-patterned DBS. In addition to these negative studies, a few studies with positive benefits to temporally-patterned DBS have been reported. In a rat model of epilepsy, Cota and colleagues (2009) found that a temporally-patterned DBS was a more effective anticonvulsant than conventionally-patterned DBS. Finally, in a non-human hemiparkinsonian model, Baker and colleagues (2011) found that a temporally-patterned DBS was just as effective and required less current than conventionally-patterned DBS at producing behavioral improvement.

In the specific context of CT/DBS, there is only a handful of articles to compare the results of this thesis to. CT/DBS has been investigated in intact rats (Shirvalkar, Seth, Schiff, & Herrera, 2006), brain injured rats (Mair and Hembrook, 2008), macaque monkeys (Smith *et al.*, 2009), and one human case study (Schiff *et al*., 2007). In all of these studies, CT/DBS increased motor activity or enhanced performance on a cognitive task. With CT/DBS, these studies describe enhanced performance on a novel object recognition task (Shirvalkar, Seth, Schiff, & Herrera, 2006); enhanced working memory (Mair & Hembrook, 2008); sustained attention (Smith *et al*., 2009); and functional recovery in a MCS patient

(Schiff *et al.*, 2007). The data presented in this thesis add this body of evidence that CT/DBS can increase generalized arousal and enhance cognition.

While there is one clinical trial into the efficacy of DBS in TBI patients listed in clinicaltrials.gov, very little is published on the use of this neurological intervention in brain-injured patients or animal models of brain injury. In the pre-clinical literature, there is a handful of articles that describe molecular and functional benefits to stimulation in rat models of ischemia. In the clinical literature, the majority of articles are open label studies into the efficacy of DBS in DOC with only a single controlled cross-over study with a single MCS subject. More research is needed on the effects of DBS in brain injury models as well as more controlled studies of DBS in brain injury. The data presented in this thesis add more evidence to these articles that suggest that deficits caused by acquired brain injury can be ameliorated by DBS.

CAVEATS

This thesis investigates the effects of a previously unexplored parameter of stimulation, temporal pattern. It is not within the scope of the work to fully explore all possible temporal patterns: the permutations of possible temporal pattern are enormous. To constrain this thesis within the limits of the experimental equipment, a small set of temporal patterns was tested, and to maximize the benefit of the information gained, these temporal patterns were chosen under the

hypothesis that nonlinear dynamics are important to the control of generalized arousal and included an independently patterned control. These experiments barely scratch the surface of temporally-patterned DBS, but importantly, they confirm that temporal patterns are important in DBS and further research into this facet of DBS will highly benefit the clinical community.

In addition to temporal pattern, other parameters of DBS merit further in-depth exploration including amplitude, frequency, pulse width, pulse shape, or stimulation epoch length. It would have been prohibitively time consuming to comprehensively explore all of these parameters. Pilot experiments stimulating the basal forebrain used a low frequency of stimulation, 50 hz, and unpublished observations from one collaborator noted increased c-fos expression with 175 hz stimulation. With this information in mind, the experiments of Chapter 4 were designed using 50 hz, 125 hz, 175 hz, and 225 hz. Early studies with hippocampal DBS showed a higher likelyhood of seizure at amplitudes of 150 μA or higher, and therefore the experiments of Chapter 4 were restricted to lower amplitudes of stimulation. This work aimed to logically choose a testable set of parameters, and in Chapter 4 (page 71), the most suitable parameter set was chosen from the range of values examined.

As mentioned in the introduction, there are myriad TBI mouse models. Practical limitations due to surgery and recovery time reduced the number of

models applicable to the DBS paradigm used, and a weight drop model was chosen for its straightforward implementation, adjustability, and similarity to real injury-causing phenomena. An impact site of the side of the head instead of the more traditional top of the head was chosen because acceleration/deceleration injuries in a lateral orientation are known to produce more substantial deficits than injuries in a rostral/caudal orientation (Gaetz, 2004). While another type of brain injury, anoxia, was characterized in the lab using the operational definition of generalized arousal (Arrieta-Cruz, Pfaff, & Shelley, 2007), the response of this injury model to DBS has not been examined.

At the conclusion of the sensory experiment (Chapter 6, page 115), no statistical differences were seen between olfactory responses alone and olfactory responses paired with DBS. However, it cannot be inferred that DBS is incapable of potentiating olfactory responsiveness. It is known that the response to DBS, unlike the response to an olfactory stimulus, is not immediate, and the timing of maximal response to DBS is unknown. It may be that potentiation of olfaction by DBS happens only at an optimal time delay. As mentioned above, further experimentation of different time delays between DBS and an olfactory stimulus is necessary to elucidate whether DBS can increase arousal-mediated olfactory responsiveness.

The variability of these behavioral experiments is large and can obscure statisical results even if carefully considered and appropriately managed. In addition to mouse-to-mouse variation, data in these experiments can vary depending on sex differences, timing (dark versus light and hourly differences), electrode placement, and precise injury locus and severity of injury. Variability due to these factors may mask experimentally-generated relevant differences. In attempts to design experiments rigorously in the face of variability, (1) motor activity data were normalized to behavior just prior to stimulation; (2) order of temporally-patterned stimulation was counter-balanced over the course of the day between mice; (3) in sensory experiments, stimulation was delivered at time points with the same basline activity, *i.e.*, after 1 minute of quiescence; (4) later studies were restricted to only males; and (5) mouse strain was limited to C57BL/6J.

CLINICAL IMPLICATIONS

While CT/DBS is not a clinically proven therapy for MCS, the data in this thesis support the idea that CT/DBS can increase generalized arousal in brain-injured subjects. In all experiments using all stimulation parameters, CT/DBS increased generalized arousal as measured by motor activity during and after stimulation. If DBS shows the same effectiveness in increasing generalized arousal in further controlled clinical studies, MCS patients could see vast im-

provement. From requiring assistance for all aspects of care to being able to communicate functionally and feed themselves, MCS patients can only gain from therapeutics that facilitate emergence to consciousness. Eventually, it may be advantageous to treat patients with less drastic cognitive deficits resulting from TBI or other brain injury. As CT/DBS is designed to support cognition, applying CT/DBS to functionally conscious patients with severe cognitive deficits is a logical step.

Once CT/DBS therapy is proven efficacious for MCS, this thesis points toward previously unexplored avenues for stimulation. Since we know that temporal patterns are important in neural systems, temporally-patterned DBS may vastly benefit many patients. At the very least, temporally-patterned DBS can minimize electrical current and severity of side effects while maintaining optimal clinical outcome.

Appendix A

TEMPORAL PATTERN OF PULSES DURING DEEP BRAIN STIMULATION AFFECTS CENTRAL NERVOUS SYSTEM AROUSAL

Amy Wells Quinkert, Nicholas D. Schiff, and Donald W. Pfaff.

Behav Brain Res 214.2 (2010):399-385.

Behavioural Brain Research 214 (2010) 377–385

Contents lists available at ScienceDirect

Behavioural Brain Research

journal homepage: www.elsevier.com/locate/bbr

Research report

Temporal patterning of pulses during deep brain stimulation affects central nervous system arousal

Amy Wells Quinkert[a,*], Nicholas D. Schiff[b], Donald W. Pfaff[a]

[a] Laboratory of Neurobiology and Behavior, Rockefeller University, 1230 York Ave, New York, NY 10065, United States
[b] Laboratory of Clinical Neurophysiology, Weill Cornell Medical College, 1300 York Ave, New York, NY 10065, United States

ARTICLE INFO

Article history:
Received 21 May 2010
Accepted 5 June 2010
Available online 15 June 2010

Keywords:
Deep brain stimulation
Generalized arousal
Temporal patterning

ABSTRACT

Regulation of CNS arousal is important for a wide variety of functions, including the initiation of all motivated behaviors. Usually studied with pharmacological or hormonal tools, CNS arousal can also be elevated by deep brain stimulation (DBS), in the human brain and in animals. The effectiveness of DBS is conventionally held to depend on pulse width, frequency, amplitude and stimulation duration. We demonstrate a novel approach for testing the effectiveness of DBS to increase arousal in intact female mice: all of the foregoing parameters are held constant. Only the temporal patterning of the pulses within the stimulation is varied. To create differentially patterned pulse trains, a deterministic nonlinear dynamic equation was used to generate a series of pulses with a predetermined average frequency. Three temporal patterns of stimulation were defined: two nonlinear patterns, Nonlinear1 (NL1) and Nonlinear2 (NL2), and the conventional pattern, Fixed Frequency (FF). Female mice with bilateral monopolar electrodes were observed before, during and after hippocampal or medial thalamic stimulation. NL1 hippocampal stimulation was significantly more effective at increasing behavioral arousal than either FF or NL2; however, FF and NL2 stimulation of the medial thalamus were more effective than NL1. During the same experiments, we recorded an unpredicted increase in the spectral power of slow waves in the cortical EEG. Our data comprise the first demonstration that the temporal pattern of DBS can be used to elevate its effectiveness, and also point the way toward the use of nonlinear dynamics in the exploration of means to optimize DBS.

1. Introduction

1.1. Deep brain stimulation and generalized arousal

Deep brain stimulation (DBS) is an increasingly utilized treatment for several specific neurodegenerative and psychiatric disorders. It is FDA approved for the use in essential tremor, Parkinson's disease, primary dystonia, and obsessive–compulsive disorder, and is currently undergoing trials for application in a variety of disorders including epilepsy, cluster headache, and refractory depression [3,4]. One such clinical application seeks to develop DBS as a method to promote emergence from a minimally conscious state (MCS), a disorder of consciousness; Schiff et al. successfully use DBS of the central thalamus to facilitate a wide range of behaviors in a single patient 6 years after his initial injury [1].

The theoretical motivation for DBS of the central thalamus in MCS patients is to replace broad denervation and loss of neuromodulatory control of the central thalamus in the severely-injured brain [5]. The central thalamus receives dense innervation from ascending arousal systems and then projects to the cerebral cortex, waking up the rest of the brain and supporting consciousness and generalized arousal. Generalized arousal is that force of the central nervous system (CNS) that underlies behavior, cognition, and emotion [6]. We began by using DBS in the ventral hippocampus, a brain region closely connected to a variety of emotional and visceral functions that depend exquisitely on CNS arousal [7]. DBS has been shown to increase arousal not only in humans, but also in anesthetized rats [2]; it has also been used to increase the cognitive capacity in mice [8]. In this work, we explored increases to arousal with DBS in behaving mice.

1.2. Temporal pattern and the neural code

Building on the general hypothesis that DBS in MCS patients approximates a missing input, what is the nature of the actual input this therapy is trying to emulate? Or to put the question another way, where is the informational content in the signal DBS ther-

* Corresponding author at: Laboratory of Neurobiology and Behavior, Rockefeller University, 1230 York Ave, Box 275, New York, NY 10065, United States.
Tel.: +1 212 327 8668; fax: +1 212 327 8643.
E-mail addresses: awells@rockefeller.edu, amy.quinkert@gmail.com (A.W. Quinkert).

0166-4328/$ – see front matter © 2010 Elsevier B.V. All rights reserved.
doi:10.1016/j.bbr.2010.06.009

apy is trying to emulate? If it is true that informational content of neural responses is either irrelevant to the application of this technique or strictly in the frequency of such responses or in any static electrical response parameter, then the current standard clinical practice of choosing the proper frequency, amplitude, pulse width, and stimulation duration is valid and sufficient. If on the other hand, informational content is in the pattern of pulses and not just the values of these electrical parameters, it would stand to reason that appropriately patterned stimulation trains might more effectively mimic and substitute normal neural input.

Wasserman, in his 1992 review [9], discusses several theories of the neural code and reiterates the classic question of the pattern of neuronal cell responses: neuroscientists observe that neurons fire in particular patterns that can change with stimuli, but do these patterns carry informational content? There are many examples of physiologically relevant temporal patterns, especially in sensory systems, and how neuronal circuits can use temporal patterning to relay information about changing stimuli. If arousal systems are as sensitive to temporal patterning of neuronal responses as sensory systems, DBS to increase generalized arousal may also be responsive to different temporal patterns. In the present study, we investigated whether temporal pattern of DBS to increase generalized arousal can impact the animal's behavioral response.

2. Methods

2.1. Animals and materials

Twenty-two 6–9-week old female C57BL/6J mice were singly housed for the duration of the study. Female mice were used because the current study was inspired by a previous investigation of the effects of estrogens on arousal [10]. Mice were allowed food and water *ad libitum* and were subject to a 12 h light/dark cycle, lights off at 6 am. Stainless steel monopolar electrodes (0.3 mm diameter) with gold plated connections were insulated using epoxy resin with 0.5 mm stripped from the electrode tips prior to implantation surgery.

All animals were implanted with bilateral electrodes either in the hippocampus ($n = 19$) or, for comparison, in the medial thalamus ($n = 3$) under pentobarbital anesthesia using a stereotaxic apparatus (Kopf Instruments). Mice were also subcutaneously implanted with a small animal transmitter (Data Sciences International) capable of transmitting electroencephalogram (EEG). Post-operative care included recovery from anesthesia under a heat lamp and acetaminophen analgesia (3 mg/mL drinking water) for 3 days. Before any handling or manipulation, mice were allowed to recover from surgery for 5–7 days.

Prior to the start of data collection, mice were plugged into the stimulus generator (Multichannel Systems). EEG was measured and collected by the DSI telemetry system, and home cage activity data were collected by a 3D infrared monitor (Accuscan Instruments). After data were collected, animals were sacrificed by pentobarbital overdose and transcardial perfusion of phosphate-buffered saline and paraformaldehyde. Fixed brain tissue was then sliced at 80 μm in coronal sections, mounted on slides, and stained with cresyl violet. Stained tissue sections were observed for histological confirmation of electrode placement.

All animal procedures were in compliance with National Institutes of Health guidelines and approved by the Rockefeller University Institutional Animal Care and Use Committee.

2.2. Stimulation parameters

Stimulation was programmed and delivered by a four channel stimulus generator (Multichannel systems STG2004). Stimulation epochs lasted for 10 min and occurred every 3 h during the dark phase of the light cycle. All stimulations were biphasic with a pulse width of 0.1 ms (for both anodic and cathodic phases of the pulse) and a frequency of 50 Hz. Pulse amplitude was set at 25 μA ($n = 6$), 75 μA ($n = 3$), 100 μA ($n = 10$), or 150 μA ($n = 3$); these amperages were chosen to elicit behavioral responses but avoid seizures.

To test the hypothesis that the temporal pattern of stimulation can change behavioral response, we generated nonstandard stimulation patterns using the logistic equation: $X_n = R\,X_{n-1}\,(1 - X_{n-1})$, where X is the output at time n and R is a constant modifier that creates chaotic output at certain values. Output to the logistic equation was calculated to two or three thousand iterations with initial conditions of $R = 3.90$ and $X_0 = 0.2$. To ensure that neurons did not show depolarization block, a minimum interpulse interval (IPI) was defined as 0.3 ms, and equation output was scaled to meet that minimum. A consecutive set of output numbers was found such that the number of the set divided by the sum of the scaled output equaled the desired average frequency. Three distinct temporal patterns of stimulation were defined: Fixed Frequency (FF), the standard pattern with constant IPIs at 50 Hz (black temporal pattern, Fig. 1); Nonlinear1 (NL1), a repeating pattern of 10 pulses derived from the logistic equation with an average frequency of 50 Hz (red temporal pattern, Fig. 1); and Nonlinear2 (NL2), a repeating pattern of 50 pulses derived from the logistic equation with an average frequency of 50 Hz (blue temporal pattern, Fig. 1).

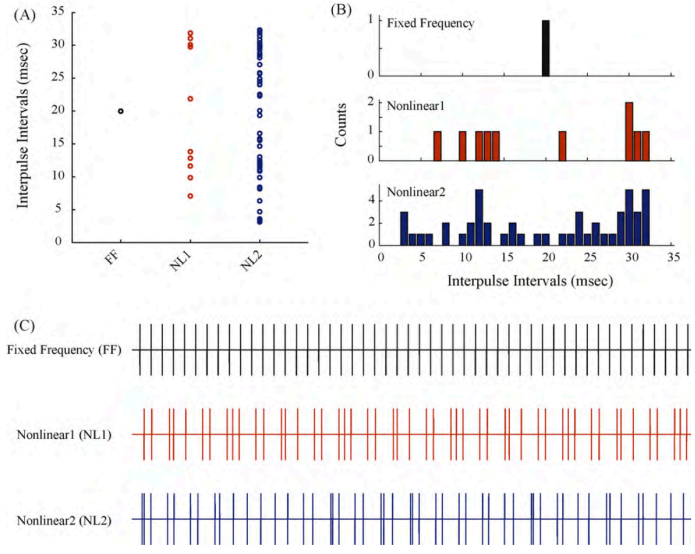

Fig. 1. Characterization of differentially patterned stimulation trains. A) Distribution of interpulse intervals for each pattern. B) Histogram of interpulse intervals for each pattern. C) Graphical representation of one second of each temporal pattern.

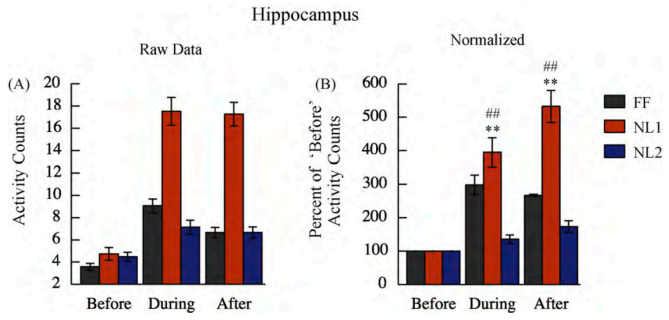

Fig. 2. NL1 hippocampal DBS increases Activity Counts more than FF or NL2. A) Raw Activity Count data. B) Normalized to 'Before' Activity Count data. Data are shown as mean ± s.e.m.; ** $p < 0.01$ compared to FF; ## $p < 0.01$ compared to NL2; black bars - FF; red bars - NL1; blue bars - NL2.

Each mouse was stimulated 4–12 times and was challenged with at least two of the three DBS patterns. All stimulation parameters were held constant for any individual mouse except for temporal pattern. To account for possible order effects, DBS temporal patterns were counterbalanced for order in each mouse and between mice as much as possible. More specifically, for four epochs of stimulation in 1 day, an example of the order of stimulation a mouse would see is as follows: FF, NL1, NL1, FF. And for every mouse that started a given day with FF stimulation, another mouse started the day with NL1 stimulation.

2.3. Data analysis

The three behavioral measures observed included whole body activity ("Activity Counts"), collected by the DSI transmitter and representing changes in field strength between the transmitter and receiver as the mouse moves; fidgeting movements ("Horizontal Activity"), collected by the home cage Accuscan system and representing the number of infrared beams broken in the horizontal plane; and ambulation ("Total Distance"), collected by the home cage Accuscan system and representing the length of the mouse's path. These data measures were recorded as the sum of activity every minute for 10 min prior to stimulation, 10 min during stimulation, and the 10 min after stimulation. In addition, EEG spectra were calculated for minute long recordings, 10 min before and 10 min after stimulation, using MATLAB's multitaper method. Spectral frequency bins were defined as follows: delta (0.5–4 Hz), theta (4.5–8 Hz), alpha (8.5–12 Hz), beta (12.5–20 Hz), and gamma (35–45 Hz). These EEG waves were then reported as relative power, that is the percent of power in each bin to the sum of the power in all five bins. Relative power of these frequency bins was not calculated during stimulation to avoid the confounding effects of stimulation artifacts. All data were normalized and recorded as the percent of measurements before stimulation.

To guarantee that our main conclusion did not depend on the exact nature of the statistics used, both standard parametric statistics as well as non-parametric statistics were performed on normalized data. To test for DBS and temporal pattern effects, two-way ANOVA and, to confirm, non-parametric Friedman analyses were performed. For more detailed post-hoc analysis, *t* tests with Bonferroni corrections and, to confirm, non-parametric Wilcoxon matched-pairs signed ranks tests were used. All inferences of significance utilized a minimum requirement of $p < 0.05$. In addition to the statistics reported below, data were also systematically compared with respect to pulse amplitude, and this comparison yielded no significant results as might have influenced the results below.

3. Results

3.1. Behavior

Electrical Stimulation both in the hippocampus and the medial thalamus increased arousal-related motor activity as measured by fidgeting movements ("Horizontal Activity"), ambulation ("Total Distance"), and an independent measure of whole body movement ("Activity Counts"). However, the measured activity increases specifically depended on the temporal pattern within the pulse train of stimulation delivered to both structures, with different temporal patterns of pulses increasing activity during stimulation of hippocampus or medial thalamus. Moreover, specific temporal patterns of pulses showed differentiable patterns of effects across measured behavioral variables.

3.1.1. Hippocampal DBS

The temporal pattern of electrical pulses affected the magnitude of the behavioral result in several ways. With respect to activity counts, two-way ANOVA confirmed an effect of DBS ($F_{2,2245} = 28.32$, $p < 0.01$) and that responses to temporal pattern were significantly different ($F_{2,2245} = 7.58$, $p < 0.01$); see Fig. 2B. DBS also increased horizontal activity ($F_{2,1675} = 65.49$, $p < 0.01$) as well as total distance ($F_{2,1515} = 107.61$, $p < 0.01$). Temporal pattern of stimulation also significantly affected horizontal activity response ($F_{2,1675} = 12.63$, $p < 0.01$) and total distance ($F_{2,1515} = 9.72$, $p < 0.01$); see Fig. 3B and D.

In general all three temporal patterns increased behavioral response to hippocampal DBS in all three behavioral measurements. As seen in Fig. 2B, FF and NL1 stimulation increased activity counts during and after stimulation compared to before stimulation (FF during: $t_{685} = 7.31$, $p < 0.01$; FF after: $t_{694} = 5.54$, $p < 0.01$; NL1 during: $t_{229} = 7.66$, $p < 0.01$; NL1 after: $t_{238} = 9.94$, $p < 0.01$). NL2 stimulation significantly increased activity counts only after stimulation ($t_{517} = 2.92$, $p < 0.05$), and its resultant increase during stimulation did not reach significance with the Bonferroni correction ($t_{526} = 2.04$, $p = 0.1245$). Horizontal activity response to stimulation increased during and after FF (during: $t_{537} = 12.15$, $p < 0.01$; after: $t_{546} = 7.92$, $p < 0.01$), NL1 (during: $t_{263} = 9.70$, $p < 0.01$; after: $t_{275} = 5.93$, $p < 0.01$), and NL2 (during: $t_{271} = 4.59$, $p < 0.01$; after: $t_{272} = 2.74$, $p < 0.05$) stimulation; see Fig. 3B. As seen in Fig. 3D, total distance response to stimulation was also increased during and after FF (during: $t_{465} = 9.10$, $p < 0.01$; after: $t_{490} = 4.42$, $p < 0.01$), NL1 (during: $t_{249} = 8.64$, $p < 0.01$; after: $t_{266} = 3.39$, $p < 0.01$), and NL2 (during: $t_{249} = 6.08$, $p < 0.01$; after: $t_{256} = 3.14$, $p < 0.05$). It is clear that all three temporal patterns of stimulation in the hippocampus increased arousal-related behavior in all three of the observed behavioral measures.

The magnitude of increase in behavior during and after stimulation depended on the temporal pattern of stimulation. While generally NL1 hippocampal stimulation increased behavior better than either FF or NL2 stimulation, the specific responses of each behavioral measure were slightly different. With regard to whole body movement (Fig. 2), NL1 stimulation increased activity counts during and after DBS greater than either FF (during: $t_{406} = -6.08$, $p < 0.01$; after: $t_{424} = -9.90$, $p < 0.01$) or NL2 stimulation (during: $t_{347} = -8.41$, $p < 0.01$; after: $t_{347} = -11.02$, $p < 0.01$). Fidgeting movements (Fig. 3A and B) also showed significant differ-

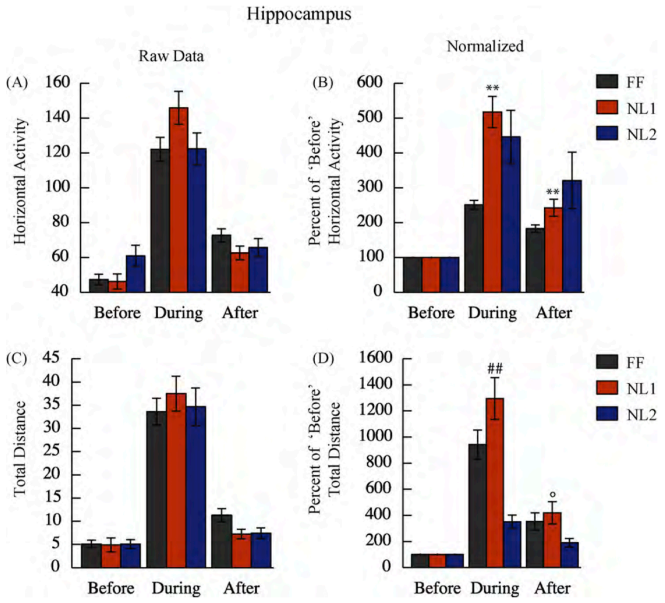

Fig. 3. NL1 hippocampal DBS increases Horizontal Activity more than FF and Total distance more than NL2. A) Raw Horizontal Activity data. B) Normalized to 'Before' Horizontal Activity data. C) Raw Total Distance data. D) Normalized to 'Before' Total Distance data. Data are shown as mean ± s.e.m.; ** $p < 0.01$ compared to FF; ## $p < 0.01$ compared to NL2;° $p = 0.055$ compared to NL2; black bars - FF; red bars - NL1; blue bars - NL2.

ences during and after stimulation between FF and NL1 patterns; FF DBS increased horizontal activity response greater than NL1 DBS (during: $t_{386} = -7.03$, $p < 0.01$; after: $t_{403} = -2.62$, $p < 0.05$). Regarding ambulation (Fig. 3C and D), significant differences were found between the two nonstandard patterns during stimulation; NL1 stimulation increased total distance response compared to NL2 stimulation during stimulation ($t_{195} = -5.32$, $p < 0.01$) but the difference between these two patterns was not significant using Bonferroni correction after stimulation ($t_{238} = -2.37$, $p = 0.0552$). In short, temporal pattern of hippocampal stimulation affected the resulting behavioral increase; NL1 stimulation of the hippocampus increased arousal-related activity greater than either other pattern.

3.1.2. Example and mouse behavioral description

In addition to quantitative behavioral measurement, infrared cameras were used to videotape behavior of some mice during the course of the study for qualitative behavioral measurement. An ethological description of the behavior of one exemplary mouse is recorded here with its corresponding quantitative measurement shown in Fig. 4.

In the 10 min before FF hippocampal stimulation, the mouse sat in one corner of her cage, occasionally moving her head or scratching her ear, but spending most of the time sitting still. During FF stimulation, she continued to sit in one corner and did not move from this spot, but did spend slightly more time moving her head or scratching than before stimulation. After FF stimulation, she sat in her corner and moved only occasionally for the first six minutes. After that, she moved from her spot and walked along the edges of the cage; see Fig. 4A for quantitative measures of this stimulation.

Before NL1 stimulation, the mouse was sitting in the corner eating and occasionally drinking. She groomed occasionally, reared once, and pivoted in a circle in her corner once. During NL1 stimulation, the mouse walked quickly around the edges of her cage several times, stopping at the corners and the water spout to drink. After NL1 stimulation, the mouse again sat in one corner, but occasionally ventured to other corners as well as to the water spout. She did not walk as much as during stimulation, but continued to move, drink, and eat while sitting; see Fig. 4B for quantitative measures of this stimulation.

Before NL2 stimulation, the mouse sat in one corner of the cage, moved her head often, took one to two steps away from her corner and returning, and pivoted in a circle one to two times. During NL2 stimulation, the mouse continued to sit in her corner and move, but did not walk around. She pivoted in a circle and moved her head to eat, but she did not walk away from her corner. After NL2 stimulation, she sat in her corner eating, and once walked only as far as the water spout before returning to the corner; see Fig. 4C for quantitative measures of this stimulation. As seen in Fig. 4 and from the above description, this mouse's behavioral activity dramatically increased during NL1 stimulation, but not during FF or NL2 stimulation.

3.1.3. Medial thalamic DBS

Similar to hippocampal stimulation, medial thalamic stimulation increased behavioral activity in all three measures of behavior. An effect of stimulation was seen in activity counts ($F_{2,635} = 19.86$, $p < 0.01$), horizontal activity ($F_{2,715} = 41.16$, $p < 0.01$) and total distance ($F_{2,595} = 13.97$, $p < 0.01$) using two-way ANOVA. The magnitude of increase in each behavioral measurement was also found to be significantly different depending on the pattern of stimulation. Activity count response was significant with respect to temporal pattern ($F_{2,635} = 19.07$, $p < 0.01$) as was horizontal activ-

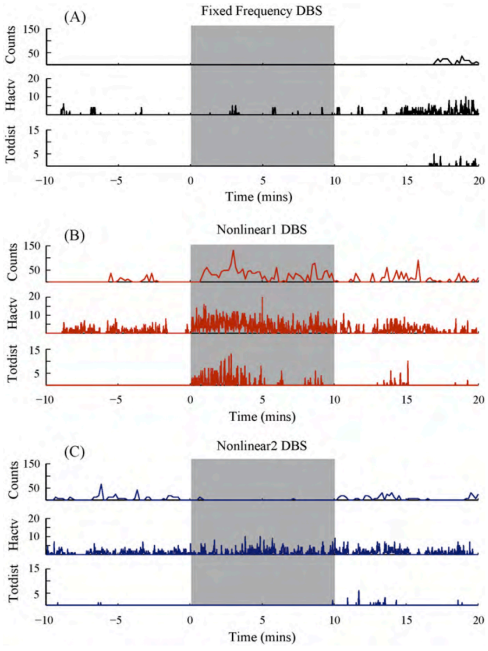

Fig. 4. High temporal resolution actograms of one mouse. One mouse's behavior 10 minutes before, 10 minutes during, and 10 minutes after hippocampal stimulation with A) Fixed Frequency, B) Nonlinear1, and C) Nonlinear2. Grey boxes delineate stimulation epochs. Activity Counts (Counts) are presented as sums of activity every 10 seconds; Horizontal Activity (Hactv) and Total Distance (Totdist) are presented as sums of activity every second.

ity response ($F_{2,715} = 16.82$, $p < 0.01$) and total distance response ($F_{2,595} = 8.92$, $p < 0.01$); see Fig. 5.

With all three types of stimulation, most behavioral measures were increased during and after stimulation. With regard to FF stimulation, all three behavioral measures increased: activity counts increased during ($t_{199} = 5.26$, $p < 0.01$) and after ($t_{199} = 6.17$, $p < 0.01$) stimulation; horizontal activity increased during ($t_{218} = 6.59$, $p < 0.01$) and after ($t_{233} = 8.17$, $p < 0.01$) stimulation; and total distance increased during ($t_{207} = 7.96$, $p < 0.01$) and after ($t_{204} = 6.12$, $p < 0.01$) stimulation; see grey bars in Fig. 5. With NL1 stimulation, however, only activity counts increased during ($t_{113} = 4.13$, $p < 0.01$) and after ($t_{114} = 3.65$, $p < 0.01$) stimulation and total distance increased during ($t_{113} = 3.03$, $p < 0.05$) but not after stimulation; see red bars in Fig. 5A and C. NL2 stimulation also increased all three behavioral measures: activity counts increased during ($t_{106} = 7.44$, $p < 0.01$) and after ($t_{103} = 4.77$, $p < 0.01$) stimulation; horizontal activity increased during ($t_{109} = 5.21$, $p < 0.01$) and after ($t_{116} = 3.90$, $p < 0.01$) stimulation; and total distance increased during ($t_{85} = 5.16$, $p < 0.01$) and after ($t_{87} = 4.63$, $p < 0.01$) stimulation; see blue bars in Fig. 5. Despite not every behavioral measure increasing during and after every temporal pattern of stimulation, in general medial thalamic stimulation also increases arousal-related behavior.

Unlike hippocampal stimulation, where NL1 stimulation elicited the largest behavioral responses, NL1 stimulation of the medial thalamus generated the smallest behavioral response increases after stimulation in all three behavioral measures. As seen in

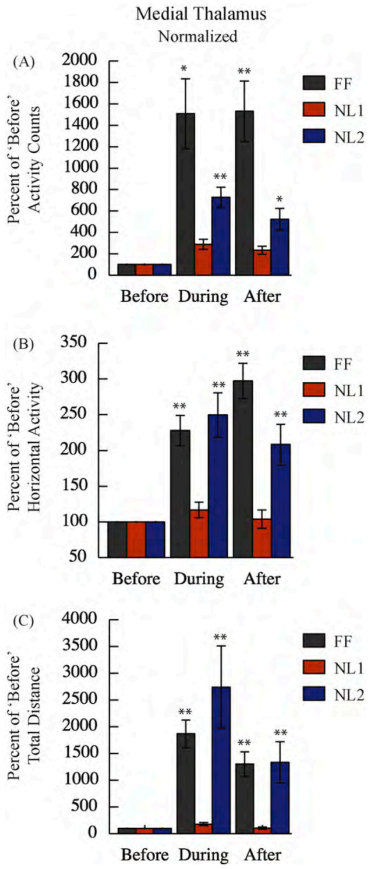

Fig. 5. FF and NL2 medial thalamic DBS increases Activity Counts, Horizontal Activity, or Total distance more than NL1. Normalized to 'Before' A) Activity Counts, B) Horizontal Activity, and C) Total Distance. Data are shown as mean ± s.e.m.; * $p < 0.05$ compared to NL1; ** $p < 0.01$ compared to NL1; black bars - FF; red bars - NL1; blue bars - NL2.

Fig. 5A, activity count response to NL1 stimulation was less than both FF during ($t_{134} = 3.06$, $p < 0.05$) and after ($t_{135} = 3.80$, $p < 0.01$) stimulation and NL2 during ($t_{101} = 4.32$, $p < 0.01$) and after ($t_{99} = 2.86$, $p < 0.05$) stimulation. NL1 stimulation increased horizontal activity less than FF during ($t_{152} = 3.69$, $p < 0.01$) and after ($t_{169} = 5.30$, $p < 0.01$) stimulation as well less than NL2 during ($t_{103} = 4.11$, $p < 0.01$) and after ($t_{112} = 3.32$, $p < 0.01$) stimulation (Fig. 5B). Regarding Total distance in Fig. 5C, NL1 increased behavioral response less than compared to FF during ($t_{142} = 5.12$, $p < 0.01$) and after ($t_{138} = 4.08$, $p < 0.01$) stimulation, and less than NL2 during ($t_{80} = 4.77$, $p < 0.01$) and after ($t_{81} = 4.35$, $p < 0.01$) stimulation. While temporal pattern of medial thalamic stimulation also affects resulting behavioral response, the specific response of medial thalamic stimulation to different temporal patterns is not the same as hippocampal stimulation. Interestingly, with DBS in medial thalamus, FF gave larger increases in arousal-related behavior than NL1.

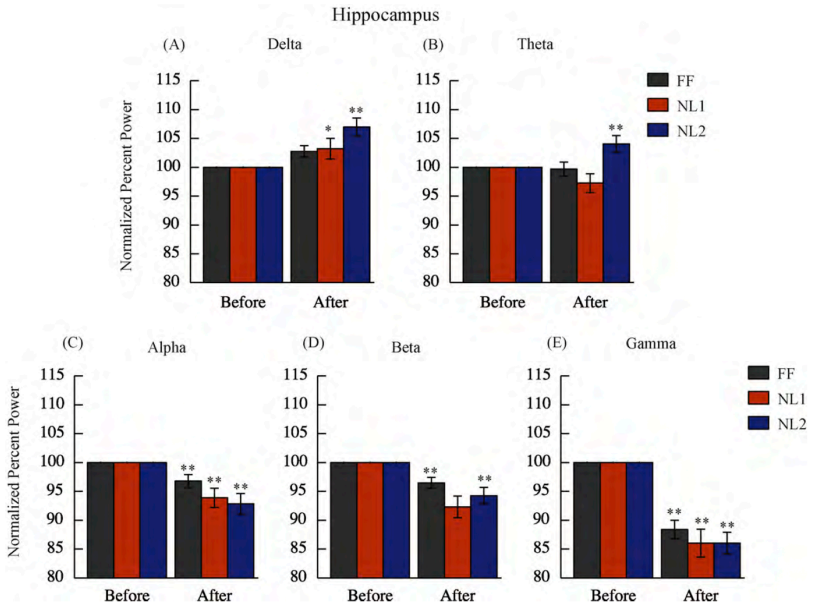

Fig. 6. Relative EEG spectral changes to differentially patterned DBS of the hippocampus. Normalized to 'Before' A) Delta waves (0.5–4 hz), B) Theta waves (4.5–8 hz), C) Alpha waves (8.5–12 hz), D) Beta waves (12.5–20 hz), and E) Gamma waves (35–45 hz). Data are shown as mean ± s.e.m.; * $p < 0.05$ compared to before, ** $p < 0.01$ compared to before.

3.2. EEG

In addition to behavioral effects, electrical stimulation altered the relative power of wave forms in specific frequency bins of the EEG with both hippocampal stimulation and medial thalamic stimulation. While stimulation of both brain regions elicited EEG changes, the specific responses to the different patterns of stimulation were different for each brain region.

3.2.1. Hippocampal DBS

EEG spectral content was altered with hippocampal stimulation in general, but showed few differences among temporal patterns of stimulation. By two-way ANOVA, all five frequency bins showed significant relative power differences after stimulation, but only one frequency bin showed differences between temporal patterns used. Surprisingly, delta waves, normally associated with sleep, increased after DBS ($F_{1,2554} = 32.18$, $p < 0.01$); see Fig. 6A. As seen in Fig. 6B, theta waves were also changed ($F_{1,2120} = 22.72$, $p < 0.01$). Alpha waves decreased after stimulation ($F_{1,2610} = 37.16$, $p < 0.01$) as did beta waves ($F_{1,2539} = 51.53$, $p < 0.01$) and gamma waves ($F_{1,2587} = 149.00$, $p < 0.01$); see Fig. 6C–E. The only frequency band that showed significant differences between responses to temporal pattern was delta waves ($F_{2,2554} = 3.03$, $p < 0.05$). Despite the apparent significant difference in delta wave response between the temporal patterns of stimulation as shown by two-way ANOVA, *t* tests failed to find significant differences between any two of the patterns with Bonferroni corrected alpha values.

3.2.2. Medial thalamic DBS

Paralleling hippocampal stimulation, medial thalamic stimulation led to a change in relative power of frequency bands of the EEG with only a few differences between different temporal patterns of stimulation. Again all five frequency bins showed a significant effect of stimulation by two-way ANOVA. As seen in Fig. 7A and B, delta and theta waves changed after stimulation (Delta: $F_{1,454} = 56.04$, $p < 0.01$; Theta: $F_{1,455} = 76.52$, $p < 0.01$). Alpha waves decreased after stimulation ($F_{1,446} = 63.17$, $p < 0.01$) as did beta waves ($F_{1,435} = 33.04$, $p < 0.01$) and gamma waves ($F_{1,437} = 11.06$, $p < 0.01$); see Fig. 7C–E.

Unlike with hippocampal stimulation, three frequency bins showed significant differences between responses to the pattern of stimulation. These three frequency bins were delta waves ($F_{2,454} = 15.24$, $p < 0.01$) theta waves ($F_{2,455} = 17.81$, $p < 0.01$) and alpha waves ($F_{2,446} = 3.58$, $p < 0.05$). With respect to pattern, Bonferroni-corrected *t* tests showed that the delta wave response to FF was greater than response to both NL1 ($t_{161} = 6.42$, $p < 0.01$) and NL2 ($t_{160} = 4.80$, $p < 0.01$), but that delta wave response to NL1 was not different from NL2 ($t_{103} = 1.80$, $p = 0.07$); see Fig. 7A. As seen in Fig. 7B, theta wave response to NL1 stimulation was greater than FF ($t_{161} = -7.43$, $p < 0.01$) and NL2 ($t_{102} = -5.84$, $p < 0.01$) stimulation. Comparing the alpha response the different temporal patterns in Fig. 7C, NL1 stimulation decreased alpha waves less than FF stimulation ($t_{153} = -2.59$, $p < 0.05$).

4. Discussion

4.1. Major findings

4.1.1. Behavior

In the current study, we conclude that temporal patterning of pulses in DBS affects arousal-related behavior. With stimulation in two different brain regions, increases in arousal-related behavior during and after stimulation were modulated by the temporal pat-

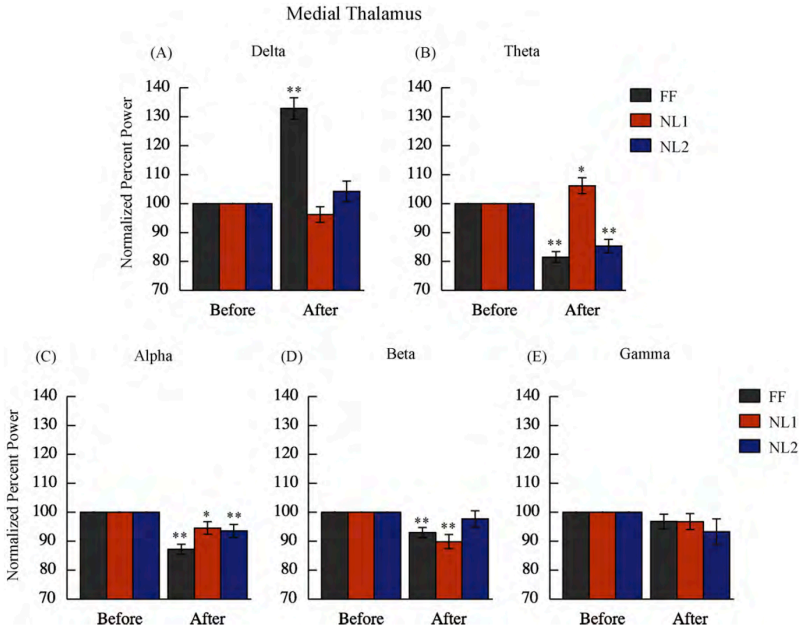

Fig. 7. Relative EEG spectral changes to differentially patterned DBS of the medial thalamus. Normalized to 'Before' A) Delta waves (0.5–4 hz), B) Theta waves (4.5–8 hz), C) Alpha waves (8.5–12 hz), D) Beta waves (12.5–20 hz), and E) Gamma waves (35–45 hz). Data are shown as mean ± s.e.m.; * $p < 0.05$ compared to before, ** $p < 0.01$ compared to before.

tern of stimulation. In the hippocampus, NL1 stimulation increased arousal-related behavior more than either FF or NL2. In the medial thalamus, stimulation with either FF or NL2 produced significantly more activity increases than NL1. We see that not only does temporal pattern make a difference, but also that the response to temporal pattern is different in each DBS target. This difference between brain regions likely depends on the physiology of the target of stimulation and its function within the particular neuronal circuit of interest.

4.1.2. EEG

EEG spectral response to temporal pattern of DBS was surprising. While there was little evidence of a difference in response to temporal pattern, we found a general effect of DBS. Most interestingly, we found a consistent increase in delta power after DBS. In conjunction with the increases seen in behavioral activity, this seemed paradoxical. Why should an EEG wave associated with sleep increase in power at the same time as an increase in behavioral activity? There might be many possibilities to explain such a phenomenon; below we propose three.

One possibility to explain our surprising increase in delta power is that it has some relation to the phenomenon of "alpha-delta arousals," usually seen in human brains as intrusions into Non-Rapid Eye Movement sleep [11]. Recordings of EEG during sleep also reveal brief arousals that include large amplitude low frequency waves in a pattern often called "*K*-complexes." Whether or not our unpredicted finding can be explained by those observations in human brain remains an open question. Secondly, another possibility is that our unexpected delta effect is a rebound phenomenon. In order to test that idea, stimulating using epochs of varying lengths would be required to find out whether very short trains could arouse the animal without the hypothetical rebound in the EEG. Finally, from a mechanistic point of view, there is the possibility that our increased delta power and decreased gamma power reflect apical dendritic potentials of the pyramidal cells and other subthreshold events that we measure as low frequency summated potentials [12], recruited by our DBS. Which of these or other interpretations of our surprising EEG result are actually correct remain to be determined.

4.2. Literature

While no paper has explored the importance of mathematically determined temporal patterning in DBS per se for affecting behavior, there is a rich history of literature describing temporally patterned neural responses, information theory analyses of temporally patterned responses, physiological explanations for the presence and possibly usage of temporal patterns, and neural network models that utilize temporal patterns. Many of these papers address the classic question: do neural systems use temporal patterns to encode information? [9]. Most descriptions of temporally patterned neural responses come from various sensory systems. There are studies exploring temporal-pattern-sensitive neurons in visual [13,14], gustatory [15,16], olfactory [17–19], auditory [20,21], tactile [22], and electro-sensing [23] systems.

Our current line of inquiry began with the observation of different robust temporal patterns resulting from different stimuli. Once these temporal patterns were observed, the question then posed was: are these temporal patterns useful for transmitting information or do they represent noise around a meaningful aver-

age? Our data suggest, for the first time, that temporal patterning, itself, may be meaningfully used. Our empirical findings are consonant with what might be proposed on the basis of information theory. Informational theoretic analyses allow for calculation of the amount of information (generally in bits/s) transmitted by a neuronal signal, taking into account various parameters of that signal [6]. In all of these analyses, when temporal patterning of the signal is included, more information is transmitted by the signal; in some cases, the amount of information encompassed by temporal patterning is necessary for what the neuron or system does *in vivo* [14,22,24,25]. Now that the idea of the importance of temporal patterning has taken hold, a body of evidence is growing that describes how receptors, neurons, and networks generate and possibly use temporal patterns [26–28]. In addition, neural network models of sensory systems emulate the complex characteristics of natural neural systems only when they include these temporal dynamics [29,30].

While most of the evidence for the usefulness of temporal patterns is indirect, there are a small number of examples, in addition to our own data, of direct experimentation on the response of a neural system to temporally-patterned input; here we list two. First, Di Lorenzo et al. used a conditioned aversion paradigm to test whether temporally patterned stimulation of the nucleus tractus solitarius would elicit a taste perception with a particular quality [15]. Using recordings from the nucleus tractus solitarius in behaving rats presented with quinine, the authors defined a temporal pattern of spike trains to simulate quinine. They found that conditioned aversion using their quinine simulating temporal pattern generalized specifically to bitter taste stimuli; additionally conditioned aversion using randomized temporal patterns generalized to more than just bitter taste stimuli. They concluded that they have shown their subjects perceive a bitter taste when stimulated with their quinine simulating temporal pattern. Second, Kimmel and Moore concluded that the frontal eye field in monkeys is sensitive to temporal pattern of input in signaling saccadic eye movement [31]. They found that an accelerating temporal pattern is most efficient at eliciting saccades; this temporal pattern was better than both a decelerating temporal pattern and a fixed interpulse interval pattern. In addition to these three temporal patterns (all with the same mean interpulse interval), the authors also used randomized temporal patters; the random temporal patterns found to elicit saccades were on average accelerating, and those that were not found to elicit saccades were on average decelerating.

4.3. Potential caveats

The magnitude of the effect of temporal patterning of DBS was not always the same. Three considerations can be brought to bear, for explaining this variability. First, from comparisons among data sets, we suspect that the background level of excitability of the mouse may differentially affect arousal responses to different temporal patterns. Second, in some of the data covered in Section 3, greater behavioral NL1 effects occurred during the 10 min immediately after DBS, whereas in other experiments, the NL1 effect was maximal (compared to FF) during DBS. Third, since these experimental subjects were female mice, it is important to note that the largest difference between NL1 and FF results were obtained in ovariectomized animals as estrogens are know to affect arousal level [10]. This may be because of the consideration raised above, namely, the importance of the background level of excitability of the test animals influence the magnitude of the NL1 effect. In addition to response variability, we also note that all of the observations we report here were made during the dark part of the daily light cycle, and thus that observations following DBS during the light part of the cycle might differ.

4.4. Outlook

While our data show that temporal patterning can be used to modulate CNS arousal in response to DBS, the dynamics of that patterning, as it affects behavioral response, have not yet been comprehensively explored. One consideration for future studies will be approaches based on randomness. This would require special consideration since some random generators are not truly random and are themselves nonlinear dynamic equations. In contrast, a full exploration of pure randomness in this experimental setting will require constructing new families of pulse trains based either on the mathematics of Poisson processes, in which timings of individual pulses are determined in a manner independent of one another [32], or on the mathematics of random sequences, their randomness proven by the inability to compress them into shorter repeating sequences [33]. In addition, besides the logistic equation, there are several other equations that generate deterministic chaos [34], and they might be explored as well. Finally, it must also be recognized that our two nonlinear temporal patterns were generated from the same equation, but resulted in different behavioral and EEG responses. Understanding exactly how these dynamics influence the CNS arousal system will be essential to find the optimal temporal pattern for maximizing behavioral arousal responses.

Increase in generalized arousal can affect more than just an animal's motor activity. We know that in an animal with greater generalized arousal, that animal exhibits not only more spontaneous motor activity, but also can manifest greater sensory responsiveness and more emotional reactivity [6]. In the current study we used motor activity as an efficient indication of arousal, but to more completely illustrate the concept of generalized arousal, future studies should include measures of sensory response and emotional reactivity.

Acknowledgments

This work was funded, in part, by a company, IntElect Medical Inc, in which Cornell University has part ownership; through the licensing of technology, one author, NDS, is a listed Cornell inventor and may benefit in the future from commercialization of intellectual property owned by Cornell.

References

[1] Schiff ND, Giacino JT, Kalmar K, Victor JD, Baker K, Gerber M, et al. Behavioural improvements with thalamic stimulation after severe traumatic brain injury. Nature 2007;448:600–3.
[2] Wu HB, Stavarache M, Pfaff DW, Kow LM. Arousal of cerebral cortex electroencephalogram consequent to high-frequency stimulation of ventral medullary reticular formation. Proc Natl Acad Sci USA 2007;104:18292–6.
[3] Larson PS. Deep brain stimulation for psychiatric disorders. Neurotherapeutics 2008;5:50–8.
[4] Miller G. Neuropsychiatry—rewiring faulty circuits in the brain. Science 2009;323:1554–6.
[5] Schiff ND. Central thalamic deep-brain stimulation in the severely injured brain: rationale and proposed mechanisms of action. Ann NY Acad Sci 2009;1157:101–16.
[6] Pfaff DW. Brain arousal and information theory: neural and genetic mechanisms. Cambridge, Mass: Harvard University Press; 2006.
[7] Petrovich GD, Canteras NS, Swanson LW. Combinatorial amygdalar inputs to hippocampal domains and hypothalamic behavior systems. Brain Res Rev 2001;38:247–89.
[8] Shirvalkar P, Seth M, Schiff ND, Herrera DG. Cognitive enhancement with central thalamic electrical stimulation. Proc Natl Acad Sci USA 2006;103:17007–12.
[9] Wasserman GS. Isomorphism, task dependence, and the multiple meaning theory of neural coding. Biol Signals 1992;1:117–42.
[10] Ribeiro AC, Pfaff DW, Devidze N. Estradiol modulates behavioral arousal and induces changes in gene expression profiles in brain regions involved in the control of vigilance. Eur J Neurosci 2009;29:795–801.
[11] Kryger MH, Roth T, Dement WC. Principles and practice of sleep medicine. 3rd ed. Philadelphia: Saunders; 2000.
[12] Doi A, Mizuno M, Katafuchi T, Furue H, Koga K, Yoshimura M. Slow oscillation of membrane currents mediated by glutamatergic inputs of rat

somatosensory cortical neurons: in vivo patch-clamp analysis. Eur J Neurosci 2007;26:2565–75.
[13] Mechler F, Victor JD, Purpura KP, Shapley R. Robust temporal coding of contrast by v1 neurons for transient but not for steady-state stimuli. J Neurosci 1998;18:6583–98.
[14] Reinagel P, Reid RC. Temporal coding of visual information in the thalamus. J Neurosci 2000;20:5392–400.
[15] Di Lorenzo PM, Leshchinskiy S, Moroney DN, Ozdoba JM. Making time count: functional evidence for temporal coding of taste sensation. Behav Neurosci 2009;123:14–25.
[16] Glendinning JI, Davis A, Rai M. Temporal coding mediates discrimination of "bitter" taste stimuli by an insect. J Neurosci 2006;26:8900–8.
[17] Laurent G, Wehr M, Davidowitz H. Temporal representations of odors in an olfactory network. J Neurosci 1996;16:3837–47.
[18] Lei H, Christensen TA, Hildebrand JG. Spatial and temporal organization of ensemble representations for different odor classes in the moth antennal lobe. J Neurosci 2004;24:11108–19.
[19] Wehr M, Laurent G. Relationship between afferent and central temporal patterns in the locust olfactory system. J Neurosci 1999;19:381–90.
[20] Kozloski J, Crawford JD. Transformations of an auditory temporal code in the medulla of a sound-producing fish. J Neurosci 2000;20:2400–8.
[21] Malone BJ, Scott BH, Semple MN. Temporal codes for amplitude contrast in auditory cortex. J Neurosci 2010;30:767–84.
[22] Arabzadeh E, Panzeri S, Diamond ME. Deciphering the spike train of a sensory neuron: counts and temporal patterns in the rat whisker pathway. J Neurosci 2006;26:9216–26.
[23] Carlson BA. Temporal-pattern recognition by single neurons in a sensory pathway devoted to social communication behavior. J Neurosci 2009;29:9417–28.
[24] Marsat G, Pollack GS. Effect of the temporal pattern of contralateral inhibition on sound localization cues. J Neurosci 2005;25:6137–44.
[25] Schnupp JWH, Hall TM, Kokelaar RF, Ahmed B. Plasticity of temporal pattern codes for vocalization stimuli in primary auditory cortex. J Neurosci 2006;26:4785–95.
[26] Sanchez JT, Gans D, Wenstrup JJ. Contribution of NMDA and AMPA receptors to temporal patterning of auditory responses in the inferior colliculus. J Neurosci 2007;27:1954–63.
[27] Williams SR, Stuart GJ. Backpropagation of physiological spike trains in neocortical pyramidal neurons: implications for temporal coding in dendrites. J Neurosci 2000;20:8238–46.
[28] Wu SH, Ma CL, Kelly JB. Contribution of AMPA NMDA, and GABAA receptors to temporal pattern of postsynaptic responses in the inferior colliculus of the rat. J Neurosci 2004;24:4625–34.
[29] Buonomano DV. Decoding temporal information: a model based on short-term synaptic plasticity. J Neurosci 2000;20:1129–41.
[30] Buonomano DV, Merzenich MM. Temporal information transformed into a spatial code by a neural network with realistic properties. Science 1995;267:1028–30.
[31] Kimmel DL, Moore T. Temporal patterning of saccadic eye movement signals. J Neurosci 2007;27:7619–30.
[32] Snyder DL, Miller MI. Random point processes in time and space. 2nd ed. New York: Springer-Verlag; 1991.
[33] Martin-Löf P. The definition of random sequences. Inform Control 1966;9:602–19.
[34] Cohen JE. Unexpected dominance of high frequencies in chaotic nonlinear population models. Nature 1995;378:610–6.

Appendix B

QUANTITATIVE DESCRIPTIONS OF GENERALIZED AROUSAL, AN ELEMENTARY FUNCTION OF THE VETEBRATE BRAIN

Amy Wells Quinkert, Vivek Vimal, Zachary M. Weil, George N. Reeke,

Nicholas D. Schiff, Jayanth R. Banavar, and Donald W. Pfaff

Proc Natl Acad Sci USA 108.suppl 3 (2011):15617-15623

Quantitative descriptions of generalized arousal, an elementary function of the vertebrate brain

Amy Wells Quinkert[a,1], Vivek Vimal[a], Zachary M. Weil[a], George N. Reeke[b], Nicholas D. Schiff[c], Jayanth R. Banavar[d], and Donald W. Pfaff[a]

[a]Laboratory of Neurobiology and Behavior and [b]Laboratory of Biological Modelling, The Rockefeller University, New York, NY 10065; [c]Laboratory of Clinical Neurophysiology, Weill Cornell Medical College, New York, NY 10065; and [d]Department of Physics, Pennsylvania State University, University Park, PA 16802

Edited by Dale Purves, Duke University Medical Center, Durham, NC, and approved April 13, 2011 (received for review February 2, 2011)

We review a concept of the most primitive, fundamental function of the vertebrate CNS, generalized arousal (GA). Three independent lines of evidence indicate the existence of GA: statistical, genetic, and mechanistic. Here we ask, is this concept amenable to quantitative analysis? Answering in the affirmative, four quantitative approaches have proven useful: (*i*) factor analysis, (*ii*) information theory, (*iii*) deterministic chaos, and (*iv*) application of a Gaussian equation. It strikes us that, to date, not just one but at least four different quantitative approaches seem necessary for describing different aspects of scientific work on GA.

deep brain stimulation | food anticipation | logistic equation | reticular formation | activation of behavior

In this brief review, we present a global concept of brain function, generalized arousal (GA), and illustrate the application of four mathematical methods to its description and analysis. Here, in order of the sections below, we (*i*) use factor analysis to help prove that GA actually exists; (*ii*) use information theory to characterize stimuli that elicit GA; (*iii*) resort to the logistic equation to speculate on how GA might make use of nonlinear dynamics; and (*iv*) having studied GA in the context of the hunger-induced activation of behavior, characterize the behavioral data with a simple Gaussian.

We have proposed that the most powerful and essential activity in any vertebrate nervous system is GA (1). As conceived, GA is universal and fundamental, initiating the activation of all behavioral responses in all vertebrate animals. The operational definition of GA is that a more-aroused animal or human is (*i*) more responsive to sensory stimuli in all modalities; (*ii*) more active motorically; and (*iii*) more reactive emotionally (1). GA's performance requirements are listed in Table 1.

Evidence for the Existence of GA of the CNS

Three independent lines of evidence indicate that generalized CNS arousal actually exists: statistical, genetic, and mechanistic.

The first line of evidence derives from recently reported behavioral results that show, statistically, the influence of GA (2). We did several experiments with mice, which tapped all three components of the operational definition of GA: S (sensory alertness) measured as motor activity in response to sensory stimuli of various modalities; M (motor activity) measured as spontaneous home cage motor activity; and E (emotional reactivity) measured as motor activity and freezing behavior in a conditioned fear paradigm. These three parameters did not covary either genetically or phenotypically. We analyzed the data using factor analysis, which probes the covariance structure of a large data set—in our case it tabulates the statistical relations among various arousal-related response measures. Factor analysis as applied here "lets the subject (in our case, a mouse) tell us" the structure of its arousal functions. Application of this analysis to our five sets of experimental data allowed us to estimate the contribution of GA, measured as the most generalized, least specific factor, as revealed by an unrotated covariance matrix and a forced one-factor solution (3). Among the five experiments, the lowest contribution by GA to explain the variance in the data was 29.7%, and the highest was 45% (2). Surprisingly, the overall conclusion that GA accounted for approximately one third of the variance of our data held true despite (*i*) different populations of mice, (*ii*) different investigators, (*iii*) different experimental manipulations and details of response measures, and (*iv*) different configurations of individual, particular factor analysis solutions involving four to six factors for each experiment. Control calculations showed that our result was robust in three ways: (*i*) the GA factor was never identical to the first factor of any particular multifactor analysis; (*ii*) it accounted for significantly more real data than in any random-number control; and (*iii*) nothing similar to the GA factor appeared in a stringent control in which marginal averages were held constant but the individual data entries were scrambled randomly (all three controls significantly different from our result, $P < 0.001$). All of these calculations indicated that the mathematical structure of arousal functions in the CNS includes a primitive, undifferentiated form we call GA. Thus, these calculations offer the first line of evidence that GA exists.

As a second line of evidence, it is possible to breed mice for high or low GA, and to the extent that this breeding program is successful, that success offers a second line of proof that a function such as GA exists. Using a high-throughput assay in mice that incorporates all three components of the operational definition of GA, mice that score high in all three components (S, M, and E) are labeled "high arousal," and mice that score low in all three components are labeled "low arousal." High-arousal males are mated to high-arousal females, and low-arousal males are mated to low-arousal females. With each generation, we expect the two lines to diverge if there is, in fact, a genetic basis for GA. We note that one cannot breed for a function that does not exist, and thus our success so far offers independent evidence for GA. Success so far, through generation 7, in this breeding program has recently been reported (4), showing that animals bred for high arousal have significantly greater measures in our GA assay than animals bred for low arousal.

In addition to the separation of the two lines of mice with the breeding experiment, we found effects of GA on behaviors that require specific forms of arousal. In GA theory, the strength of motivated behaviors that require specific arousal should be modulated by alterations in GA. In the breeding experiment, we

This paper results from the Arthur M. Sackler Colloquium of the National Academy of Sciences, "Quantification of Behavior" held June 11–13, 2010, at the AAAS Building in Washington, DC. The complete program and audio files of most presentations are available on the NAS Web site at www.nasonline.org/quantification.

Author contributions: J.R.B. and D.W.P. designed research; A.W.Q., V.V., and Z.M.W. performed research; G.N.R., and N.D.S. contributed new reagents/analytic tools; A.W.Q. analyzed data; and A.W.Q., J.R.B., and D.W.P. wrote the paper.

Conflict of interest statement: Through the licensing of technology, N.D.S. is a listed Cornell inventor and may benefit in the future from commercialization of intellectual property owned by Cornell.

This article is a PNAS Direct Submission.

[1]To whom correspondence should be addressed. E-mail: awells@rockefeller.edu.

Table 1. Operating requirements of CNS arousal systems

Operational definition
Provide alertness to sensory stimuli, body-wide, all sensory modalities
Drive voluntary motor activity, body-wide, from fidgeting to running marathons
Fuel emotional reactivity, positive and negative
Operational requirements
Lability: "Hair triggered," rapid, not sluggish
Sensitivity: Especially to the momentary state of the organism
Convergence: All sensory stimuli activate the same set of arousal subsystems, which, in turn, support each other
Divergence: Activate cerebral cortex, autonomic nervous systems, and endocrine organs to initiate behavior
Robustness: Does not fail. Survival of the organism depends on adequate CNS arousal

found that high levels of GA, as bred, had a significant impact on male sex behavior. The high-arousal male mice exhibited greater excitement and premature mounts in the presence of a receptive female and, having achieved an intromission, ejaculated significantly sooner (4). Additionally, high-arousal animals of both sexes exhibited greater levels of anxiety-like behaviors and reduced exploratory behavior in the elevated plus maze and light–dark box tasks. Taken together, these data from the breeding experiment illustrate the impact of GA on motivated behaviors.

Apart from the above breeding experiment, the *functional genomics* of CNS arousal can also be analyzed. Strikingly, more than 120 genes can be counted as contributing to arousal physiology. These have been discovered through studies of null mutant mice and through the cloning of genes whose molecular pharmacology had already implicated their gene products in arousal mechanisms (1, 2).

A third independent line of evidence for the existence of GA depends on a wealth of neuroanatomical, neurophysiological, and genomic data on the proximate mechanisms that underlie CNS arousal. One could not cite mechanisms for a CNS function that does not exist. Thus, it is important to note, as summarized previously (1, 5), that neuroscientists are beginning to understand how CNS arousal works in terms of neuroanatomical, neurophysiological, and molecular mechanisms. The classic neuroanatomical pathways ascending from the lower brainstem toward or in the forebrain can signal arousal using norepinephrine, dopamine, serotonin, histamine, and acetylcholine as transmitters.

Neuroanatomy. Four sensory modalities feed these ascending pathways in obvious ways: touch (including pain), taste, vestibular, and auditory. The ascending pathways (summarized in Fig. 1*A*) include norepinephrine-containing systems that tend to emphasize projections to the more posterior cerebral cortex (except for occipital cortex) and to support sensory alertness. Dopaminergic systems tend to project more strongly to anterior, frontal cortex and to foster directed motor acts. Serotonergic neurons tend to project preferentially to a more ancient form of cortex ("limbic cortex") and hypothalamus, and to be involved in emotional behaviors and autonomic regulation. Cholinergic neurons (ACh) in the basal forebrain support arousal by their widespread projections across the cerebral cortex, and pedunculopontine ACh cells drive thalamic neurons for thalamocortical excitation. Histamine-producing neurons likewise have extremely widespread projections, which actually originate in the hypothalamus and are strongly associated with increased CNS arousal.

A crucial feature of these ascending arousal pathways is that they show a tremendous degree of redundancy, which has the effect of protecting arousal systems from total failure after small insults. Among human patients, only *bilateral* damage to a substantial fraction of these pathways, particularly at the mesencephalic/diencephalic junction, causes coma or a vegetative state, as a result of focal injuries.

Descending neuroanatomical pathways (summarized in Fig. 1*B*) projecting from the forebrain toward the brainstem are also important. Lateral hypothalamic area hypocretin/orexin neurons project down to monoamine-expressing cell groups in the lower brainstem and even to the spinal cord. Oxytocin and arginine vasopressin-expressing neurons in the parvocellular portion of the paraventricular hypothalamic nucleus control autonomic arousal through the lower brainstem and spinal cord and affect EEG arousal through projections to locus coeruleus. Histamine-containing hypothalamic neurons in the tuberomammillary nucleus have widespread projections and receive inputs from a "biological clock," the suprachiasmatic nucleus. Preoptic area neurons have descending axons that affect sleep and autonomic physiology. For example, neurons in the preoptic area connect to lower brain regions, which control the viscera. Likewise, the paraventricular nucleus of the hypothalamus has axonal projections that, in principle, could contribute to all aspects of arousal: cerebral cortical, autonomic, endocrine, and behavioral. In sum, although the ascending arousal systems have relatively few neurons, only sparse abilities to encode particular stimuli, and are responsible for "waking up" the cerebral cortex, descending arousal systems prepare the body for action by empowering reticulospinal neurons to activate our big posture-supporting trunk muscles, modifying sensory excitability, and activating autonomic systems.

Summarizing the neuroanatomy of CNS arousal pathways, we believe they are bilateral, bidirectional, and universal among vertebrate animals including humans and that they are always involved in response potentiation of either approach or avoidance responses (1).

Neurophysiology. To gather electrophysiological evidence about arousal pathways, one looks for multimodal nerve cells that respond to a wide variety of salient stimuli across a range of sensory modalities. Such nerve cells are found up and down the brainstem (reviewed in ref. 1; see also ref. 6), from the medulla and the pons into the midbrain.

Some of the most fascinating cells in arousal systems are found in the hindbrain reticular formation near its midline toward the bottom of the brain. These large neurons have axons that split into ascending and descending limbs and could contribute both to ascending systems (for arousal of the cerebral cortex) and to descending systems (for arousal of the autonomic pathways controlling cardiovascular events and the viscera) at the same time (references in ref. 1). Regarding their sensory inputs, studied electrophysiologically, some of the neurons in this region have the large receptive fields and multimodal response characteristics expected of neurons serving GA (6–8). Likewise, their involvement in the control over a wide variety of motor activities suggests their capacity to subserve GA (9). Electrical stimulation of neurons in this area of the medullary reticular formation elevates cortical arousal (10), whereas dampening activity of medullary reticular neurons via the activation of GABA receptors decreases behavioral arousal (11). Moreover, in the spirit of

"reverse engineering," these neurons may serve as the middle of a "bow tie" configuration, having a wide range of inputs converging upon them and distributing a wide range of outputs. Control engineering theorist John Doyle (12, 13) has envisioned ways in which such a "bow tie" configuration confers robust system performance in the face of great uncertainty and variability in its environment.

Genomics. In addition to the genetic information cited above, we note the existence of gene products that are essentially involved in CNS arousal. Among classical neurotransmitters, histamine is an arousal transmitter *par excellence.* Among neuropeptide genes, hypocretin/orexin not only supports normal forms of arousal, but certain mutations in this gene or those for its receptors lead to narcolepsy (14, 15).

With three lines of evidence that an elementary function called GA exists, how might we describe environments or stimuli that elicit GA?

Information Theory in the Description of GA

GA is conceived most easily with the use of classic Shannon information theory, which was first applied to nervous systems by MacKay and McCulloch (16) and, more recently, has been introduced in didactic form to theoretical neuroscience by Dayan and Abbott (17). The communications engineer Claude Shannon (18) successfully devised a method useful for quantifying the transfer of information. His equation, Eq. **1** below, states that in a series of events ($i = 1$ to n):

$$H = -\sum_{i=1}^{n} p_i(\log p_i) \qquad [1]$$

where H is the informational entropy, a measure of information, and p_i is the probability of the i^{th} event. For example, in a binary choice between A and B, information is minimized when the probability of either A or B approaches 1.0 and is maximized at $P = 0.5$, when uncertainty is the greatest. In other words, more information is transferred when the outcome is uncertain. During several decades, neuroscientists have endeavored to apply information theory to signaling in the CNS (19–22). Despite many different methods for quantifying information, here we refer to only those methods that stem from Shannon's classic equation above.

Traditional approaches to the estimation of information content in temporal series of neuronal action potentials (23) break up the time line into a series of narrow bins so that the probabilities of 1's (spikes) and 0's (no spike) can be counted. Because calculating information content in neurophysiological data can encounter problems related to the sizes of temporal bins that are chosen, methods for calculation that include the construction of vector spaces and the estimation of interval entropy from an analytic distribution, methods that avoid bins, have been introduced (24–26). Additionally, information calculations are not restricted to single neuron action potential sequences and can be applied to sets of firing neurons (27). The concept of mutual information, the reduced amount of information encoded by cell A, for example, given knowledge of the activity in cell B that influences cell A, has also been presented as useful for the examination of neural networks (28).

The importance of information content for the activation of behavior is supported by the universality of a phenomenon known as *habituation* (references in ref. 1). In this context, habituation is defined as the decline in the vigor of a behavioral response when a stimulus is repeated and is considered an example of nonassociative memory (29, 30). This learning process is casually described as information storage. Although information theory has not been used formally in the description of habituation, we can use the language of information theory to describe how informational entropy of a stimulus affects an animal's behavioral response. At the first exposure to a stimulus, the animal knows nothing about the stimulus; therefore, the stimulus' informational entropy is high, and the animal's behavioral response is correspondingly high. If the stimulus is associated with neither aversive nor beneficial events, the animal learns nothing new with each successive exposure, and the stimulus' informational entropy decreases. As informational entropy decreases, so does behavioral response to the stimulus. Here, we are content to think of classic Shannon information calculations as a useful metric to predict CNS arousal to a stimulus or a set of stimuli.

Nonlinear Dynamics and GA

Theory of How a GA Function May Work. Although the use of information theory, above, to give a *static* description of environmental circumstances that can be arousing seems to work adequately, we have also sought an approach that might well describe the *dynamics* of CNS arousal.

Ever since the discovery of deterministic chaos, scientists have been interested in applying this form of mathematics to biology (31, 32). However, it has been difficult to generate neurobiological data that would show the power of this thinking for explaining aspects of brain function. In our case, no one would believe that GA systems work in a linear manner. Instead we seek a dynamic, nonlinear system capable of providing the rapid lability and great power of amplification that would allow a disturbing sensory stimulus to cause the entire CNS to swing into action. The logistic equation, one of several forms of mathematics that yield deterministic chaos (33), appealed to us, as a first step, consonant with our previously stated hypothesis (34).

For an initial set of experiments we were attracted to the use of the logistic equation because of its capacity for producing large and rapid changes in output and its sensitivity to small changes in the input, and because of its link to our previous theory about phase transitions in the regulation of CNS arousal (34). Of course, other nonlinear dynamic systems have similar characteristics, but the long history of intense work on the logistic equation recommended it to us (35–37).

$$X_n = R\,X_{n-1}(1\text{-}X_{n-1}) \qquad [2]$$

This equation, shown in Eq. **2**, describes an output variable, X, generated recursively by some closed system at time n, and whose value is between 0 and 1. X_{n-1} denotes the previous state of the system, whereas X_n gives the current state of the system. This time series of outputs can be stable or chaotic depending on the constant R, chosen to be between 0 and 4. We propose that arousal systems take advantage of these kinds of nonlinear dynamics when they are in a chaotic phase. Arousal systems, however, could not operate in a chaotic domain for very long and still produce organized behavioral responses, and so we were forced to conceive dynamics in which primitive neural systems, that will generate CNS arousal, operate in a chaotic zone but operate close to a phase transition, occasioned by critical slowing, during which a system relaxes to equilibrium much more slowly. As a result of this phase transition, these arousal systems are proposed (Fig. 2) to enter orderly, well-organized states capable of controlling motor behaviors (34).

Consider, as we have before (34), a classic example of an exquisitely sensitive state of matter characterized by a rapid phase transition, the liquid crystal phase (38). We propose an analogy to a phase transition in CNS arousal systems from a state of quietude to a state in which behavioral activity is rapidly initiated. We suggest that the unaroused state is a "controlled chaotic" phase (39).

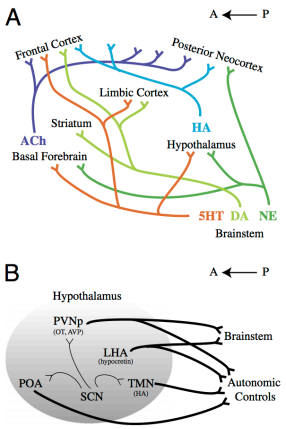

Fig. 1. (*A*) Simplified schematic representation of ascending arousal regulatory pathways. Norepinephrine-containing systems (NE, also known as noradrenergic) tend to emphasize projections to the more posterior cerebral cortex and to support sensory alertness. Dopaminergic systems (DA) tend to project more strongly to anterior, frontal cortex and to foster directed motor acts. Serotonergic (5HT) neurons project preferentially to limbic cortex and hypothalamus and are involved in emotional behaviors and autonomic controls. Cholinergic neurons (ACh) in the basal forebrain support arousal by their widespread projections across the cerebral cortex. Histamine-producing neurons (HA) likewise have extremely widespread projections that actually originate in the hypothalamus and are strongly associated with increased CNS arousal. (*B*) Simplified schematic representation of descending arousal regulatory pathways. Lateral hypothalamic area (LHA) hypocretin/orexin neurons project to monoamine-expressing cell groups in the lower brainstem and even the spinal cord. Neurons that express oxytocin (OT) and arginine vasopressin (AVP) in the parvocellular portion of the paraventricular hypothalamic nucleus (PVNp) control autonomic arousal through the lower brainstem and spinal cord and affect EEG arousal through projections to locus coeruleus. Hypothalamic neurons containing histamine (HA) in the tuberomammillary nucleus (TMN) have widespread projections and receive inputs from a biological clock, the suprachiasmatic nucleus (SCN). Preoptic area (POA) neurons have descending axons that affect sleep and autonomic physiology. Adapted from ref. 1.

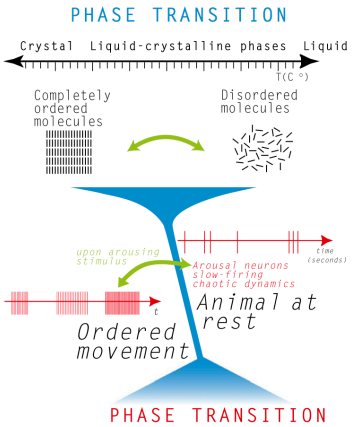

Fig. 2. Analogy between phases of matter and our hypothesis for CNS arousal. *Upper:* Schematic phase diagram for liquid crystals ranging from high temperatures and liquid phase (disordered, "random" molecules on right) to low temperatures and crystalline phase (completely ordered molecules on left). T, temperature. The liquid crystal phase is considered one of the most sensitive phases of matter because of its proximity to a phase transition to the liquid phase. *Lower:* In the quiescent animal at rest (depicted on right), large numbers of arousal-related neurons (the firing of a typical neuron is illustrated by the vertical lines as a function of time, t) have their rates of firing subject to chaotic dynamics, so that the effects of small perturbations from the arousing stimulus can be amplified selectively and very rapidly. When a movement in response to that stimulus is initiated, cortical and subcortical controls take over, moving the system across the nearby phase transition into the domain of orderly, high rates of firing (depicted on left). The system accrues significant advantages by not only being in the chaotic regime but also because it is poised in the vicinity of a phase transition. Adapted from ref. 34.

Chaotic systems have the potential to exhibit diverse behaviors. The exquisite sensitivity of chaotic systems to tiny perturbations is a powerful means of directing the trajectories in useful ways. Most important, the nonlinear dynamics of deterministic chaos provide exponential amplification of intrinsic fluctuations. Work on the control of chaos has demonstrated how one may use this sensitivity to develop feedback mechanisms for maintaining a system near dynamically unstable trajectories, thus vastly improving the flexibility in its performance. Furthermore, the unpredictability associated with chaos need not be a factor in the CNS because of the relatively short time that the system is in a chaotic state after receiving an arousing sensory input. This sensitivity to initial conditions and the inherent nonlinearity of a chaotic system near a phase transition (Fig. 2) would account for the organism's rapid response to an arousing stimulus.

We envision that a sensory input of sufficient magnitude in any modality (6) would trigger a rapid, nonlinear amplification of electrical activity in the defined neural circuits serving arousal. These could be, for example, norepinephrine-producing cells in the locus coeruleus, but they could also be cells expressing other small molecules or gene products related to arousal. When threshold firing rates of these arousal-driving neurons have been reached, the combination of the sensory input and the ascending arousal signals modulate neuronal activity in the cerebral cortex in a synchronized manner consistent with immediate attention. These cortical neurons, through their descending projections, then impose ordered patterns of activity not only to control excitability in arousal pathways but also to generate well-organized motor responses promptly.

The order/chaos phase transition has been considered before as an important feature of biological systems (28, 31). Our hypothesis simply proposes that CNS arousal systems have evolved such that they also take advantage of operating near a phase transition (31, 40). That is, they enjoy the benefits of chaotic lability and flexibility, and then, as soon as the organism is aroused, orderly, regular patterns of activity dominate. Along these lines, Rajan et al. (41) have recently carried out studies of the influence of the resonant effects of external stimuli on large chaotic neural networks and predict that the variance of neural responses ought to be significantly reduced, leading to elimination of chaos at frequencies in the range of many sensory systems. More generally, their calculations underscore the importance of the system being poised in the vicinity of the phase transition between a chaotic regime and one in which the chaos is completely absent.

There are three ways by which one could test the notion that GA systems in the mammalian brain operate in a manner that reflects chaotic dynamics: (*i*) recording neuronal activity in arousal-related neurons to search for evidence of chaotic attractors; (*ii*) simulating neural networks and looking for outputs that reflect in some way the operation of the logistic equation or other

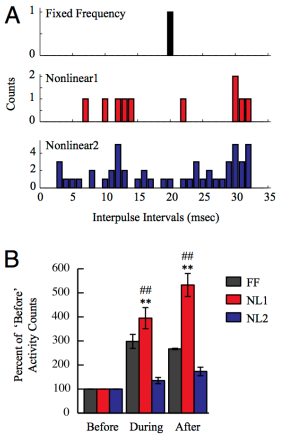

Fig. 3. (*A*) Histogram of interpulse intervals for three temporal patterns of DBS. Counts represent the number of interpulse intervals that fall within the bin range. (*B*) Behavioral response to three temporal patterns of DBS. All stimulations were physically identical except with respect to temporal patterning. Data represent 10 min during and 10 min immediately after stimulation; are normalized to 10 min immediately before; and are reported as mean ± SEM. $^{**}P < 0.01$ vs. Fixed Frequency (FF); $^{\#\#}P < 0.01$ vs. Nonlinear2 (NL2). Adapted from ref. 46.

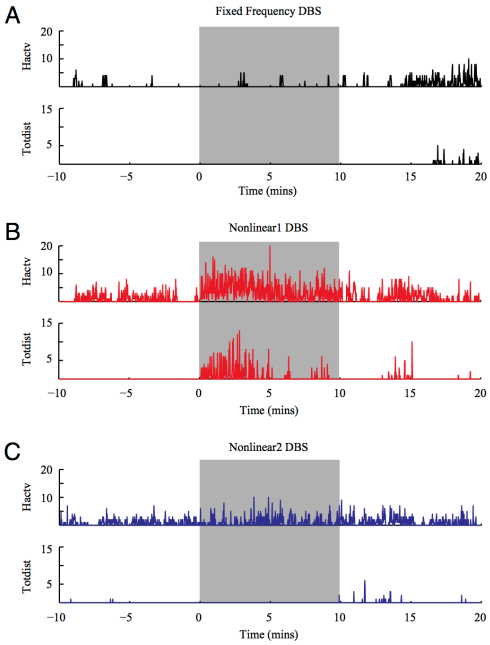

Fig. 4. Behavioral response of one mouse to three temporal patterns of DBS. Data reported represent behavior 10 min before, 10 min during, and 10 min after hippocampal stimulation with (*A*) Fixed Frequency, (*B*) Nonlinear1, and (*C*) Nonlinear2. Gray boxes delineate stimulation epochs. Horizontal Activity (Hactv) and Total Distance (Totdist) are presented as sums of activity every second. Adapted from ref. 46.

chaotic dynamics; and (*iii*) stimulating arousal-related neurons and looking for unusual results when pulse trains dictated by the logistic equation are applied.

Upon reflection, regarding approach (*i*), recording activity, we realized that even in low-dimensional systems, impossibly large amounts of data would have to be searched for evidence of chaotic dynamics and that the search would be even harder in the inevitable presence of biological noise. Therefore, we have worked on (*ii*), simulation, and (*iii*), stimulation. Approach (*ii*), simulating large neural nets, did lead to sudden breaks in activity at the value $R = 3$ (42), but neither the implications of that finding nor the network characteristics necessary for producing that finding is yet clear. Therefore, we have concentrated on approach (*iii*), deep brain stimulation (DBS).

Electrical Stimulation Using Temporally Patterned Pulse Trains. DBS has been used to increase arousal in humans (43) and rats (10); one study also showed that stimulation can improve cognition in mice (44). However, these studies and all clinical applications of DBS have used simple fixed-frequency temporal patterns. Although neuroscientists observe temporally patterned neuronal responses, especially in sensory systems (45), it is still an open question whether these patterns are actually used by the CNS. A recently published study tested the hypothesis that, in DBS that increases arousal, temporally patterned electrical pulse trains work significantly better to support the animal's initiation of behavior, compared with conventional pulse trains that are physically identical in every way except the temporal patterning (46). Total number of pulses was also held constant.

In this study (46), mice were implanted with bilateral monopolar electrodes either in the ventral hippocampus or the medial thalamus. During the study, behavioral motor activity of each mouse was measured using an infrared home cage monitoring system. After recovery from surgery, animals were stimulated every 3 h during the dark phase of the light cycle for up to 3 d. The distributions of interpulse intervals in the three pulse trains used in this study are shown in Fig. 3*A*: the standard pattern of Fixed Frequency is in black and the two nonlinear patterns, Nonlinear1 and Nonlinear2, are shown in red and blue, respectively. Each animal was challenged with Fixed Frequency and at least one of the two nonlinear patterns. Order of stimulation for each pattern was counterbalanced as much as possible.

The temporal patterning of pulses within DBS affected the arousal-related behavior; specifically, Nonlinear1 increased whole-body movement (recorded as activity counts) during and after stimulation more than either Fixed Frequency or Nonlinear2 (Fig. 3*B*). Although these data are averaged across animals, the same effect can be seen in raw data from an individual. In Fig. 4, two activity outputs are displayed at high temporal resolution for the same animal during three different stimulations. Despite the fact that we know little about the mechanism of how temporal dynamics effect arousal, our data offer proof that temporal patterning within a pulse train can make a difference when all other physical parameters of the pulses are held constant. Under no circumstances would we assert that Nonlinear1 and -2 are unique, but instead these results show that temporal patterning of a pulse train for DBS is important, even when all other physical characteristics of the pulse train are held constant (46). These results suggest that work on the temporal dynamics of arousal systems will foster a deep understanding of how they work.

Gaussian Distribution Describes the Activation of Behavior Due to Hunger

A different approach to the quantification of arousal is the use of an experimental manipulation to suddenly increase arousal when otherwise it would remain at a low level. That is, one of the most incisive ways to discover neuronal mechanisms underlying GA is to set up forces that regulate arousal against each other. Mistlberger (47) and a host of other scientists have done this by requiring hungry animals, in the absence of an alarm or any signal other than their hunger, to wake up and become active during the time of day they normally would be sleeping to receive food: they generate food-anticipatory activity (FAA). Although the neural network that generates FAA is still under investigation, we emphasize the importance of the ventromedial nucleus of the hypothalamus, a cell group in which we found the earliest activation of neurons that apparently support or even initiate FAA (48). Surprisingly, LeSauter et al. (49) discovered that a Gaussian distribution, shown below in Eq. **3**,

$$f(x) = \frac{1}{\sqrt{2\pi\sigma^2}} e^{-\frac{(x-\mu)^2}{2\sigma^2}}, \qquad [3]$$

closely represents the process of accumulating arousal, revealed by a correlation of $r = 0.99$ between the rising limb of the best-fit Gaussian and the cumulative activity. In this particular case, $f(x)$ represents cumulative behavior at time x. The two parameters μ (mean) and σ (SD) were varied to achieve the excellent fit with the data. As LeSauter et al. (49) reasoned, "the close fit to the Gaussian indicates that the mechanisms underlying these data include a large number of individual neuronal go, no-go decisions with an increasing proportion of 'go' decisions as feeding time draws near."

Further, this experiment (49) included an analysis of gene/behavior relations. It compared the FAA of ghrelin gene knockout animals with their wild-type littermates. Again, in the gene knockout animals, the excellent fit of the data to a Gaussian distribution suggests that the decision to activate this appetitive behavior can be understood as a series of repetitive binary choices, but the probability of a positive decision is only approximately half as large in the ghrelin knockout animals. The height of the Gaussian for the ghrelin knockout animals was half that of their wild-type littermates. In this sense, the comparison of the shapes and amplitudes of the Gaussians yields a mathematical description of a gene/behavior relationship.

Multiplicity of Approaches

We have used not just one but multiple quantitative approaches to conceive and describe a primitive, elementary CNS function. One of the three lines of evidence for the very existence of generalized CNS arousal depended on factor analysis, a mathematical statistical approach that uses a matrix of correlations among quantitative endpoints. Then, second, a conception of generalized CNS arousal used Shannon's equation to express "information" in mathematical terms. Third, following the initial conceptualization, we theorized that the most fundamental arousal mechanisms in the brainstems of all vertebrate animals operate in a nonlinear zone. A quantitative expression of our idea lay in the logistic equation, a formulation that has the capacity of yielding chaotic dynamics. Fourth, a Gaussian function accurately describes the increase in arousal caused by the anticipation of food. Under no circumstances would we claim that these four independent approaches are unique or that other equally useful approaches do not exist.

In addition to the multiplicity of quantitative approaches described here, it is important to understand that individual differences in this primitive function, GA, may be contributing to behavioral outcomes of various sorts without investigators realizing it, controlling for it, or incorporating it into their interpretations. By providing a quantitative assessment of GA based on simple behavioral measures, we hope to help investigators maximize the effectiveness of their studies and make further inroads into understanding the contribution of more specific variables to behavioral outputs.

In summary, we suspect that even for the analysis of elementary brain functions, let alone complex functions such as learning and memory, well-chosen sets of multiple equations will be required for their description and analysis.

ACKNOWLEDGMENTS. We thank Christopher Kim and William Weinberger in the D.W.P. laboratory for their important work supplying some of the data on neural networks and the following readers for their useful feedback: Prof. T. James Matthews, Prof. Peggy Mason, Prof. Ralph Mistlberger, and Dr. Ilia Karatsoreos. This work was funded, in part, by a company, IntElect Medical Inc., in which Cornell University has part ownership. This work is also supported by National Institutes of Health Grants HD-05751 and MH-38273.

1. Pfaff DW (2006) *Brain Arousal and Information Theory: Neural and Genetic Mechanisms* (Harvard Univ Press, Cambridge, MA), p vi.
2. Garey J, et al. (2003) Genetic contributions to generalized arousal of brain and behavior. *Proc Natl Acad Sci USA* 100:11019–11022.
3. Gorsuch RL (1983) *Factor Analysis* (Lawrence Erlbaum Associates, Hillsdale, NJ), 2nd Ed, p xvii.
4. Weil ZM, Zhang Q, Hornung A, Blizard D, Pfaff DW (2010) Impact of generalized brain arousal on sexual behavior. *Proc Natl Acad Sci USA* 107:2265–2270.
5. Pfaff D, Martin EM, Weingarten W, Vimal V (2008) The central neural foundations of awareness and self-awareness. *Prog Theor Phys Suppl* 173:79–98.
6. Martin EM, Pavlides C, Pfaff D (2010) Multimodal sensory responses of nucleus reticularis gigantocellularis and the responses' relation to cortical and motor activation. *J Neurophysiol* 103:2326–2338.
7. Leung CG, Mason P (1998) Physiological survey of medullary raphe and magnocellular reticular neurons in the anesthetized rat. *J Neurophysiol* 80:1630–1646.
8. Leung CG, Mason P (1999) Physiological properties of raphe magnus neurons during sleep and waking. *J Neurophysiol* 81:584–595.
9. Serafin M, Vidal PP, Mühlethaler M (1996) Electrophysiological study of nucleus gigantocellularis neurons in guinea-pig brainstem slices. *Neuroscience* 73:797–805.
10. Wu HB, Stavarache M, Pfaff DW, Kow LM (2007) Arousal of cerebral cortex electroencephalogram consequent to high-frequency stimulation of ventral medullary reticular formation. *Proc Natl Acad Sci USA* 104:18292–18296.
11. Mackersey K, Litvin Y, Pfaff DW, Martin EM (2009) GABA-A receptor antagonism in the medullary gigantocellular reticular nucleus leads to increased responsiveness in isoflurane anesthetized mice. *Society for Neuroscience* Program No. 276.272. 2009 Neuroscience Meeting Planner, Chicago.
12. Csete M, Doyle J (2004) Bow ties, metabolism and disease. *Trends Biotechnol* 22:446–450.
13. Doyle J, Csete M (2005) Motifs, control, and stability. *PLoS Biol* 3:e392.
14. Mikkelsen JD, et al. (2001) Hypocretin (orexin) in the rat pineal gland: A central transmitter with effects on noradrenaline-induced release of melatonin. *Eur J Neurosci* 14:419–425.
15. Taheri S, Zeitzer JM, Mignot E (2002) The role of hypocretins (orexins) in sleep regulation and narcolepsy. *Annu Rev Neurosci* 25:283–313.
16. MacKay DM, McCullouch WS (1952) The limiting information capacity of a neuronal link. *Bull Math Biophys* 14:127–135.
17. Dayan P, Abbott LF (2001) *Theoretical Neuroscience: Computational and Mathematical Modeling of Neural Systems* (Massachusetts Institute of Technology Press, Cambridge, MA), p xv.
18. Shannon CE (1948) A mathematical theory of communication. *Bell Syst Tech J* 27:379–423.
19. Paulin MG, Hoffman LF, Assad C (2004) Distributed coding by single spikes in the bullfrog vestibular nerve: A basis for dynamical computation in neural systems. *Neurocomputing* 58-60:73–77.
20. Rokem A, et al. (2006) Spike-timing precision underlies the coding efficiency of auditory receptor neurons. *J Neurophysiol* 95:2541–2552.
21. Pogosyan A, et al. (2006) Elevations in local gamma activity are accompanied by changes in the firing rate and information coding capacity of neurons in the region of the subthalamic nucleus in Parkinson's disease. *Exp Neurol* 202:271–279.
22. Nemenman I, Lewen GD, Bialek W, de Ruyter van Steveninck RR (2008) Neural coding of natural stimuli: information at sub-millisecond resolution. *PLoS Comput Biol* 4:e1000025.
23. Strong SP, Koberle R, de Ruyter van Steveninck RR, Bialek W (1998) Entropy and information in neural spike trains. *Phys Rev Letts* 80:197–200.
24. Victor JD (2002) Binless strategies for estimation of information from neural data. *Phys Rev E Stat Nonlin Soft Matter Phys* 66:051903.

25. Reeke GN, Coop AD (2004) Estimating the temporal interval entropy of neuronal discharge. *Neural Comput* 16:941–970.
26. Nemenman I, Bialek W, de Ruyter van Steveninck R (2004) Entropy and information in neural spike trains: Progress on the sampling problem. *Phys Rev E Stat Nonlin Soft Matter Phys* 69:056111.
27. Yu YG, Crumiller M, Knight B, Kaplan E (2010) Estimating the amount of information carried by a neuronal population. *Front Comp Neurosci* 4:10.
28. Greenfield E, Lecar H (2001) Mutual information in a dilute, asymmetric neural network model. *Phys Rev E Stat Nonlin Soft Matter Phys* 63:041905.
29. Kandel ER (2000) Cellular mechanisms of learning and the biological basis of individuality. *Principles of Neural Science*, ed Kandel ER (McGraw-Hill, Health Professions Division, New York), 4th Ed.
30. Sanderson DJ, et al. (2010) Spatial working memory deficits in GluA1 AMPA receptor subunit knockout mice reflect impaired short-term habituation: Evidence for Wagner's dual-process memory model. *Neuropsychologia* 48:2303–2315.
31. Kauffman SA (1993) *The Origins of Order: Self-organization and Selection in Evolution* (Oxford Univ Press, New York), p xviii.
32. May R (2002) The best possible time to be alive. *It Must Be Beautiful: Great Equations of Modern Science*, ed Farmelo G (Granta Books, London), pp 28–45.
33. Cohen JE (1995) Unexpected dominance of high frequencies in chaotic nonlinear population models. *Nature* 378:610–612.
34. Pfaff D, Banavar JR (2007) A theoretical framework for CNS arousal. *Bioessays* 29: 803–810.
35. Anderson RM, May RM (1978) Regulation and stability of host-parasite population interactions. 1. Regulatory processes. *J Anim Ecol* 47:219–247.
36. Feigenbaum MJ (1978) Quantitative universality for a class of non-linear transformations. *J Stat Phys* 19:25–52.
37. Feigenbaum MJ (1979) Universal metric properties of non-linear transformations. *J Stat Phys* 21:669–706.
38. de Gennes PG, Prost J (1993) *The Physics of Liquid Crystals* (Oxford Univ Press, Oxford), 2nd Ed, p xvi.
39. Ott E, Sauer T, Yorke JA (1994) *Coping with Chaos: Analysis of Chaotic Data and the Exploitation of Chaotic Systems* (Wiley-Interscience, New York), p 418.
40. Kauffman SA, Johnsen S (1991) Coevolution to the edge of chaos: Coupled fitness landscapes, poised states, and coevolutionary avalanches. *J Theor Biol* 149:467–505.
41. Rajan K, Abbott LF, Sompolinsky H (2010) Stimulus-dependent suppression of chaos in recurrent neural networks. *Phys Rev E Stat Nonlin Soft Matter Phys* 82:011903.
42. Vimal V, Quinkert AW, Weingarten WF, Reeke GN, Pfaff DW (2010) Chaotic dynamics reflected in the output of a simulated neural network. *Society for Neuroscience*: Program No. 208.231. 2010 Neuroscience Meeting Planner, San Diego.
43. Schiff ND, et al. (2007) Behavioural improvements with thalamic stimulation after severe traumatic brain injury. *Nature* 448:600–603.
44. Shirvalkar P, Seth M, Schiff ND, Herrera DG (2006) Cognitive enhancement with central thalamic electrical stimulation. *Proc Natl Acad Sci USA* 103:17007–17012.
45. Wasserman GS (1992) Isomorphism, task dependence, and the multiple meaning theory of neural coding. *Biol Signals* 1:117–142.
46. Quinkert AW, Schiff ND, Pfaff DW (2010) Temporal patterning of pulses during deep brain stimulation affects central nervous system arousal. *Behav Brain Res* 214: 377–385.
47. Mistlberger RE (2009) Food-anticipatory circadian rhythms: Concepts and methods. *Eur J Neurosci* 30:1718–1729.
48. Ribeiro AC, LeSauter J, Dupré C, Pfaff DW (2009) Relationship of arousal to circadian anticipatory behavior: Ventromedial hypothalamus: One node in a hunger-arousal network. *Eur J Neurosci* 30:1730–1738.
49. LeSauter J, Hoque N, Weintraub M, Pfaff DW, Silver R (2009) Stomach ghrelin-secreting cells as food-entrainable circadian clocks. *Proc Natl Acad Sci USA* 106: 13582–13587.

Appendix C

TEMPORAL PATTERNS OF DEEP BRAIN STIMULATION GENERATED WITH A TRUE RANDOM NUMBER GENERATOR AND THE LOGISTIC EQUATION: EFFECTS OF CNS AROUSAL IN MICE

Amy Wells Quinkert and Donald W. Pfaff

Behav Brain Res 229.2 (2012):340-358

Behavioural Brain Research 229 (2012) 349–358

Contents lists available at SciVerse ScienceDirect

Behavioural Brain Research

journal homepage: www.elsevier.com/locate/bbr

Research report

Temporal patterns of deep brain stimulation generated with a true random number generator and the logistic equation: Effects on CNS arousal in mice

A.W. Quinkert*, D.W. Pfaff

Rockefeller University, Laboratory of Neurobiology and Behavior, 1230 York Ave. Box 275, New York, NY 10065, United States

ARTICLE INFO

Article history:
Received 2 November 2011
Received in revised form 9 January 2012
Accepted 12 January 2012
Available online 21 January 2012

Keywords:
Deep brain stimulation
Temporal patterns
Generalized arousal
Logistic equation

ABSTRACT

Deep brain stimulation (DBS) has shown promise in the treatment of many neurological and psychiatric disorders as well as a disorder of consciousness, the minimally conscious state (MCS). In the clinic, DBS is always monotonic standard pulses; however, we have hypothesized that temporally patterned pulses might be more efficient in achieving desired behavioral responses. Here we present two experiments on DBS of the central thalamus to increase arousal, as measured by motor activity, and to affect the electroencephalogram (EEG). In the first, we optimized amplitude and frequency in standard stimulation of the central thalamus in intact mice. In the second, the optimized fixed frequency was compared to two alternative temporal patterns, chaotic and random, which were physically identical to each other and fixed frequency in all ways except temporal pattern. In both experiments and with all types of stimulation, DBS of the central thalamus increased arousal as measured by motor activity. These data also revealed that temporal patterning of pulses can modulate response to stimulation. That temporal patterns in DBS of the central thalamus were found to alter motor activity response implies possible usefulness of temporal patterns in DBS of other contexts. More investigation into exactly how temporally patterned stimulation may affect neuronal circuit dynamics is necessary.

1. Introduction

Deep brain stimulation (DBS) is growing in popularity as a neurosurgical technique because of its wide applicability, adjustability, and reversibility. It is used in a large number of brain targets to treat widespread neurological and psychiatric illnesses and has been successfully applied for the treatment of movement disorders [1–3], affective disorders [4–6], and chronic pain [7–9]. Another promising application of DBS is the treatment of patients with disorders of consciousness; in particular, a diagnosis of minimally conscious state (MCS) is amenable to treatments such as DBS. Central thalamus DBS (CT/DBS) has been shown to facilitate functional recovery in MCS patients. In a double-blinded crossover study of one MCS patient, Schiff et al. show great improvement of patient awareness and ability to communicate with CT/DBS [10]. Six years after the initial brain injury, the patient presented with behavior fluctuations consistent with MCS, and with no improvement since two years post-injury. Almost immediately after stimulation started, the patient began showing improvement, and by the end of the six months of the study, he had much greater functional ability including being able to feed himself and communicate with words.

For the particular application of DBS for MCS, the chosen target is the central thalamus. The central thalamus is uniquely poised for modulation in the severely injured brain because of its neuroanatomical placement and role in regulating generalized arousal. Anatomically located between the major ascending and basal forebrain arousal systems and the cortex, the central thalamus is recruited to support overall cerebral activation and maintain that activation during high arousal states [11]. This level of cerebral activation is obviously absent in the severely injured brain; Schiff theorizes that while MCS patients retain thalamo-cortical connections needed to support cerebral activation, they lack sufficient innervation from the arousal systems. It is suggested that CT/DBS in a severely injured brain approximates this missing arousal input, allowing the central thalamus to function normally in supporting cerebral activity and cognition [12].

Assuming DBS for increasing arousal does mimic a missing arousal input, what is the nature of that input? There are various theories of how information is coded in neuronal action potentials; one such hypothesis is that information is contained in temporal patterns of neuronal spike trains [13–15]. If information is carried by temporal patterns, responses to DBS of different patterns might be larger than standard stimulation. Temporally patterned DBS might be more effective for increasing arousal than conventional fixed frequency stimulation. Assuming this is true, it would be possible to minimize electric current directed into brain by optimizing temporal pattern to maximize response to DBS. In our previously

* Corresponding author. Tel.: +1 212 327 8668; fax: +1 212 327 8643.
E-mail addresses: awells@rockefeller.edu, amy.quinkert@gmail.com (A.W. Quinkert).

0166-4328/$ – see front matter © 2012 Elsevier B.V. All rights reserved.
doi:10.1016/j.bbr.2012.01.025

published work [16], we showed that temporal patterning of pulses altered motor activity response to DBS.

There is a multitude of patterns or ways to pattern a series of pulses. To narrow down the possibilities, we first chose to use deterministic chaos to generate temporal patterns. In our previously published work [16], the logistic equation was chosen for our first temporal pattern because it is a simple discrete chaotic equation and because it coincides with our previous hypothesis that nonlinear dynamics may be important in the control of CNS arousal systems [17]. Chaotic systems have the advantage of being able to quickly amplify the smallest of perturbations. In that original study, we compared two different temporal patterns generated by the logistic equation to the standard fixed frequency. Here in addition to our chaotic temporal pattern, we wanted an alternate temporal pattern that would also serve as a control. Since our chaotic temporal pattern is deterministic, we wanted our second temporal pattern to be internally independent; therefore, a true random number generator was chosen. True random number generators use physical measurements (such as measurements of atmospheric noise) instead of deterministic algorithms to create series of numbers.

In this paper, we present two experiments; in the first, we optimize amplitude and frequency of CT/DBS, and in the second we compare our optimized fixed frequency with chaotic and random temporal patterns. While the highest amplitude tested (125 μA) significantly increased behavioral response to DBS, we were conservative in our choice of 100 μA for subsequent studies. There were no significant differences between the four frequencies we tried, but 125 Hz increased behavioral activity more than the other three. We also saw a significant effect of light phase, and this difference seems to be due to the low baselines of behavior in the light which result in larger relative changes with stimulation than in the dark. In the second experiment, we found a general effect of temporal pattern. In both studies, CT/DBS increased generalized arousal as measured by motor activity and EEG waves. We also confirmed that temporal patterning makes a difference in behavioral response, but using conservative statistical methods, these differences were not always significant.

2. Methods

2.1. Animals and materials

A total of 26 six- to nine-week-old C57BL/6 mice were singly housed on a reversed 12 h light/dark cycle with food and water available *ad libitum* for the duration of the study. Monopolar stainless steel electrodes (Plastics One) were implanted bilaterally into the central thalamus under ketamine/xylazine anesthesia (80/12 mg/kg) using a Kopf stereotaxic apparatus. Coordinates used were as follows: anterior–posterior, −1.70 mm from bregma; lateral, ±0.75 mm from midline; and depth, −3.00 mm from the surface of the brain. Only mice histologically confirmed with at least unilateral electrode placement in the central thalamus are reported here. Mice were also subcutaneously implanted with a small animal transmitter (Data Sciences International) capable of transmitting electroencephalogram (EEG). EEG electrodes were positioned to touch the intact dura and secured to the skull with super glue; the drilled holes for the electrodes were located on the left posterior and right anterior portions of the parietal bone of the skull. Post-operative care included recovery from anesthesia under a heat lamp and flunazine analgesia (50 mg/kg) for 2 days. Before any handling or manipulation, mice were allowed to recover from surgery for 5–7 days. At the end of the study, mice were euthanized by isoflurane anesthesia and decapitation. Fresh frozen brains were collected and then cut at 40 μm on a cryostat, and electrode placements were confirmed by acetylcholinesterase staining [18] (see Figure S1 for diagram of electrode placements). All animal procedures were in compliance with National Institutes of Health guidelines and approved by the Rockefeller University Institutional Animal Care and Use Committee.

Supplementary material related to this article can be found, in the online version, at doi:10.1016/j.bbr.2012.01.025.

2.2. Parametric experiment

In this experiment, mice ($n = 10$) were stimulated for 10 min for a maximum of 24 stimulations over the course of three days. To space stimulations evenly over the course of the study, stimulation epochs occurred every 3 h. Three amplitudes (75, 100, and 125 μA) and four frequencies (50, 125, 175, and 225 Hz) were tested. While amplitude was increased systematically over the three days in all animals, frequency was counterbalanced for order.

2.3. Temporal pattern experiment

Based on the motor activity data from the parametric experiment, we chose 125 Hz and 100 μA as the parameters for the temporal pattern experiment. Two temporal patterns were chosen in addition to our optimized fixed frequency pattern. One pattern, based on the logistic equation, was chosen subsequent to our previous study using nonlinear patterns [16] as well as our hypothesis that nonlinear dynamics may be important in the control of CNS arousal systems [17]. The second pattern, based on a true random number generator, was chosen as a patterned control; based on independent true random numbers, the random temporal pattern was used to give perspective on the internally structured chaotic temporal pattern. Mice ($n = 16$) were stimulated for 10 min for a total of six stimulations over the course of one day. To space stimulations evenly over the course of that day, stimulation epochs occurred every 4 h. Each mouse was challenged with all three temporal patterns, counterbalanced for order.

The other two temporal patterns were generated using a true random number generator (based on atmospheric noise) and the logistic equation. The logistic equation, $X_n = RX_{n-1}(1 - X_{n-1})$, where X is the output at time n, has a constant modifier, R, that creates chaotic output at certain values. The true random number generator used here takes atmospheric noise measurements to generate three thousand uniformly distributed numbers [19]. Output to the logistic equation was calculated to two or three thousand iterations with initial conditions to ensure chaotic behavior of the equation ($R = 3.90$ and $X_0 = 0.2$). To ensure that depolarization block did not occur, a minimum interpulse interval (IPI) was defined as 0.3 ms, and chaotic and random sequences were scaled to meet that minimum. For both sequences of numbers, a consecutive set of numbers was found such that the number of elements in the set divided by the sum of the scaled output equaled the desired average frequency. In this manner, we defined a set of 50 pulses from the logistic equation output and named it 'chaotic' and a set of 50 pulses from the true random number generator output and named it 'random.' To ensure the only difference between the three patterns was the temporal patterning of pulses, the three temporal patterns were identical with respect to pulse shape, pulse duration, amplitude, average frequency, and stimulation duration. All stimulation, in both experiments, was constant current, monopolar, symmetric biphasic stimulation with a total pulse duration of 0.2 ms.

2.4. Data analysis

During the course of each study, one channel EEG and three behavioral data measures were collected. Two data collection systems were utilized; a 3D infrared beam home cage activity monitor (Accuscan Instruments) was used to collect motor activity data, and an implantable transmitter telemetry system (Data Sciences International or DSI) was used to collect EEG as well as motor activity data. The three behavioral measures observed included: (1) activity counts (whole body activity, designated "Counts" below), collected by the DSI transmitter and representing changes in field strength between the transmitter and receiver as the mouse moves; (2) horizontal activity (fidgeting movements, designated "Hactv" below), collected by the home cage Accuscan system and representing the number of infrared beams broken in the horizontal plane; and (3) total distance (ambulation, designated "Totdist" below), collected by the home cage Accuscan system and representing non-repeating infrared beam breaks in the horizontal plane. EEG, collected by the DSI system, was divided into minute long epochs and its power spectra were estimated using the multitaper method. EEG waves were integrated over the following frequency bins: delta (0.5–4 Hz), theta (4.5–8 Hz), alpha (8.5–12 Hz), beta (12.5–20 Hz), and gamma (35–45 Hz). EEG data are reported as the relative power of each frequency bin to the summed power in all five frequency bins. Data were reported for 10 min before, 10 min during (only for behavioral measures), and 10 min after each stimulation. Data collected during and after stimulation were normalized to data collected directly before stimulation. Because motor activity and EEG inherently change over the course of the light dark cycle, we restricted our analyses to the half hour surrounding stimulation to avoid the intrinsic fluctuations of our outcome measures.

For statistical evaluation, each data measure was analyzed by multiple factor ANOVA and post-hoc two-tailed t-tests with Bonferroni corrections for multiple comparisons. Multiple factor ANOVA is a common method for determining the relative effects of multiple independent variables as well as their interactions on a single outcome measure [20,21]. The factors included in our analyses were stimulation, stimulation parameters (amplitude and frequency in the parametric experiment, temporal pattern in the temporal pattern experiment), phase of the light dark cycle, as well as any interactions between these factors. Since no significant interactions were found, these analyses were not included in the following for discussion. Despite obvious strong differences where the standard error of the means did not overlap, several post-hoc comparisons were not significant with Bonferroni-corrected t-tests. Even though these Bonferroni corrections were very conservative, we included them during our interpretation of the results. In subsequent evaluation

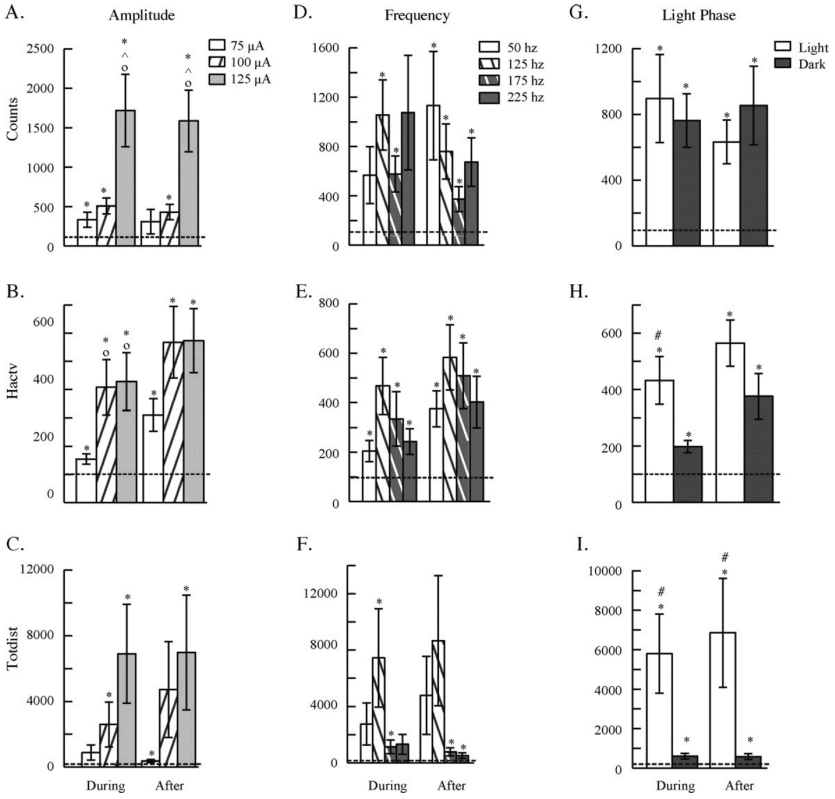

Fig. 1. *Parametric experiment: behavior*. Behavioral response to amplitude (A, B and C), frequency (D, E and F.), and light phase (G, H and I) of CT/DBS. Three behavioral measures are shown: activity counts (whole body movement), horizontal activity (fidgeting), and total distance (ambulation). ANOVA analyses revealed an overall effect of CT/DBS in activity counts ($p < 0.001$), horizontal activity ($p < 0.001$), and total distance ($p < 0.01$). ANOVA also showed an effect of amplitude in activity counts (A, $p < 0.001$), horizontal activity (B, $p < 0.001$), and total distance (C, $p < 0.01$). An overall effect of frequency was found in horizontal activity (E, $p < 0.05$) and total distance (F, $p < 0.001$). Light phase of CT/DBS was found to be significant in horizontal activity (H, $p < 0.001$) and total distance (*I*, $p < 0.001$). Panels include 10 min of data during and 10 min of data after CT/DBS, all normalized to before stimulation. Data are presented as mean ± S.E.M. $^{*}p < 0.05$ compared to before, $^{\circ}p < 0.05$ compared to 75 µA, $\hat{}p < 0.05$ compared to 100 µA, $^{\#}p < 0.05$ compared to dark phase.

of the behavioral data, we utilized multiple factor MANOVA with Wilks' lambda to determine if our findings held true when considering the behavioral data as a whole [21]. MANOVA analysis of both experiments confirmed all of our major findings except for the main effect of light phase in the parametric experiment.

Extensive analyses of data from both experiments were done to determine if any sex differences in response to stimulation exist. All differences found were small and inconsistent across data measures and between the two data sets; therefore, data presented here are pooled from males and females.

3. Results

3.1. Parametric experiment

In addition to looking for differences caused by the stimulation itself, we investigated differences caused by amplitude of stimulation, frequency of stimulation, light phase during which stimulation occurred, and any correlation between data measures (scattergrams and correlation coefficients for EEG data can be found in Figure S2). First and foremost, we found an effect of central thalamus DBS (CT/DBS) in all three behavioral measures (counts: $F_{2,100} = 14.23$, $p < 0.001$; Hactv: $F_{2,902} = 32.33$, $p < 0.001$; Totdist: $F_{2,914} = 5.66$, $p < 0.01$; see Fig. 1) and four of five EEG waves (theta: $F_{1,780} = 69.78$, $p < 0.001$; alpha: $F_{1,772} = 14.58$, $p < 0.001$; beta: $F_{1,760} = 21.89$, $p < 0.001$; gamma: $F_{1,771} = 42.44$, $p < 0.001$; see Fig. 2). CT/DBS increased motor activity, decreased theta waves in the EEG, and increased alpha, beta, and gamma waves in the EEG. These data replicate our finding that CT/DBS increases generalized arousal.

Supplementary material related to this article can be found, in the online version, at doi:10.1016/j.bbr.2012.01.025.

3.1.1. Amplitude effects

ANOVA analyses also revealed an effect of amplitude, when all other factors are held constant, in all three behavioral measures (counts: $F_{2,1000} = 15.68$, $p < 0.001$; Hactv: $F_{2,902} = 7.83$, $p < 0.001$; Totdist: $F_{2,914} = 5.13$, $p < 0.01$; see Fig. 1). Comparing individual amplitudes, 125 µA stimulation increased activity counts greater than either 75 µA (during: $t_{197} = -3.06$, $p < 0.01$; after: $t_{200} = -3.15$, $p < 0.01$) or 100 µA (during: $t_{202} = -2.72$, $p < 0.05$; after: $t_{202} = -3.03$,

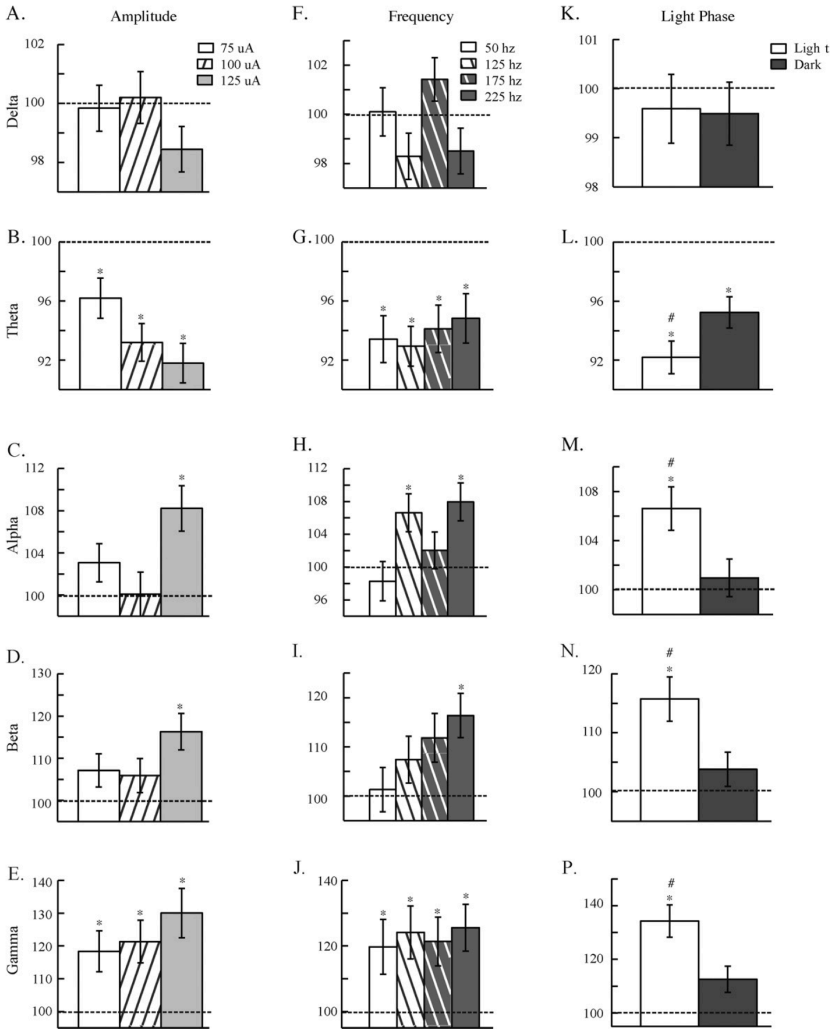

Fig. 2. *Parametric experiment: EEG.* EEG response to amplitude (A–E), frequency (F–J), and light phase (K–P) of CT/DBS. EEG waves are defined by the following frequency bins: delta (0.5–4 Hz), theta (4.5–8 Hz), alpha (8.5–12 Hz), beta (12.5–20 Hz), and gamma (35–45 Hz). ANOVA analyses revealed an overall effect of CT/DBS in theta ($p < 0.001$), alpha ($p < 0.001$), beta ($p < 0.001$), and gamma ($p < 0.001$) waves. ANOVA also showed an effect of amplitude in theta (B, $p < 0.05$) and alpha (C, $p < 0.01$) waves. An effect of frequency was found in alpha (H, $p < 0.05$) waves. Light phase of CT/DBS was found to be significant in theta (L, $p < 0.05$), alpha (M, $p < 0.01$), beta (N, $p < 0.01$), and gamma (P, $p < 0.001$) waves. Panels include 10 min of data after CT/DBS, normalized to before stimulation. Data are presented as mean ± S.E.M. $^{*}p < 0.05$ compared to before, $^{\#}p < 0.05$ compared to dark phase.

$p < 0.01$) during and after stimulation (see Fig. 1A). Looking at horizontal activity, 75 μA stimulation increased motor activity less than 100 μA ($t_{178} = -2.76$, $p < 0.05$) or 125 μA ($t_{175} = -2.90$, $p < 0.05$) during stimulation (see Fig. 1B). Confirming an effect of stimulation, all amplitudes increased all three behavioral measures during and after stimulation compared to before.

In the ANOVA analyses of EEG waves, an effect of amplitude, holding all other factors constant, was found in two of five EEG waves (theta: $F_{2,780} = 3.06$, $p < 0.05$; alpha: $F_{2,772} = 5.08$, $p < 0.01$; see Fig. 2). Despite the overall effect of amplitude in theta and alpha waves, there were no statistically significant differences between individual amplitudes in those two EEG waves. Comparing response after stimulation to before however, significant differences were found. Theta waves decreased with all three amplitudes of stimulation (75 μA: $t_{278} = 2.92$, $p < 0.01$; 100 μA: $t_{279} = 5.56$, $p < 0.001$; 125 μA: $t_{250} = 6.32$, $p < 0.001$; see Fig. 2B).

125 μA increased alpha ($t_{248} = -3.98$, $p < 0.001$; see Fig. 2C) and beta ($t_{235} = -4.14$, $p < 0.001$; see Fig. 2D) waves after stimulation. Gamma waves were increased after all three amplitudes (75 μA: $t_{283} = -3.00$, $p < 0.01$; 100 μA: $t_{279} = -3.41$, $p < 0.01$; 125 μA: $t_{236} = -4.38$, $p < 0.001$; see Fig. 2E) of stimulation. These data also support the idea that more current in CT/DBS increases generalized arousal to a higher degree. To avoid negative side effects of injecting too much current into the brain, we decided on the conservative choice of 100 μA for future studies.

3.1.2. Frequency effects

Investigation of the frequency of stimulation led to the determination there was a significant effect of frequency in two of behavioral measures (Hactv: $F_{3,902} = 3.70$, $p < 0.05$; Totdist: $F_{3,914} = 5.98$, $p < 0.001$; see Fig. 1E and F). Despite this overall effect of frequency, none of the Bonferroni-corrected *t*-tests showed significant differences between individual frequencies. Comparing response during and after stimulation to before, 125 Hz stimulation increased motor activity in activity counts during ($t_{196} = -4.00$, $p < 0.001$) and after ($t_{196} = -3.50$, $p < 0.01$; see Fig. 1D) stimulation, horizontal activity during ($t_{184} = -4.12$, $p < 0.001$) and after ($t_{184} = -4.72$, $p < 0.001$; see Fig. 1E) stimulation, and total distance during ($t_{187} = -2.66$, $p < 0.05$; see Fig. 1F) stimulation. An example of high temporal resolution raw behavioral data for all four frequencies in a single mouse can be found in Fig. 3.

Only one of the EEG waves displayed an effect of frequency when all other factors are held constant (alpha: $F_{3,772} = 3.57$, $p < 0.05$; see Fig. 2H), and again, despite this ANOVA result, none of the Bonferroni-corrected *t*-tests showed significant differences between individual frequencies. EEG response after stimulation was also compared to before stimulation. Theta waves decreased with all four frequencies (50 Hz: $t_{198} = 4.30$, $p < 0.001$; 125 Hz: $t_{223} = 5.40$, $p < 0.001$; 175 Hz: $t_{197} = 3.86$, $p < 0.001$; 225 Hz: $t_{187} = 3.22$, $p < 0.01$; see Fig. 2G) after stimulation. Alpha waves increased with 125 Hz ($t_{215} = -3.06$, $p < 0.01$) and 225 Hz ($t_{184} = -3.64$, $p < 0.01$; see Fig. 2H) while beta waves only increased significantly with 225 Hz ($t_{186} = -3.80$, $p < 0.001$; see Fig. 2I) after stimulation. Finally, gamma waves increased with all four frequencies (50 Hz: $t_{192} = -2.53$, $p < 0.05$; 125 Hz: $t_{213} = -3.25$, $p < 0.01$; 175 Hz: $t_{203} = -2.92$, $p < 0.05$; 225 Hz: $t_{188} = -3.69$, $p < 0.001$; see Fig. 2J) after stimulation. While we do see an overall effect of frequency in some data measures, these effects of CT/DBS are inconsistent across data measures. Since 125 Hz tended to increase arousal more than the other frequencies, we chose 125 Hz for future studies.

Secondary analysis uncovered a multivariate interaction effect of amplitude and frequency ($F_{18,2048} = 2.59$, $p < 0.001$). This effect was primarily exhibited in the behavioral measure horizontal activity ($F_{6,902} = 3.82$, $p < 0.01$). The highest increases in horizontal activity during and after stimulation occurred with 125 Hz stimulation at 100 μA. This result further supported our choice of 125 Hz and 100 μA as stimulation parameters for future studies.

3.1.3. Daily light phase effects

In addition to the various parameters of stimulation manipulated above, we found that the light phase during which stimulation occurred had an effect, holding all other factors constant, on response to DBS in two behavioral measures (Hactv: $F_{1,902} = 14.03$, $p < 0.001$; Totdist: $F_{1,914} = 16.07$, $p < 0.001$; see Fig. 1H and I). Motor activity increased with light phase stimulation more than dark phase stimulation in horizontal activity during stimulation ($t_{257} = 2.82$, $p < 0.01$; see Fig. 1H) and total distance during ($t_{263} = 2.49$, $p < 0.01$) and after stimulation ($t_{264} = 2.20$, $p < 0.05$; see Fig. 1I).

In ANOVA analyses of EEG waves, light phase of stimulation had a significant effect on response to stimulation in four EEG

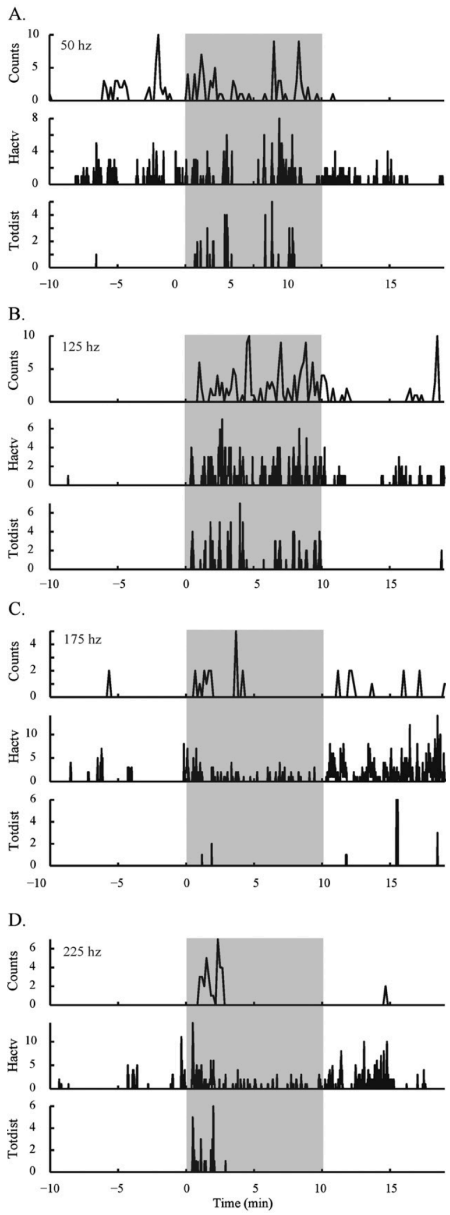

Fig. 3. *Parametric experiment – example of behavior at high temporal resolution.* Motor activity behavior of one mouse at four frequencies of stimulation, 100 μA, in the light phase. (A) 50 Hz, (B) 125 Hz, (C) 175 Hz, (D) 225 Hz. Activity counts ('counts') shown at one sample every 10 s, horizontal activity ('Hactv') and total distance ('Totdist') shown at one sample every 1 s. Grey boxes mark epochs of stimulation.

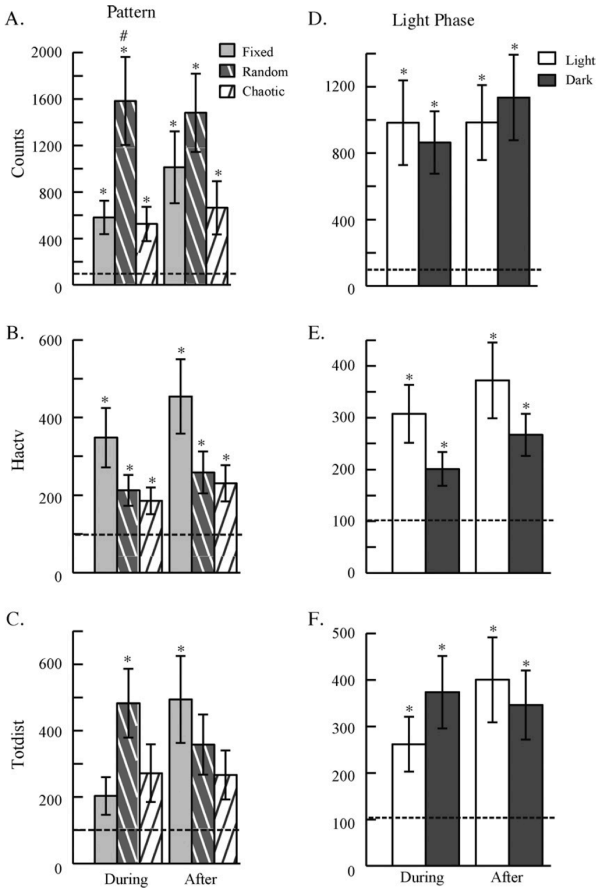

Fig. 4. *Temporal pattern experiment: behavior*. Behavioral response to temporal pattern (A–C) and light phase (D–F) of CT/DBS. Three behavioral measures are shown: activity counts (whole body movement), horizontal activity (fidgeting), and total distance (ambulation). ANOVA analyses revealed an overall effect of temporal pattern in activity counts (A, $p < 0.001$) and horizontal activity (B, $p < 0.01$). Panels include 10 min of data during and 10 min of data after CT/DBS, all normalized to before stimulation. Data are presented as mean ± S.E.M. $^{*}p < 0.05$ compared to before, $^{\#}p < 0.05$ compared to chaotic.

waves (theta: $F_{1,780} = 5.80$, $p < 0.05$; alpha: $F_{1,772} = 8.10$, $p < 0.01$; beta: $F_{1,760} = 9.05$, $p < 0.01$; gamma: $F_{1,771} = 12.40$, $p < 0.001$; see Fig. 2L–P). Theta waves decreased more with stimulation in the light phase than dark phase ($t_{389} = -1.99$, $p < 0.05$; see Fig. 2L). Additionally, alpha ($t_{381} = 2.42$, $p < 0.05$; see Fig. 2M), beta ($t_{369} = 2.54$, $p < 0.05$; see Fig. 2N), and gamma ($t_{380} = 2.82$, $p < 0.01$; see Fig. 2P) waves all increased more with DBS during the light phase than the dark. These data coincided with previous observations that increases to arousal due to stimulation are larger in the light than the dark.

3.2. Temporal pattern experiment

In the analysis of the temporal pattern experiment, we looked for differences caused by the stimulation itself and investigated differences caused by pattern of stimulation, light phase during which stimulation occurred, and any correlation between data measures (scattergrams and correlation coefficients for EEG data can be found in Figure S3). As with the Parametric data set, we found a significant effect of stimulation in all three behavioral measures (counts: $F_{2,453} = 21.47$, $p < 0.001$; Hactv: $F_{2,513} = 15.19$, $p < 0.001$; Totdist: $F_{2,504} = 12.56$, $p < 0.001$; see Fig. 4) and four of the EEG waves (delta: $F_{1,271} = 8.76$, $p < 0.01$; theta: $F_{1,258} = 13.29$, $p < 0.001$; beta: $F_{1,258} = 5.57$, $p < 0.05$; gamma: $F_{1,261} = 8.25$, $p < 0.01$; see Fig. 5). Again, we replicate findings here and elsewhere that CT/DBS increases generalized arousal as measured by motor activity and EEG response.

Supplementary material related to this article can be found, in the online version, at doi:10.1016/j.bbr.2012.01.025.

3.2.1. Temporal pattern effects

ANOVA analyses also revealed an effect of temporal patterning, while all other factors remain constant, in two behavioral measures (counts: $F_{2,453} = 8.56$, $p < 0.001$; Hactv: $F_{2,513} = 6.44$,

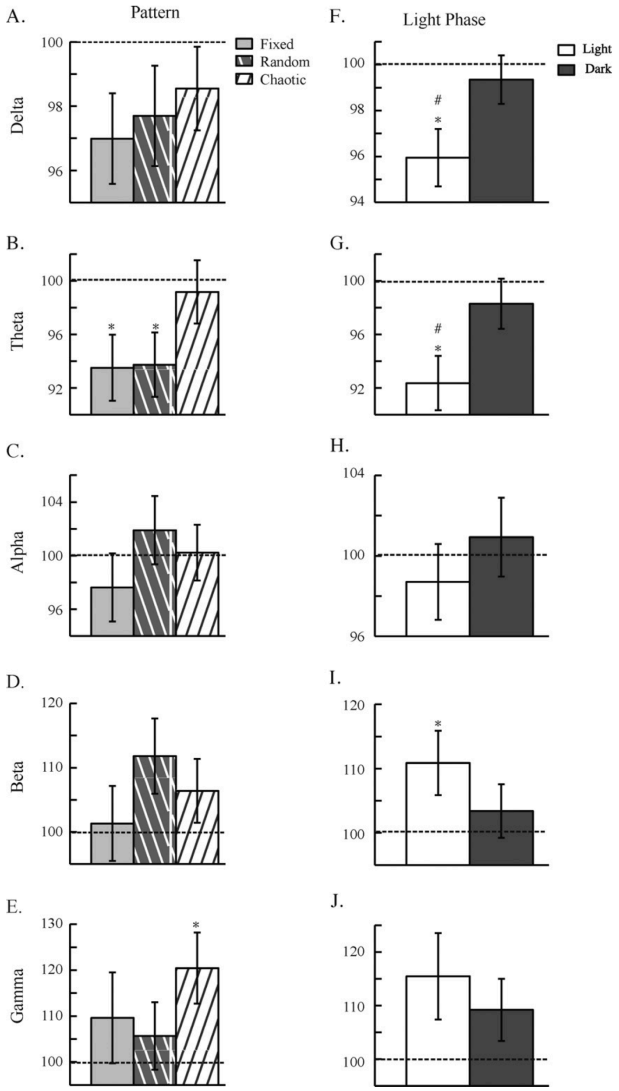

Fig. 5. *Temporal pattern experiment: EEG.* EEG response to temporal pattern (A–E) and light phase (F–J) of CT/DBS. EEG waves are defined by the following frequency bins: delta (0.5–4 Hz), theta (4.5–8 Hz), alpha (8.5–12 Hz), beta (12.5–20 Hz), and gamma (35–45 Hz). ANOVA analyses revealed an effect of CT/DBS in activity counts ($p < 0.001$), horizontal activity ($p < 0.001$), and total distance ($p < 0.001$) light phase of CT/DBS also had a significant effect in delta (F, $p < 0.05$) and theta (G, $p < 0.05$) waves. Panels include 10 min of data after CT/DBS, normalized to before stimulation. Data are presented as mean ± S.E.M. $^{*}p < 0.05$ compared to before, $^{\#}p < 0.05$ compared to dark phase.

$p < 0.01$; see Fig. 4A and B). While an overall effect of pattern was found, only one post-hoc comparison between patterns was significant. Random stimulation increased activity counts significantly more than chaotic during stimulation ($t_{96} = 2.52$, $p < 0.05$; see Fig. 3A). Comparing response during and after stimulation to before, all patterns increased motor activity compared to before in activity counts during (fixed: $t_{103} = -3.83$, $p < 0.001$; random: $t_{113} = -4.39$, $p < 0.001$; chaotic: $t_{105} = -2.35$, $p < 0.01$) and after stimulation (fixed: $t_{104} = -3.38$, $p < 001$; random: $t_{114} = -4.56$, $p < 0.001$; chaotic: $t_{106} = -2.76$, $p < 0.05$; see Fig. 4A), horizontal activity during (fixed: $t_{116} = -3.33$, $p < 0.01$; random: $t_{121} = -2.93$, $p < 0.05$; chaotic: $t_{116} = -2.55$, $p < 0.05$) and after stimulation (fixed: $t_{115} = -3.79$, $p < 0.01$; random: $t_{121} = -3.10$, $p < 0.01$; chaotic: $t_{116} = -2.86$, $p < 0.05$; see Fig. 4B), and total distance

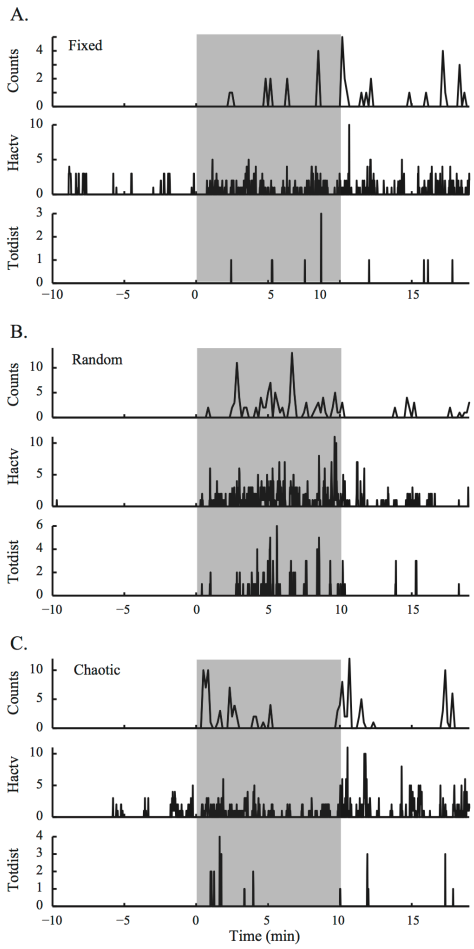

Fig. 6. *Temporal pattern experiment – example of behavior at high temporal resolution.* Motor activity behavior of one mouse at three temporal patterns of stimulation, 100 μA, in the light phase. (A) Fixed, (B) random, and (C) chaotic. Activity counts ('counts') shown at one sample every 10 s, horizontal activity ('Hactv') and total distance ('Totdist') shown at one sample every 1 s. Grey boxes mark epochs of stimulation.

during (random: $t_{120} = -3.87$, $p < 0.001$) and after stimulation (fixed: $t_{114} = -3.12$, $p < 0.01$; random: $t_{119} = -3.02$, $p < 0.01$; see Fig. 4C). An example of high temporal resolution raw behavioral data for all three patterns in a single mouse can be found in Fig. 6.

In the EEG analysis, there was no overall effect of pattern in any of the EEG waves, but in comparing responses after DBS to before, some significant differences emerged. Fixed and random DBS decreased theta waves after stimulation (fixed: $t_{84} = 2.96$, $p < 0.05$; random: $t_{95} = 2.81$, $p < 0.05$; see Fig. 5B), and chaotic DBS increased gamma waves after stimulation ($t_{90} = -2.77$, $p < 0.05$; see Fig. 5E). Despite an overall effect of temporal pattern and large obvious differences, conservative Bonferroni-corrected post-hoc analyses reveal few significant differences between specific temporal patterns.

3.2.2. Daily light phase effects

An effect of daily light phase was found in two of the EEG waves (delta: $F_{1,271} = 4.24$, $p < 0.05$; theta: $F_{1,258} = 6.49$, $p < 0.05$; see Fig. 5F and G). This general effect was confirmed by post-hoc *t*-tests comparing light to dark (delta: $t_{136} = -2.09$, $p < 0.05$; theta: $t_{123} = -2.14$, $p < 0.05$) after stimulation (see Fig. 5F and G). In three EEG waves, response after light phase DBS was significantly different from before. Delta ($t_{132} = 3.38$, $p < 0.001$) and theta ($t_{127} = 4.10$, $p < 0.001$) waves decreased with stimulation in the light (see Fig. 5F and G), and beta ($t_{124} = -2.44$, $p < 0.05$) waves increased with stimulation in the light (see Fig. 5I). This recapitulates our result that higher relative responses to stimulation occur during the light phase.

4. Discussion

4.1. Major findings

4.1.1. Behavior

Considering the behavioral results of both experiments presented above, we conclude that generalized arousal as measured by spontaneous motor activity can be increased by CT/DBS. This increase can be modulated by various parameters of stimulation. Amplitude of DBS increases behavioral response in an expected way; more current yields a concomitant increase in motor activity. Behavioral responses to various frequencies of DBS also differ, but in this particular circumstance the differences between the specific frequencies chosen were not significant. Light phase during which DBS occurs can also affect degree of increase in behavior; larger increases during and after stimulation occur during the light phase and are most likely due to the low baseline activity during the light. Most importantly we have found that temporal pattern of stimulation affects behavioral response to CT/DBS. This effect of temporal pattern in behavioral response to DBS replicates our previous findings [16] that temporal patterning makes a difference.

Our behavioral data revealed an overall effect of temporal pattern, but only one specific significant difference in the Bonferroni-corrected post-hoc analysis and only in the activity counts behavioral measure. In that instance, random CT/DBS increased motor activity during stimulation more than chaotic. This result is unexpected. Since we theorized [17] that nonlinear dynamics play a role in controlling arousal systems, we hypothesized that chaotic CT/DBS would increase arousal more than either fixed or random; instead we see that random does better. At the moment, it is unclear why one temporal pattern did better than another in one behavioral measure. Given that our results ran counter to our expectations, it might be that some singular undefined characteristic of the random temporal pattern was responsible for the temporal pattern's success instead of theoretical method by which it was generated.

4.1.2. EEG

EEG responses to DBS were as expected. In both experiments, EEG waves changed significantly with CT/DBS and in a direction consistent with an increase in arousal. Delta and theta waves, associated with sleep and quiet wakefulness [22], decreased with CT/DBS, while alpha, beta, and gamma waves, associated with wakefulness and higher cognitive functions such as attention [23], increased with CT/DBS. Degree of response to DBS was modulated by amplitude of stimulation, but these changes were small and often not significant. Differences between response to various frequencies of stimulation were also subtle and only significant in

alpha waves. EEG response to DBS during the two phases of the light cycle were also different; changes after DBS were larger in the light phase than in the dark. We assume these larger responses during the light phase are due to the nocturnal nature of mice; since mice are often quiescent during the light phase, they respond more dramatically to an arousing stimulus then. We saw no differences in response to our three patterns of stimulation. The EEG data presented here do not coincide with our previously published results [16]. It was discovered that a typographical error in the analysis script for these previously collected EEG data altered the results and their interpretation. Upon reanalyzing these data, we found that delta waves did not increase significantly with either hippocampal or central thalamus stimulation and that gamma waves did increase significantly with central thalamus stimulation. These corrected results coincide with our expectations as well as the results presented here. Other differences can be explained by different brain regions stimulated as well as different stimulation parameters used.

4.2. Literature

Due to the novelty of this work, there is only a handful of articles, reporting work done in varying contexts, to compare our results to. CT/DBS has been investigated in intact rats [24], brain injured rats [25], macaque monkeys [26], mice [16], and one human case study [10]. Concurrent with what we observe here, CT/DBS increased motor activity or enhanced performance on a cognitive task in all of these studies; however, none of the work mentioned above explored the importance of temporal pattern of stimulation. Shirvalkar et al. showed increased early action gene expression in cortical and basal ganglia regions as well as enhanced performance on a novel object recognition task with CT/DBS in intact rats [24]. In a DMTP rat model, Mair et al. showed enhanced working memory with CT/DBS [25]. Smith et al. used bayesian statistical methods to analyze the effect of CT/DBS on a sustained attention task in macaque monkeys [26]. This method was also used to further analyze data collected from the human case study of CT/DBS in a MCS patient. It was confirmed that CT/DBS helped facilitate functional recovery in this patient [10,26]. These studies represent the body of evidence that CT/DBS can increase arousal and enhance cognition, but there are still questions to explore such as what stimulation parameters, including pattern, are best and how do these parameters need to be adjusted, patient to patient.

4.3. Potential caveats

Like many behavioral studies with multiple subjects, especially mice, these experiments show a large variability. Three potential sources of variance are considered: baseline activity level, exact electrode placement, and sex differences. First, it is clear that baseline activity level does influence response to stimulation. Mice respond differentially to stimulation in the light and dark; responses during the light phase, when mice are more often quiescent, are relatively larger than those during the dark phase. Fluctuations of baseline activity on a smaller scale are likely causes of intra-subject variability. Second, small variations in electrode placement might affect inter-subject variability. These small position differences change the electrical field of stimulation and which specific neurons are influenced by this field. These changes might alter the efficiency of stimulation as well as the magnitude of response during and directly after stimulation. Finally, we observed small, inconsistent sex differences as mentioned in Section 2.1. While these differences were not statistically significant, it is likely they affected inter-subject variability once the data from males and females were pooled.

4.4. Conclusions

Here we have presented more evidence that temporal patterning of DBS can affect the magnitude of desired responses. While a comprehensive exploration of temporal patterns in DBS is outside the scope of this paper, possible avenues to continue this work would be to investigate (1) longer sequences of pulses that would presumably permit still more entropy, (2) specific local characteristics of the temporal patterns presented here to determine why random was better than chaotic, (3) other deterministic chaotic equations [27], and (4) playbacks of temporal patterns recorded from central thalamus or from arousal systems that project to the central thalamus. Additionally, it stands to reason that because we found that temporal patterns of CT/DBS are important in modulating motor activity and EEG response, temporal patterns of stimulation might modulate desired responses to DBS in other, medically important contexts. More research is needed into how neuronal circuits of interest function in normal and diseased states as well as how DBS can be used to effect desired changes in these circuits. This is essential to the future of DBS therapy because the more we know about diseased neuronal circuits and how DBS affects them, the better able we will be to logically choose stimulation parameters and design DBS regimes. Choosing a stimulation regime for a specific disorder or set of symptoms will be much more efficient than the current method for finding stimulation parameters, by trial and error.

Acknowledgments

We appreciate the intellectual support of Nicolas D Schiff as well as the funding from his NIH grant NS067249. This work was also funded in part by Intelect Medical, Inc.

References

[1] Benabid AL, Chabardes S, Mitrofanis J, Pollak P. Deep brain stimulation of the subthalamic nucleus for the treatment of Parkinson's disease. Lancet Neurol 2009;8:67–81.
[2] Castrioto A, Lozano AM, Poon YY, Lang AE, Fallis M, Moro E. Ten-year outcome of subthalamic stimulation in Parkinson disease: a blinded evaluation. Arch Neurol 2011.
[3] Obeso JA, Guridi J, Rodriguez-Oroz MC, Agid Y, Bejjani P, Bonnet AM, et al. Deep-brain stimulation of the subthalamic nucleus or the pars interna of the globus pallidus in Parkinson's disease. N Engl J Med 2001;345:956–63.
[4] Greenberg BD, Suzanne SLR, Haber SN. Invasive circuitry-based neurotherapeutics: stereotactic ablation and deep brain stimulation for OCD. Neuropsychopharmacology 2010;35:317–36.
[5] Hirschfeld RMA. Deep brain stimulation for treatment-resistant depression. Am J Psychiatry 2011;168:455–6.
[6] Wichmann T, DeLong MR. Deep brain stimulation for neurologic and neuropsychiatric disorders. Neuron 2006;52:197–204.
[7] Coffey RJ. Deep brain stimulation for chronic pain: results of two multicenter trials and a structured review. Pain Med 2001;2:183–92.
[8] Levy R, Deer TR, Henderson J. Intracranial neurostimulation for pain control: a review. Pain Physician 2010;13:157–65.
[9] Rasche D, Rinaldi PC, Young RF, Tronnier VM. Deep brain stimulation for the treatment of various chronic pain syndromes. Neurosurg Focus 2006; 21:E8.
[10] Schiff ND, Giacino JT, Kalmar K, Victor JD, Baker K, Gerber M, et al. Behavioural improvements with thalamic stimulation after severe traumatic brain injury. Nature 2007;448:600–3.
[11] Schiff ND. Central thalamic contributions to arousal regulation and neurological disorders of consciousness. Mol Biophys Mech Arousal Alertness Attention 2008;1129:105–18.
[12] Schiff ND. Central thalamic deep-brain stimulation in the severely injured brain: rationale and proposed mechanisms of action. Ann N Y Acad Sci 2009;1157:101–16.
[13] Kumar A, Rotter S, Aertsen A. Spiking activity propagation in neuronal networks: reconciling different perspectives on neural coding. Nat Rev Neurosci 2010;11:615–27.
[14] Panzeri S, Brunel N, Logothetis NK, Kayser C. Sensory neural codes using multiplexed temporal scales. Trends Neurosci 2010;33: 111–20.
[15] Wasserman GS. Isomorphism, task dependence, and the multiple meaning theory of neural coding. Biol Signals 1992;1:117–42.

[16] Quinkert AW, Schiff ND, Pfaff DW. Temporal patterning of pulses during deep brain stimulation affects central nervous system arousal. Behav Brain Res 2010;214:377–85.
[17] Pfaff D, Banavar JR. A theoretical framework for CNS arousal. Bioessays 2007;29:803–10.
[18] Paul CA, Beltz BS, Berger-Sweeney J, Discovering Neurons. The experimental basis of neuroscience. Cold Spring Harbor Laboratory Press; 1997.
[19] Haahr M. Random integer generator. Random.org; 1998. Available at http://www.random.org/integers [accessed 16 June 2010].
[20] Brown MB, Forsythe AB. 372: The Anova and multiple comparisons for data with heterogeneous variances. Biometrics 1974:719–24.
[21] Tabachnick BG, Fidell LS. Using multivariate statistics. 4th ed. Boston, MA: Allyn and Bacon; 2001.
[22] Niedermeyer E. Sleep and EEG. In: Niedermeyer E, Lopes da Silva F, editors. Electroencephalography: basic principles, clinical applications, and related fields. 5th ed. Philadelphia: Lippincott Williams and Wilkins; 2005.
[23] Niedermeyer E. The normal EEG of the waking adult. In: Niedermeyer E, Lopes da Silva F, editors. Electroencephalography: basic principles, clinical applications, and related fields. 5th ed. Philadelphia: Lippincott Williams and Wilkins; 2005.
[24] Shirvalkar P, Seth M, Schiff ND, Herrera DG. Cognitive enhancement with central thalamic electrical stimulation. Proc Natl Acad Sci USA 2006;103:17007–12.
[25] Mair RG, Hembrook JR. Memory enhancement with event-related stimulation of the rostral intralaminar thalamic nuclei. J Neurosci 2008;28:14293–300.
[26] Smith AC, Shah SA, Hudson AE, Purpura KP, Victor JD, Brown EN, et al. A Bayesian statistical analysis of behavioral facilitation associated with deep brain stimulation. J Neurosci Methods 2009;183:267–76.
[27] Cohen JE. Unexpected dominance of high frequencies in chaotic nonlinear population models. Nature 1995;378:610–6.

References

Arabzadeh, E., Panzeri, S., & Diamond, M. E. (2006). Deciphering the Spike Train of a Sensory Neuron: Counts and Temporal Patterns in the Rat Whisker Pathway. *J Neurosci*, 26(36), 9216-9226.

Armed Forces Health Surveillance Center. (2010). *TBI numbers by severity - All Armed Forces: 2002-2006.* Retrieved from http://www.dvbic.org/Archive-of-DoD-Numbers-for-TBI.aspx.

Arrieta-Cruz, I., Pfaff, D. W., & Shelley, D. N. (2007). Mouse model of diffuse brain damage following anoxia, evaluated by a new assay of generalized arousal. *Exp Neurol*, 205(2), 449-460.

Aston-Jones, G., Chen, S., Zhu, Y., & Oshinsky, M. L. (2001). A neural circuit for circadian regulation of arousal. *Nat Neurosci*, 4(7), 732-738.

Aston-Jones, G., Rajkowski, J., Kubiak, P., Valentino, R. J., & Shipley, M. T. (1996). Role of the locus coeruleus in emotional activation. *Prog Brain Res*, 107, 379-402.

Baker, K. B., Zhang, J. Y., & Vitek, J. L. (2011). Pallidal stimulation: Effect of pattern and rate on bradykinesia in the non-human primate model of Parkinson's disease. *Exp Neurol*, 231(2), 309-313.

Birdno, M. J., Kuncel, A. M., Dorval, A. D., Turner, D. A., & Grill, W. M. (2008). Tremor varies as a function of the temporal regularity of deep brain stimulation. *Neuroreport*, 19(5), 599-602.

Birdno, M. J., Kuncel, A. M., Dorval, A. D., Turner, D. A., Gross, R. E., & Grill, W. M. (2012). Stimulus features underlying reduced tremor suppression with temporally patterned deep brain stimulation. *J Neurophys*, 107(1), 364-383.

Bourne, S. K., Eckhardt, C. A., Sheth, S. A., & Eskandar, E. N. (2012). Mechanisms of deep brain stimulation for obsessive compulsive disorder: effects upon cells and circuits. *Front Integr Neurosci*, 6, 29.

Buonomano, D. V. (2000). Decoding Temporal Information: A Model Based on Short-Term Synaptic Plasticity. *J Neurosci*, 20(3), 1129-1141.

Buonomano, D. V., & Merzenich, M. M. (1995). Temporal information transformed into a spatial code by a neural network with realistic properties. *Science*, 267(5200), 1028-1030.

Carlson, B. A. (2009). Temporal-pattern recognition by single neurons in a sensory pathway devoted to social communication behavior. *J Neurosci*, 29(30), 9417-9428.

CDC. (2010). *Traumatic brain injury in the United States: emergency department visits, hospitalizations and deaths, 2002–2006.* Atlanta, GA: US Department of Health and Human Services, CDC. Retrieved from: http://www.cdc.gov/traumaticbraininjury/tbi_ed.html.

Coffey, R. J. (2001). Deep brain stimulation for chronic pain: results of two multicenter trials and a structured review. *Pain Med*, 2(3), 183-192.

Cohen, J. E. (1995). Unexpected dominance of high frequencies in chaotic nonlinear population models. *Nature*, 378(6557), 610-616.

Cota, V. R., Medeiros, D. D., Vilela, M. R. S. D., Doretto, M. C., & Moraes, M. F. D. (2009). Distinct patterns of electrical stimulation of the basolateral amygdala influence pentylenetetrazole seizure outcome. *Epilepsy & Behav*, 14, 26-31.

Di Lorenzo, P. M., Leshchinskiy, S., Moroney, D. N., & Ozdoba, J. M. (2009). Making Time Count: Functional Evidence for Temporal Coding of Taste Sensation. *Behav Neurosci*, 123(1), 14-25.

Doi, A., Mizuno, M., Katafuchi, T., Furue, H., Koga, K., & Yoshimura, M. (2007). Slow oscillation of membrane currents mediated by glutamatergic inputs of rat somatosensory cortical neurons: in vivo patch-clamp analysis. *Euro J Neurosci*, 26(9), 2565-2575.

Flierl, M. A., Stahel, P. F., Beauchamp, K. M., Morgan, S. J., Smith, W. R., & Shohami, E. (2009). Mouse closed head injury model induced by a weight-drop device. *Nat Protoc*, 4(9), 1328-1337.

Fox, S. H., Katzenschlager, R., Lim, S. Y., Ravina, B., Seppi, K., Coelho, M., et al. (2011). The Movement Disorder Society Evidence-Based Medicine Review Update: Treatments for the Motor Symptoms of Parkinson's Disease. *Movement Disorders*, 26, S2-S41.

Gaetz, M. (2004). The neurophysiology of brain injury. *Clin Neurophys*, 115(1), 4-18.

Giacino, J., Fins, J. J., Machado, A., & Schiff, N. D. (2012). Central Thalamic Deep Brain Stimulation to Promote Recovery from Chronic Posttraumatic Minimally Conscious State: Challenges and Opportunities. *Neuromod*, 15, 339–349.

Giacino, J. T., Ashwal, S., Childs, N., Cranford, R., Jennett, B., Katz, D. I., et al. (2002). The minimally conscious state: definition and diagnostic criteria. *Neurol*, 58(3), 349-353.

Glendinning, J. I., Davis, A., & Rai, M. (2006). Temporal Coding Mediates Discrimination of "Bitter" Taste Stimuli by an Insect. *J Neurosci*, 26(35), 8900-8908.

Goodman, W. K., & Alterman, R. L. (2012). Deep Brain Stimulation for Intractable Psychiatric Disorders. *Ann Rev Med*, Vol 63, 63, 511-524.

Graham, D. I., Adams, J. H., Nicoll, J. A. R., Maxwell, W. L., & Gennarelli, T. A. (1995). The Nature, Distribution and Causes of Traumatic Brain Injury. *Brain Pathol*, 5(4), 397-406.

Haahr, M. (1998). *Random Integer Generator.* Retrieved from http://www.random.org

Hassler, R., Ore, G. D., Dieckman.G, Bricolo, A., & Dolce, G. (1969). Behavioural and EEG Arousal Induced by Stimulation of Unspecific Projection Systems in a Patient with Post-Traumatic Apallic Syndrome. *Electroenceph Clin Neurophysiol*, 27(3), 306-310.

Hirschberg, R., & Giacino, J. T. (2011). The Vegetative and Minimally Conscious States: Diagnosis, Prognosis and Treatment. *Neurol Clin*, 29(4), 773-86.

Jones, B. E. (2003). Arousal systems. *Front Biosci*, 8, s438-451.

Kimmel, D. L., & Moore, T. (2007). Temporal Patterning of Saccadic Eye Movement Signals. *J Neurosci*, 27(29), 7619-7630.

Kozloski, J., & Crawford, J. D. (2000). Transformations of an Auditory Temporal Code in the Medulla of a Sound-Producing Fish. *J Neurosci*, 20(6), 2400-2408.

Kryger, M. H., Roth, T., & Dement, W. C. (2000). *Principles and practice of sleep medicine* (3rd ed.). Philadelphia: Saunders.

Kumar, A., Rotter, S., & Aertsen, A. (2010). Spiking activity propagation in neuronal networks: reconciling different perspectives on neural coding. *Nat Rev Neurosci*, 11(9), 615-627.

Larson, P. S. (2008). Deep brain stimulation for psychiatric disorders. *Neurotherapeutics*, 5(1), 50-58.

Laurent, G., Wehr, M., & Davidowitz, H. (1996). Temporal Representations of Odors in an Olfactory Network. *J Neurosci*, 16(12), 3837-3847.

Lei, H., Christensen, T. A., & Hildebrand, J. G. (2004). Spatial and Temporal Organization of Ensemble Representations for Different Odor Classes in the Moth Antennal Lobe. *J Neurosci*, 24(49), 11108-11119.

Leker, R. R., Shohami, E., & Constantini, S. (2002). Experimental models of head trauma. *Acta Neurochir Suppl*, 83, 49-54.

Levy, R., Deer, T. R., & Henderson, J. (2010). Intracranial Neurostimulation for Pain Control: A Review. *Pain Physician*, 13(2), 157-165.

Liu, B., Li, J., Li, L., Yu, L., & Li, C. (2012). Electrical stimulation of cerebellar fastigial nucleus promotes the expression of growth arrest and DNA damage inducible gene β and motor function recovery in cerebral ischemia/reperfusion rats. *Neurosci Letters*, 520(1), 110–114.

Liu, Y., Postupna, N., Falkenberg, J., & Anderson, M. E. (2008). High frequency deep brain stimulation: What are the therapeutic mechanisms? *Neurosci Biobehav Rev*, 32(3), 343-351.

Mair, R. G., & Hembrook, J. R. (2008). Memory Enhancement with Event-Related Stimulation of the Rostral Intralaminar Thalamic Nuclei. *J Neurosci*, 28(52), 14293-14300.

Malone, B. J., Scott, B. H., & Semple, M. N. (2010). Temporal Codes for Amplitude Contrast in Auditory Cortex. *J Neurosci*, 30(2), 767-784.

Martin, E. M., Pavlides, C., & Pfaff, D. (2010). Multimodal sensory responses of nucleus reticularis gigantocellularis and the responses' relation to cortical and motor activation. *J Neurophysiol*, 103(5), 2326-2338.

Martin-Löf, P. (1966). The definition of random sequences. *Information and Control*, 9(6), 602-619.

Mechler, F., Victor, J. D., Purpura, K. P., & Shapley, R. (1998). Robust Temporal Coding of Contrast by V1 Neurons for Transient But Not for Steady-State Stimuli. *J Neurosci*, 18(16), 6583-6598.

Miller, G. (2009). Neuropsychiatry. Rewiring faulty circuits in the brain. *Science*, 323(5921), 1554-1556.

Montgomery, E. B., Jr., & Gale, J. T. (2008). Mechanisms of action of deep brain stimulation(DBS). *Neurosci Biobehav Rev*, 32(3), 388-407.

Morales, D. M., Marklund, N., Lebold, D., Thompson, H. J., Pitkanen, A., Maxwell, W. L., et al. (2005). Experimental models of traumatic brain injury: Do we really need to build a better mousetrap? *Neurosci*, 136(4), 971-989.

Niedermeyer, E. (2005). The Normal EEG of the Waking Adult In E. Niedermeyer & F. Lopes da Silva (Eds.), *Electroencephalography: Basic Principles, Clinical Applications, and Related Fields* (5th ed.). Philadelphia: Lippincott Williams and Wilkins.

Niedermeyer, E. (2005). Sleep and EEG. In E. Niedermeyer & F. Lopes da Silva (Eds.), *Electroencephalography: Basic Principles, Clinical Applications, and Related Fields* (5th ed.). Philadelphia: Lippincott Williams and Wilkins.

Panzeri, S., Brunel, N., Logothetis, N. K., & Kayser, C. (2010). Sensory neural codes using multiplexed temporal scales. *Trends Neurosci*, 33(3), 111-120.

Paxinos, G., & Franklin, K. B. J. (2001). *The Mouse Brain in Stereotaxic Coordinates* (2nd ed.). San Diego: Academic Press.

Pfaff, D., & Banavar, J. R. (2007). A theoretical framework for CNS arousal. *Bioessays*, 29(8), 803-810.

Pfaff, D. W. (2006). *Brain arousal and information theory: neural and genetic mechanisms.* Cambridge, MA: Harvard University Press.

Pfaff, D. W., Martin, E. M., & Faber, D. (2012). Origins of arousal: roles for medullary reticular neurons. *Trends Neurosci*, 35(8), 468-476.

Quinkert, A. W., & Pfaff, D. W. (2012). Temporal patterns of deep brain stimulation generated with a true random number generator and the logistic equation: Effects on CNS arousal in mice. *Behav Brain Res*, 229(2), 349-358.

Quinkert, A. W., Schiff, N. D., & Pfaff, D. W. (2010). Temporal patterning of pulses during deep brain stimulation affects central nervous system arousal. *Behav Brain Res*, 214(2), 377-385.

Quinkert, A. W., Vimal, V., Weil, Z. M., Reeke, G. N., Schiff, N. D., Banavar, J. R., et al. (2011). Quantitative descriptions of generalized arousal, an elementary function of the vertebrate brain. *Proc Natl Acad Sci USA*, 108(suppl 3), 15617-15623.

Rasche, D., Rinaldi, P. C., Young, R. F., & Tronnier, V. M. (2006). Deep brain stimulation for the treatment of various chronic pain syndromes. *Neurosurg Focus*, 21(6), E8.

Reilly, P. L. (2001). Brain injury: the pathophysiology of the first hours. 'Talk and Die revisited'. *J Clin Neurosci*, 8(5), 398-403.

Reinagel, P., & Reid, R. C. (2000). Temporal Coding of Visual Information in the Thalamus. *J Neurosci*, 20(14), 5392-5400.

Ribeiro, A. C., Pfaff, D. W., & Devidze, N. (2009). Estradiol modulates behavioral arousal and induces changes in gene expression profiles in brain regions involved in the control of vigilance. *Eur J Neurosci, 29*(4), 795-801.

Sanchez, J. T., Gans, D., & Wenstrup, J. J. (2007). Contribution of NMDA and AMPA Receptors to Temporal Patterning of Auditory Responses in the Inferior Colliculus. *J Neurosci*, 27(8), 1954-1963.

Schiff, N. D. (2008). Central thalamic contributions to arousal regulation and neurological disorders of consciousness. *Ann NY Acad Sci*, 1129, 105-118.

Schiff, N. D. (2009). Central thalamic deep-brain stimulation in the severely injured brain: rationale and proposed mechanisms of action. *Ann NY Acad Sci*, 1157, 101-116.

Schiff, N. D. (2010). Recovery of consciousness after brain injury: a mesocircuit hypothesis. *Trends Neurosci*, 33(1), 1-9.

Schiff, N. D., Giacino, J. T., Kalmar, K., Victor, J. D., Baker, K., Gerber, M., et al. (2007). Behavioural improvements with thalamic stimulation after severe traumatic brain injury. *Nature*, 448(7153), 600-603.

Shirvalkar, P., Seth, M., Schiff, N. D., & Herrera, D. G. (2006). Cognitive enhancement with central thalamic electrical stimulation. *Proc Natl Acad Sci USA*, 103(45), 17007-17012.

Smith, A. C., Shah, S. A., Hudson, A. E., Purpura, K. P., Victor, J. D., Brown, E. N., et al. (2009). A Bayesian statistical analysis of behavioral facilitation associated with deep brain stimulation. *J Neurosci Met*, 183(2), 267-276.

Snyder, D. L., & Miller, M. I. (1991). *Random point processes in time and space*. (2nd ed.). New York: Springer-Verlag.

So, R. Q., McConnell, G. C., Hilliard, J. D., & Grill, W. M. (2011). Irregular High Frequency Patterns Decrease the Effectiveness of Deep Brain Stimulation in a Rat Model of Parkinson's Disease. Proceedings from *5th International IEEE/ EMBS Conference on Neural Engineering*, 322-325.

Sturm, V., Kuhner, A., Schmitt, H. P., Assmus, H., & Stock, G. (1979). Chronic electrical stimulation of the thalamic unspecific activating system in a patient with coma due to midbrain and upper brain stem infarction. *Acta Neurochir (Wien)*, 47(3-4), 235-244.

Van der Werf, Y. D., Witter, M. P., & Groenewegen, H. J. (2002). The intralaminar and midline nuclei of the thalamus. Anatomical and functional evidence for participation in processes of arousal and awareness. *Brain Res Brain Res Rev*, 39(2-3), 107-140.

Vedam-Mai, V., van Battum, E. Y., Kamphuis, W., Feenstra, M. G., Denys, D., Reynolds, B. A., et al. (2012). Deep brain stimulation and the role of astrocytes. *Mol Psychiatry*, 17(2), 124-131.

Washington Headquarters Services: Directorate for Information Operations and Reports. (2006). *Active duty military personnel strengths by regional area and country: September 30, 2002-2006*. Retrieved from http://siadapp.dmdc.osd.mil/personnel/MILITARY/miltop.htm

Wasserman, G. S. (1992). Isomorphism, task dependence, and the multiple meaning theory of neural coding. *Biol Signals*, 1(3), 117-142.

Wehr, M., & Laurent, G. (1999). Relationship between Afferent and Central Temporal Patterns in the Locust Olfactory System. *J Neurosci*, 19(1), 381-390.

Weil, Z. M., Zhang, Q. Y., Hornung, A., Blizard, D., & Pfaff, D. W. (2010). Impact of generalized brain arousal on sexual behavior. *Proc Natl Acad Sci USA*, 107(5), 2265-2270.

Williams, S. R., & Stuart, G. J. (2000). Backpropagation of Physiological Spike Trains in Neocortical Pyramidal Neurons: Implications for Temporal Coding in Dendrites. *J Neurosci,* 20(22), 8238-8246.

Wu, S. H., Ma, C. L., & Kelly, J. B. (2004). Contribution of AMPA, NMDA, and GABAA Receptors to Temporal Pattern of Postsynaptic Responses in the Inferior Colliculus of the Rat. *J Neurosci*, 24(19), 4625-4634.

Yamamoto, T., Katayama, Y., Kobayashi, K., Oshima, H., Fukaya, C., & Tsubokawa, T. (2010). Deep brain stimulation for the treatment of vegetative state. *Euro J Neurosci*, 32(7), 1145-1151.

Zhang, G., Zhang, J. H., Feng, J., Li, Q., Wu, X., & Qin, X. (2011). Electrical stimulation of olfactory bulb downregulates RGMa expression after ischemia/reperfusion injury in rats. *Brain Res Bulletin*, 86(3-4), 254–261.